STRUCTURAL IDENTIFICATION OF THE SEHZADE MEHMED MOSQUE THROUGH STATIC AND DYNAMIC ANALYSES

by

Musa Artar

B.S., Civil Engineering, Istanbul Technical University, 2002

Submitted to the Institute for Graduate Studies in
Science and Engineering in the partial fulfillment of
the requirements for the degree of
Master of Science

Graduate Program in Civil Engineering
Boğaziçi University
2006

ACKNOWLEDGMENTS

I would like to express my deepest gratitude to my supervisor, Prof. Dr. Gülay Altay for her wide angle of engineering approach, enormous guidance, encouragement and technical support that she has provided during all the steps of this thesis.

I thank to my family for their infinite patience and encouragement that they gave me during all the steps of this thesis.

ABSTRACT

STRUCTURAL IDENTIFICATION OF THE SEHZADE MEHMED MOSQUE THROUGH STATIC AND DYNAMIC ANALYSES

Built between 1543-1548 by the great Turkish architect Mimar Sinan to commemorate the memory of one of the legendary Ottoman Emperor Süleyman's sons, the prince Mehmet, the Sehzade Mehmet Mosque is considered to be one of the first masterpieces of the Ottoman architecture.

It is a fact that the research studies carried out up today towards the determination of the earthquake performance of this masterpiece of Ottoman-Turkish Engineering is very limited. Before any numerical or physical analyses, it is essential to make a deep historical survey. So, firstly, I started to research on five historical mosques (the Fatih Mosque, the Beyazit Mosque, the Mihrimah Mosque, the Rüstem Pasa Mosque and the Sehzade Mehmet Mosque) built in the classical ottoman architecture era in order to have detailed information about historical development of the structural features of the Sehzade Mehmet Mosque and then, I studied on the structural characteristics of Sehzade Mehmet Mosque. In this study, the three dimensional finite element model of the Sehzade Mehmet Mosque was constructed in order to investigate the linear structural behavior of the mosque under static and dynamic conditions. Natural frequencies were obtained by the modal analysis of the Sehzade Mehmet Mosque. Finally, the analysis of the improved model under a scenario earthquake for Istanbul was carried out.

ÖZET

STATİK VE DİNAMİK ANALİZLER YARDIMIYLA ŞEHZADE MEHMET CAMİSİ'NİN YAPISAL OLARAK TANIMLANMASI

1543-1548 yılları arasında büyük Türk mimar Mimar Sinan tarafından, efsanevi Osmanlı İmparatoru Süleyman'ın oğullarından biri olan Şehzade Mehmet'in anısına inşa edilen Şehzade Mehmet Camisi, Osmanlı mimarisinin ilk başyapıtlarından biri olarak düşünülür.

Bu Osmanlı-Türk başyapıtının deprem performansının belirlenmesi yönünde bugüne kadar yapılmış olan araştırma çalışmalarının çok kısıtlı olduğu bir gerçektir. Herhangi bir nümeriksel ve fiziksel analizden önce detaylı bir tarihi araştırma gereklidir. Bu yüzden ilk olarak Şehzade Mehmet Camisinin yapısal özelliklerinin tarihi gelişimi hakkında detaylı bir bilgiye sahip olmak amacıyla Klasik Osmanlı Mimarisi Döneminde yapılan beş cami (Fatih Camisi, Beyazıt Camisi, Edirnekapı Mihrimah Camisi, Rüstem Paşa Camisi ve Şehzade Mehmet Camisi) üzerine araştırma yaptım. Daha sonra Şehzade Mehmet Camisinin yapısal karakteristikleri üzerine çalıştım. Bu çalışmada Şehzade Mehmet Camisinin statik ve dinamik koşullarda lineer davranışını araştırmak amacıyla üç boyutlu sonlu elemanlı modeli yapılmıştır. Modal analiz yardımıyla Şehzade Mehmet Camisinin doğal frekansları elde edilmiştir. Çalışmanın son aşamasında ise geliştirilmiş model üzerinde İstanbul için olası bir senaryo depreminin etkisi analiz edilmiştir.

TABLE OF CONTENTS

LIST OF FIGURES

LIST OF TABLES

LIST OF SYMBOLS

F_{11}	Axial plane force in the 1-direction
F_{12}	Shear force in the 1-2 plane
F_{22}	Axial plane force in the 2-direction
Fmin	Minimum principal force
Fmax	Maximum principal force
[K]	Stiffness matrix
m	Constant
[M]	Mass matrix
M_{11}	Bending moment in the 2-direction for shell elements
M_{12}	Twisting moment in the 1-2 plane for shell elements
M_{22}	Bending moment in the 1-direction for shell elements
Mmin	Minimum principal moment for shell elements
Mmax	Maximum principal moment for shell elements
Pk	Snow load
{R}	Vector of applied loads
S_{11}	Stress in the local 1-axis in the 2-3 plane for shell elements (hoop stress) and solid elements
S_{22}	Stress in the local 2-axis in the 1-3 plane for shell elements (radial stress) and solid elements
S_{33}	Stress in the local 3-axis in the 1-2 plane for solid elements
S_{12}	Stress in the local 2-axis in the 2-3 plane for solid elements
S_{21}	Stress in the local 1-axis in the 1-3 plane for solid elements
S_{13}	Stress in the local 3-axis in the 2-3 plane for solid elements
S_{31}	Stress in the local 1-axis in the 1-2 plane for solid elements
S_{23}	Stress in the local 3-axis in the 1-3 plane for solid elements
S_{32}	Stress in the local 2-axis in the 1-2 plane for solid elements
Smin	Minimum principal stress for shell and solid elements
Smax	Maximum principal stress for shell and solid elements
{u}	Displacement vector
{ü}	Acceleration vector

$[\Omega^2]$	Diagonal matrix giving eigen-values (modal frequencies)
{ Ø }	Vector of mode shapes corresponding with the modal frequencies

l. INTRODUCTION

Built between 1543-1548 by the great Turkish architect Mimar Sinan to commemorate the memory of one of Süleyman's sons, the prince Mehmet, the Sehzade Mehmet Mosque is considered to be one of the first masterpieces of the Ottoman architecture. Sinan (1492-1588) developed his structural ingenuity first as a military engineer. He served, for almost half a century, as a military engineer of the Ottoman Empire, during which he was involved directly or indirectly with the construction of nearly five hundred works including mosques, bridges, hydraulic structures, hospitals, palaces, schools, etc.

The Sehzade Mehmet Mosque is considered to be one of the first masterpieces of the Ottoman architecture and has successfully sustained against more than 89 major earthquakes without any severe damages [11], [19].

The present study on the Sehzade Mehmet Mosque is mainly aimed at the exploration of the static and dynamic characteristics of the structure, eventually to determine dynamic performance during earthquakes. But, before any numerical or physical analyses, it is essential to make a deep historical survey. So, firstly, I started to research on historical backgrounds and architectural features of the five historical mosques (the Fatih Mosque, the Beyazit Mosque, the Mihrimah Mosque and the Rüstem Pasa Mosque, the Sehzade Mehmet Mosque) built in the classical ottoman architecture era in order to have detailed information about historical development of the structural features of the Sehzade Mehmet Mosque and then, I studied on the structural characteristics of Sehzade Mehmet Mosque. The three dimensional finite element model of the Sehzade Mehmet Mosque was constructed in order to investigate the linear structural behavior of the mosque under static and dynamic conditions. Natural frequencies were obtained by the modal analysis of the Sehzade Mehmet Mosque and then, the analysis of the improved model under a scenario earthquake for Istanbul was carried out.

2. HISTORICAL SURVEY

Figure 2.1. The Ottoman symbol [3]

Classical Period (1437-1703) is the era when one single and large inner space was being searched for religious architecture and a single dome was tried to cover this inner space. Monumentality is the major feature in architecture of this period. The major examples of structures of which many types appeared, are: Edirne Three Galleries (of a minaret) Mosque, Fatih Group of Buildings, Bayezid Group of Buildings, Sehzade Group of Buildings, Suleymaniye Group of buildings, Edirne Selimiye Mosque, Kanuni Tomb, Rustem Pasha medresse, Koprulu Library, Bayezid Bath, Mahmud Pasha Inn and Cevahir Drapery Market. Mimar Sinan, Mimar Davut and Mimar Kasim are the important arhitects of the time [2].

2.1. The main features of the mosques built in Istanbul, in the classical ottoman architecture era

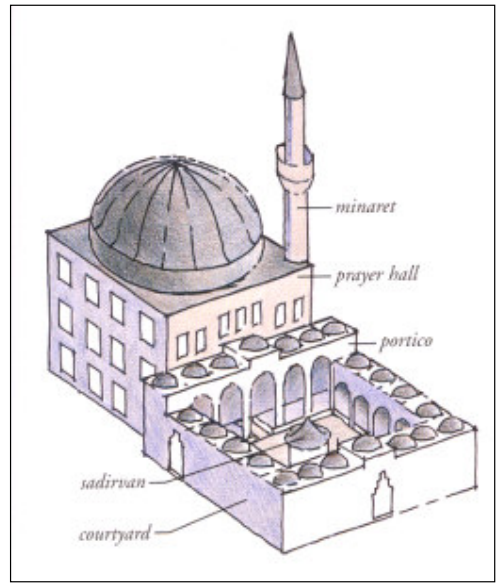

Figure 2.2. General view of a mosque built in the era [3]

The spiritual centerpiece of the entire complex were the mosques, and the heart of the mosques were their prayer halls. There were a number of absolute requirements, the most important of which was that the front wall, or kibla wall, of this room must face Mecca. When praying, the congregation would assemble in rows parallel to and facing the kibla wall and in turn the holy city and its most important shrine, the Kaaba. At floor level in the center of the kibla wall was the mihrab-a niche symbolizing the entrance to paradise [3].

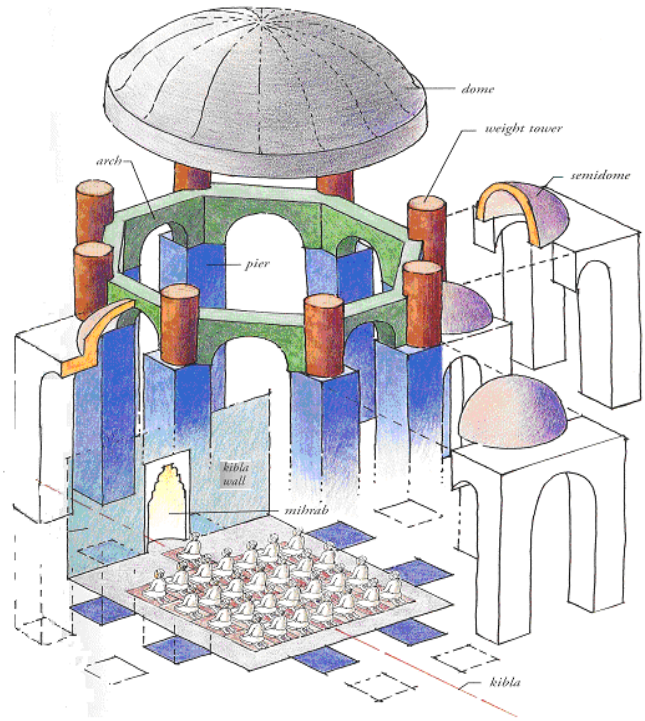

Figure 2.3. General parts of a mosque built in the era [3]

It was from in front of the mihrab that the imam would lead the congregation in prayer. The kibla itself is an imaginary line that points toward and radiates from Mecca. The kibla wall was placed perpendicular to the kibla, and the mihrab stood right on top of it. Directly opposite the mihrab was the portal—the main entrance to the prayer hall. Protecting the portal outside and providing covered space for latecomers to Friday services was a high portico, and beyond it an arcaded courtyard. In the center of the courtyard stood the sadirvan—the fountain at which the faithful would wash their hands and feet before entering the prayer hall. Like the mihrab, the main portal and the sadirvan also stood on the kibla.The last and, next to the dome, the most recognizable element of the mosque was the tall minaret, from which the faithful would be called to prayer five times a day [3].

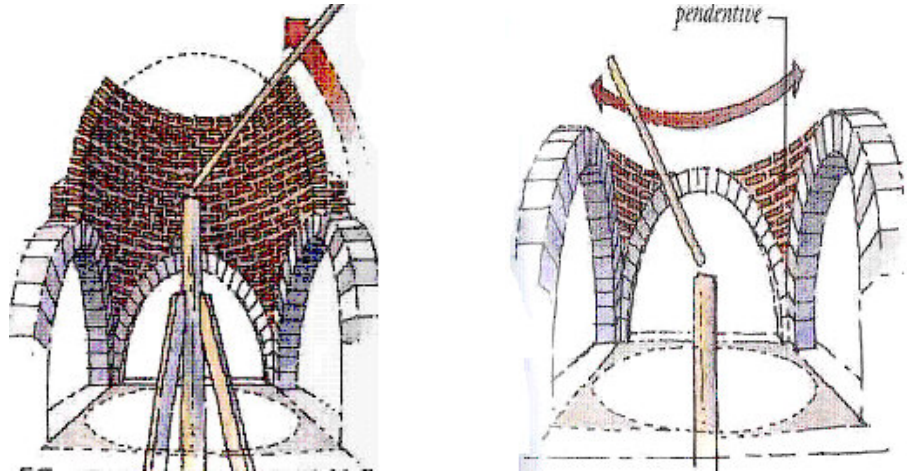

Figure 2.4. Views of dome and pendentive during construction stage [3]

There was no separation between architecture and engineering. There were two basic problems, both of which involved the use of the dome. The first was one of geometry. How does one support a circular roof over a square room without filling the space with walls or columns? The solution that had evolved over the years was a system of piers and arches. The piers were placed either in corners or around the perimeter of the square, and the arches tied them together. Not only did this arrangement create a suitable base for the dome above, but the space below the arches remained open and unobstructed [3].

The second problem was one of structure. Because of the dome's hemispherical shape, there are hidden forces within it trying to push the sides outward. While piers and arches could easily be designed to support the great weight of a masonry dome, they could not, on their own, counteract its self-destructive tendencies. Architects reduced some of these forces by strengthening the sides of the dome, where it was most vulnerable. Then, to channel the remaining forces safely down through the piers and walls to the foundations below, they added extra weight to the tops of the piers and buttressed the arches with a symmetrical arrangement of semidomes [3].

2.2. Historical background and architectural features of the Fatih Mosque

Figure 2.5. Aerial view of the Fatih Mosque [20]

This was the first great Turkish complex to be built on an urban scale in the city after the conquest. The patron was Mehmet (Fatih) (1451-1481) himself. Construction of the complex took place between 1463-1470. Architecturally it is one of the most well integrated and successful groups of buildings of its type on that scale [20].

The site of the mosque was originally that of a church (Hagion Apostolon) during the Byzantine period, and the site of the imperial cemetery. Excavations carried out during the building of the mosque revealed the tombs of the emperors, which were transferred to the courts of Topkapi Palace and are now in the Archeological museum [4].

The architect Atik Sinan built the largest complex in Ottoman Art History. The complex consisted of medreses, kervansaray, hamam, a hospital, baths, a kitchen for the poor, a library, and a koranic school. The complex has been preserved in its original form

[24]. The original mosque was destroyed in the great earthquake of 22 May 1766. Mustafa III undertook its reconstruction and the present building was completed in 1771. The mosque has a very large central dome 26 meters in diameter. The painted decoration is fussy in detail and dull in color. The mihrab is from the original building. In the graveyard, behind the mosque, are the tombs of Sultan Mehmet and his wife Gulbahar [4].

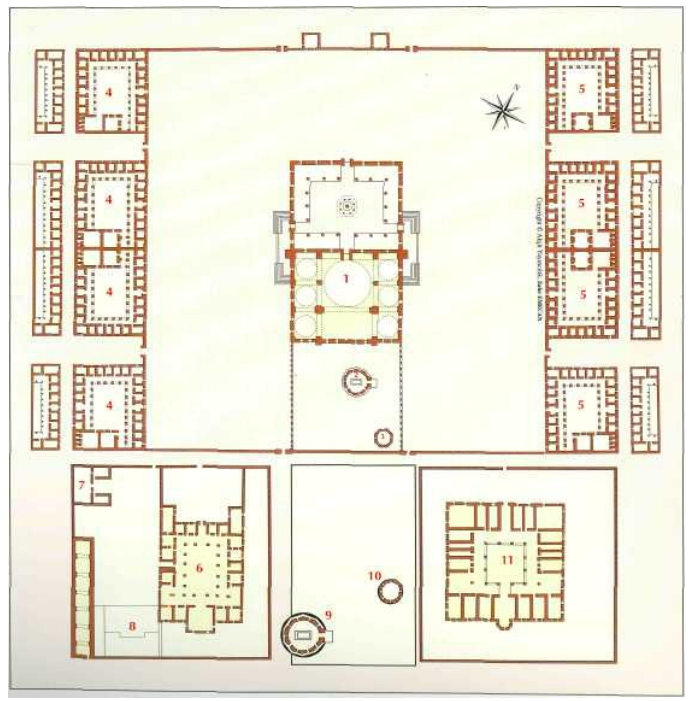

Figure 2.6. Plan of the Fatih Complex [4]

Sultan Mehmed II conquered Constantinople, and he converted the Church of Hagia Sophia into a mosque and also ordered another such structure to be built in his name. The decision was made to build the mosque in Fatih, one of the seven hills of Istanbul. Situated on this site was the Church of the Apostoleion which was constructed by Justinian in the 16 century. But that sacred church was in a state of ruin when the decision was made to construct a complex in its stead in the mid-l5th century. This complex consisted of a mosque, soup kitchen, school of theology, small hospital, hospice, caravanserai, library and baths. Today's Shoemaker Market is in one of the buildings belonging to the complex whereas its mosque is accessible through Çorekci Kapi and Boyaci Kapi from

the west and Çorba Kapi from the east [20]. An inscription above the entrance gate tells us that the architect of the mosque was Atik Sinan, that he started construction in 1470 and finished it three years later. However, the complex was restored by Bayezid I following an earthquake in 1509. The dome of the mosque collapsed in the 1766 earthquake and Mustafa III later ordered the architect Mehmed Tahir Aga to restore it [4].

The frontal court of the mosque is original, as are the faience panels over the windows of the mosque. The court is surrounded by a colonnade arcade, in which 18 granite columns support 22 cupolas. The main dome of the mosque is flanked by four semidomes and four cupolas flanking them. The main dome rests on arches separated by four piers [4].

The mosque had large entry hall with a tall dome supported by a semi-dome of equal radius over the mihrab and three colossal arches on the remaining three sides. This ensemble was flanked by three domed bays to the east and west and was entered through an arcaded courtyard to the north. Three wings of the original courtyard have remained to our day. The new mosque by Mustafa III has also incorporated the portal, the mihrab and the lower shafts of the minarets belonging to the original structure [4].

The new mosque is slightly wider than the old one and has a tall central dome held by semi-domes on all four sides in ways that resemble the classical mosques of the sixteenth century. Four small domes complete the corners of the pyramid-like space. The plan, oriented 32 degrees east of south, is wider than it is deep and is equal in size to the open courtyard that precedes the mosque [4].

The courtyard has one main and two side entrances. The main portal is located to the northwest, on axis with the entry to the mosque and the ablution fountain at the center of the courtyard. It is adorned with seven rows of stalactites inside three arches. The side entrances, with cascading steps on the outside, are located where the courtyard gallery meets the taller portico of the mosque. Windows placed low in each bay of the gallery creates visual connection between the mosque courtyard and the lower grounds. The gallery columns are carved of granite, white marble and green stone. The tympana of each window is adorned with Koranic inscriptions in white and green marble on the precinct

side. Ceramic tiles other inscriptions decorate the tympana of two windows inside the mosque portico [4].

The central dome, supported by two elephant piers and two porphyry columns in the old structure, is carried on four large piers that section the interior space. The decorative painting of the interior reflects the baroque influence on 18th century Ottoman architecture. The original Fatih Mosque had two minarets with single balconies. They were rebuilt with two minarets after the earthquake, incorporating the old foundations and the lower shafts. The minarets were refurbished in empire style during the 19th century; their stone spires were replaced by lead spires in 1965, with no alteration to the balconies. The mosque is currently under restoration to repair damage caused by the earthquake on August 18, 1999 [4].

The center of this monumental mosque is covered with a dome which is 26 m. wide and 44 m. high whereas four semi-domes surround the main dome. Arches holding up the great main dome and semi-domes are supported by four large elephantine pillars. These arches separate the center from its sides as well. The top of its sides are also covered with three smaller domes supported by high columns. Thus, the mosque has a vast area measuring 2400 m2 without any divisions. Its niche was constructed in colorful marble, whereas the original architectural style of the inner courtyard in front is still maintained. It is covered with 22 domes supported by 18 columns of granite and Egriboz marble. It is accessible through three doors, two of which are on the sides and the other is in front [4].

2.3. Historical background and architectural features of the Beyazit Mosque

Figure 2.7. Aerial view of the Beyazit Mosque [21]

Beyazit, son of the Conqueror Mehmet II had it built the mosque of Beyazit in 1501-1505. It is one of the classical examples of Ottoman Architecture. Again, the architect of Beyazit Mosque looked to the Ayasofya, employing a central dome buttressed by semi-domes and a long nave with double arcades, although the mosque is half the size of the church. The Beyazit Mosque also borrows elements from the Fatih Mosque, imitating the system of buttressing and the use of great columns alongside the dome. Thanks to Sultan Beyazit II's patronage, the Ottomans found a style of their own, which served as a bridge to later classical Ottoman architecture [9].

The sultan, who died in 1512, is buried at the back of the gardens. The placing of the courtyard and the gates reflect the Selçuk influence; the arcades of the courtyard rest on

20 columns of green and grey granite, the white marble capitals and the marble stalactites depending from them, are in the Turkish style; the 24 cupolas rising from the columns follow the encircling line of the monument. The interior of the mosque is simple in plan, being a variation on that of Saint-Sophia. The central dome is supported by two half-domes which themselves rest on two solid columns. These columns, 6 meters in height and 1 meter 40 cm in circumference, are made of Egyptian porphyry [9].

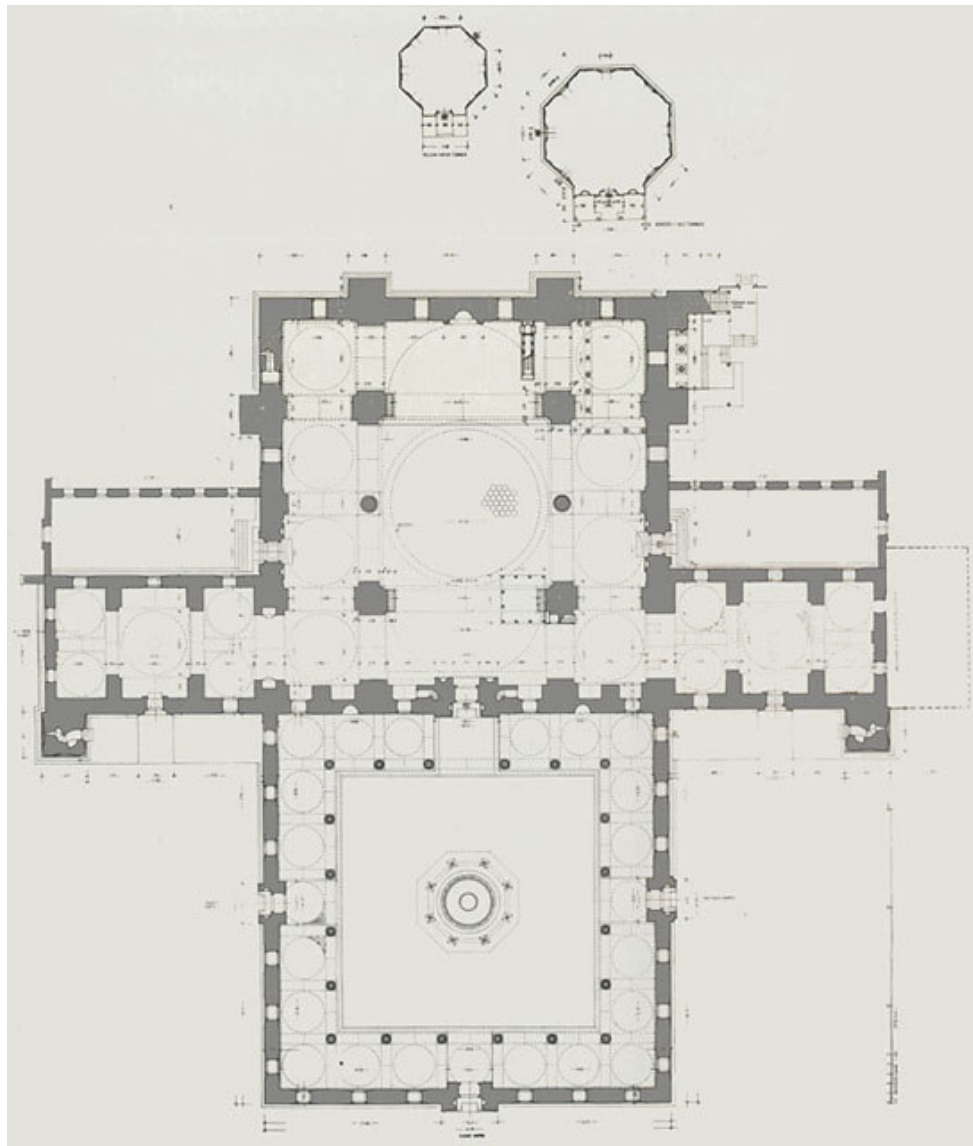

Figure 2.8. Plan of the Beyazit Mosque [5]

The buildings of the complex are placed without any apparent order on the large site, with no traces of an outer precinct wall. The soup-kitchen, caravanserai, quranic school and the tombs are clustered around the mosque to the west, while the madrasa and the baths are separated out, positioned about 120 and 250 meters to the west of the mosque respectively.

The mosque dome was partially rebuilt after the 1509 earthquake, and Mimar Sinan conducted repairs in 1573-74. The minarets were burnt separately in 1683 and 1764 and the dome was repaired again in 1754. An inscription above the northeast courtyard entrance suggests that repairs were also conducted in 1767. A restoration is currently under way at the mosque, while the madrasa, baths and quranic school were restored at different dates to house library and museums [5].

The structure of the Bayezid mosque is considered a stepping stone between early Ottoman architecture and classical Ottoman architecture, characterized by a central dome held by semi-domes on all four sides. Although the mosque is constructed entirely of cut stone, colored stones and marbles appropriated from Byzantine ruins were used throughout the exterior and interior to highlight the architecture, such as red porphyry columns marking entrance bays along the courtyard arcade. Muqarnas carvings embellish all capitals and portals, the mihrab niche and minaret balconies.

The minbar, the sultan's lodge and the women's section, which is a balcony placed above the prayer hall entrance, exhibit the fine stone latticework of the period and the original wood carvings can be seen on doors and windowpanes.

The Mosque of Beyazid II, designed by Hayreddin, is the first building in which new achievements within an independent tradition can be seen. In its use of space, the mosque is very similar to the Church of St. Sophia. The dome is supported by two half-domes and two arches. The pendentives connect the dome with the walls [6].

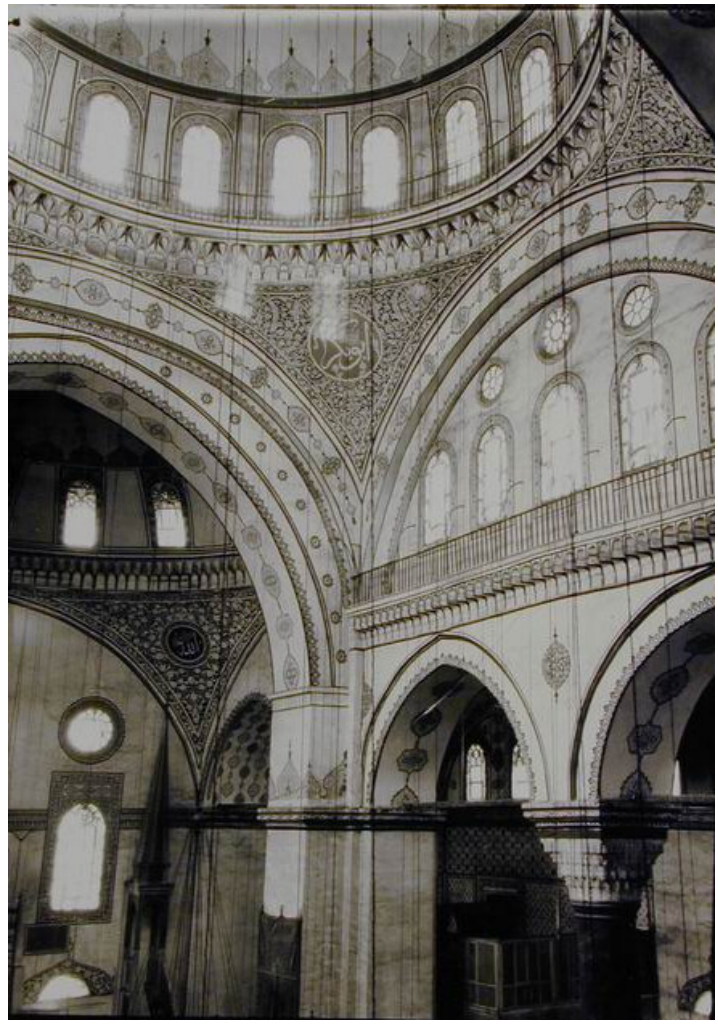

Figure 2.9. Interior view of the Beyazit Mosque [5]

If one compares this design with that of St. Sophia, it appears that similar forms have produced different space-effects. The fusing of spherical forms which had been so easily achieved in St. Sophia by doing away with clear outlines, are altogether avoided in. the Beyazid Mosque. In St. Sophia there is a single transition from the large arch to the half-dome. No outline points clearly to the principal supporting arch. In the Beyazid Mosque, however, massive arches hinder the effect of effortless suspension. The half-dome is, moreover, slightly raised by a concealed tambour. The dome of St. Sophia is a pure hemisphere, and viewed from beneath, it seems even more as though it were about to open at its outer edges. Compared with the Beyazid dome it appears complete and self-contained. A further essential difference between the two interiors is the way in which the aisles supplement the central hall. The aisles, galleries and adjoining rooms of St. Sophia

form a darker surround to the bright central hall. Between lightly polished columns and capitals, these rooms seem to stretch away to infinity. The limits of the Beyazid rooms, however, are clearly visible, and supplement the central hall. The general effect, therefore, is that of an undivided interior, a solid, unmoving mass. The architect of the Beyazid Mosque stresses outlines. The emphasis on the solidity of a single element of building is not tectonic; and here, Hayreddin remains faithful to the new style begun in Bursa. Pillars, arches, pendentives and the small lateral arches seem to have been fused [6].

An examination of Sinan's mosques will show us that Beyazid is still in the early stages of stylistic conflicts, and is therefore not altogether divorced from stylistic conflicts. Hayreddin's genius is evident wherever he creates within his own tradition, in the Beyazid complex in Edirne, and in the courtyard of the Beyazid Mosque in Istanbul. Indeed, the style here of his windows and portals later became an established pattern.

2.4. Historical background and architectural features of the Edirnekapi Mihrimah Sultan Mosque

Figure 2.10. Exterior view of the Edirnekapi Mihrimah Sultan Mosque [22]

The Mihrimah Sultan Mosque is also designed by Mimar Sinan. It was built in 1562-5 for Mihrimah Sultan, the daughter of Suleyman the Magnificent. The mosque is filled with an abundance of light since it has 161 windows [7].

The architect Sinan, in his Mosque of Mihrimah in Edirnekapi, Istanbul, achieved a strong and singularly effective architectonic expression by indicating the curved form of the pendentive on the exterior. Furthermore, he pushed in the walls and opened a great many large windows in them to obtain a screen-like quality in order to emphasize the essential structural nature of the big arches where pendentives are used. The pendentive is meaningful when the dome sits on four arches and not on walls. In a single-unit building which has a strict cubic form the use of pendentives results in a misleading geometry. Turkish triangles or squinches are more appropriate transition systems, since they define the relationship between the walls and the dome in a straightforward manner. The Ottoman Turkish architect seems to have sensed this aesthetic subtlety. The early architects did not use pendentives in their solidly built square structures. When they did adopt the pendentive, they did not consider it simply another structural system but developed it into an element of visual appeal both within and without [8].

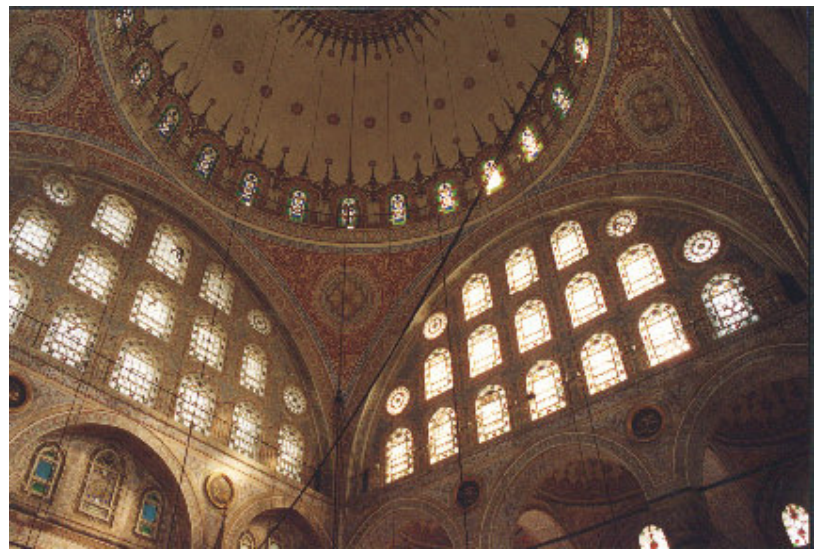

Figure 2.11. Interior view, looking up pendentives and dome [22]

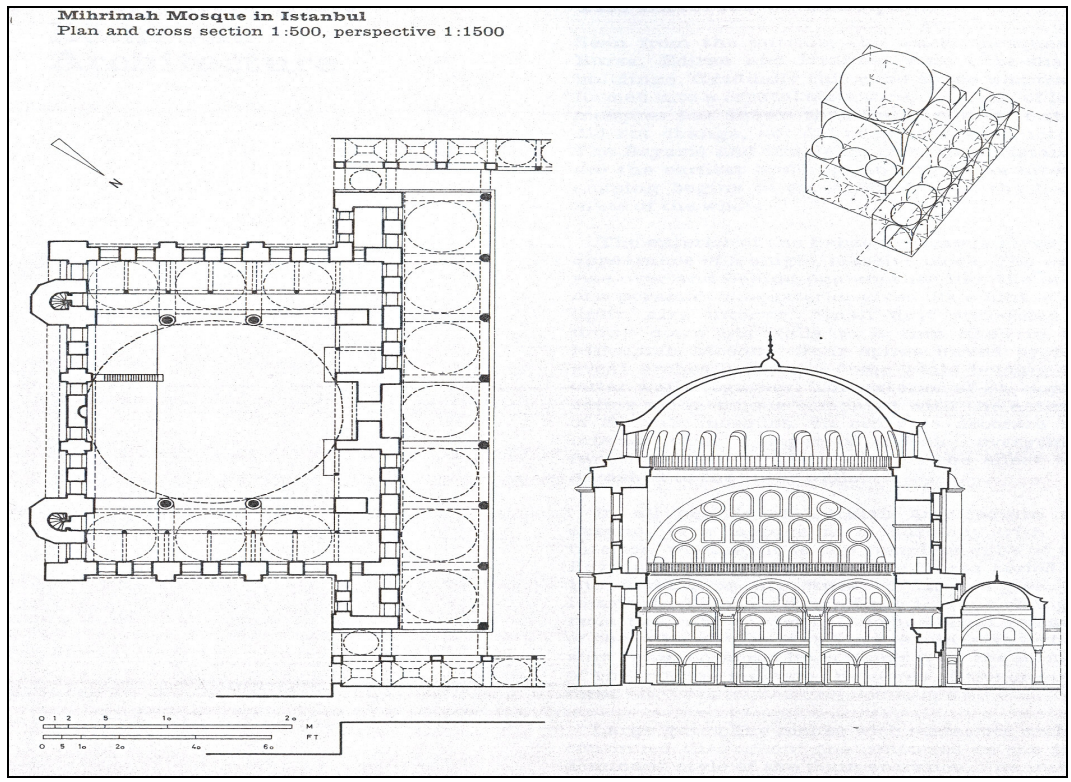

Figure 2.12. Plan of the Edirnekapi Mihrimah Sultan Mosque [6]

This mosque is unprecedented with its supporting system and dome. Four arches that spring from four piers hold up the dome, which has an astonishing height (35 m.). There are very narrow, domed aisles on the east and west sides of the building. These aisles do not lend a support to the covering system. In addition to this drawback in the supporting system, the four tympana (:walls filling the arches) are excessively fenestrated through three layers of windows ,which render the walls transparent curtains. The qibla wall below the southern tympanum also contains windows. On the inside, two rows of double granite columns bear the thrust of the eastern and western tympana. They also separate aisles from the domed central area. On the other hand, the southern and northern tympana are not buttressed any way [8].

The 39.50 by 28.00 meter prayer room of the Edirnekapi Mihrimah Sultan Mosque is surmounted by a central dome, 20.25 meters in diameter, flanked on each side by three 6.00 meter domes in a row [7]. Inside the hall, the low triple domes press down on two granite columns with stalactite capitals. In between these the lofty central dome on

pendentives rises on four piers which turn into weight towers above the cornice level of the walls to rivet the four great arches of the square baldachin. The clarity of the mosque's central structural system is, in one sense, the outcome of the logical relationship between the weight towers and the great arches. In another, it is due to the visual impact the great arches produce by being pulled out from the many-windowed walls. The receded screen walls which only support their own weight give the load-bearing arches a structural definition. It is true that Sinan stressed the great arches earlier in the Suleymaniye Mosque; but within the context of the complicated superstructural system of the Suleymaniye this architectonic subtlety was often lost [8].

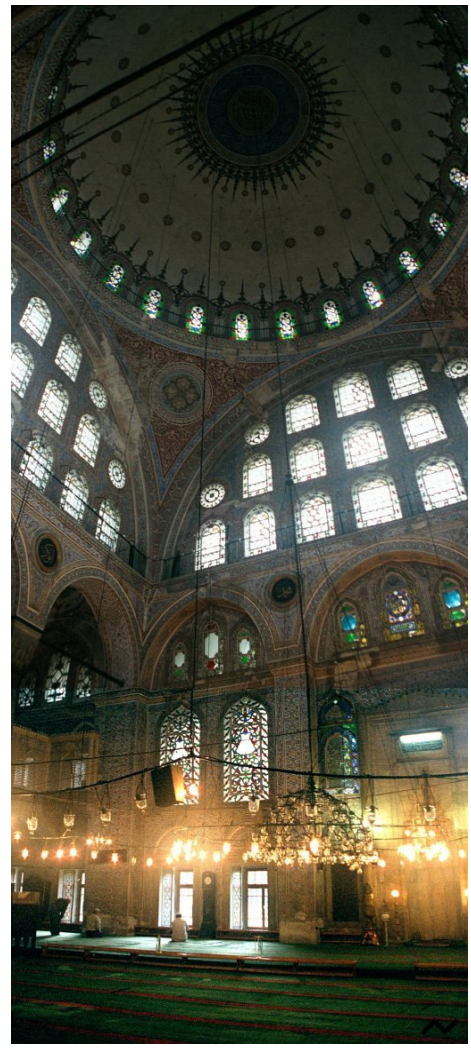

Figure 2.13. Interior view, looking up pendentives and dome [22]

In the Edirnekapi Mihrimah Sultan, on the other hand, by making almost a separate entity of the central dome through exaggerating its height, and also by contrasting the heavy solid arches with the lace-like curtain walls on four sides, he achieved a dramatic architectural expression which the eye cannot ignore. This single domed mosque on a square based plan is simpler than some of Sinan's earlier mosques. Protruding corner piers support broad arches, equal on all four sides, which carry the single dome.

The Edirnekapi Mihrimah is a spacious and well-lighted mosque. It contains three tiers of windows on the walls of its prayer hall: twenty-six at ground level, thirty above these, and forty-eight on the third row, totaling one hundred and four in all. An additional seventy-six windows are located inside the great arches: seven each on the fourth and fifth rows and five on the sixth, on all four sides. With the twenty-four encircling the drum, the number of windows in the mosque reaches two hundred and four altogether [8].

Figure 2.14. Interior view of the Edirnekapi Mihrimah Sultan Mosque [22]

The Mihrimah Mosque was the next major building in which Sinan attempted to solve the same problems, but from another angle. He had used four half-domes in the Sehzade Mosque, but here he does away with them altogether. Four narrow, arcaded walls, interrupted by windows, and four spherical spandrels effect the transition from the cube-like central hall to the dome. Sinan also restricts the use of old Turkish elements — stalactites, for example, are confined wholly to the pillar capitals. In this building he attempted to improve on Byzantine structures (arcaded walls and pendentives). The walls in the Mihrimah Mosque appear very distinct when compared with those in the Sehzade Mosque. Hard, sharply defined edges stress the various areas and transitional points. Also strongly reminiscent of St. Sophia is the way in which corners are treated — the vaulted corner arches have no visible means of support. Yet the artistic effect of these analogous treatments of the corner is not the same [6].

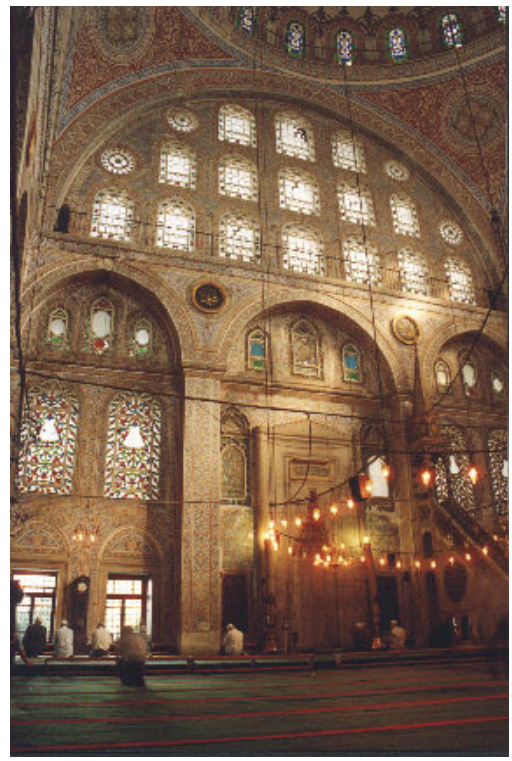

Figure 2.15. Interior view of the Edirnekapi Mihrimah Sultan Mosque [22]

The shell of the Mihrimah Mosque does not appear to float like a 'weightless bell.' On closer observation we realize that Sinan has used the same principle of structure as in the Sehzade Mosque. There is no differentiation between vault, pilaster and walls. The spandrels and arches do not differ from one another; the surface of the vaults merges immediately into the shape of the dome. If we were to imagine that all those parts which fill in the shell were removed, the remaining arches and walls beneath would not form a skeleton that would stand up on its own. No single part of the system of walls could be subtracted — all the parts must be there for the building to have any unity [6].

The Edirnekapi Mihrimah Sultan Complex included besides the mosque, a madrasa, a school, a turbe, a double hamam, and a long row of vaulted shops in the substructure of the terrace on which the mosque and madrasa share a common courtyard. These shops have been torn down, but the main buildings have survived. The Edirnekapi Mihrimah Sultan Mosque has suffered damages in the earthquakes of 1640, 1690, 1719, and 1894. In 1719 its domes collapsed. After 1894, it remained derelict for many years before the Ministry of Pious Foundations undertook its reparation. Upon the proclamation of the Second Constitution in 1908, however, the work was discontinued. It was not reactivated until 1956 when the mosque was extensively restored and saved. Despite a few amateurish mistakes such as the theater-set kind of back wall of the demolished shops facing the square on the east, the 1956 restoration was, on the whole, successful. It was proper that the external side galleries and the outer portico had not been rebuilt because the available clues provided by the stone consoles on the side walls would have been insufficient for an accurate reconstruction. The tie-beam sockets in front would likewise have produced an imaginary outer portico. The only thing one can be certain about the double portico of the Edirnekapi Mihrimah Sultan Mosque is that, unlike its counterpart in the Uskudar Mihrimah Sultan Mosque, it did not embrace the inner arcade on three sides, but screened it front ally, much like an awning [7].

2.5. Historical background and architectural features of the Rustem Pasha Mosque

Figure 2.16. Exterior view of the Rustem Pasha Mosque [23]

In 1560, Rüstem Pahsa, Grand Vizier of Sultan Süleyman the Magnificent, commissioned Mimar Sinan to construct The Rustem Pasha Mosque in Tahtakale (The Period after the Suleyman Mosuque) that is renown for its tiles. Four years after the completion of the Suleyman Mosque (156O) Sinan began work on the Rustem Pasha Mosque, and here revealed a new style. The mosque was donated by the Vizier, Rustem Pasha, husband of Princess Mihrimah. The plan of the mosque is very similar to that of the Mihrimah Mosque : a square central interior with aisles, each of which consists of three cross-beamed vaults. However, these rooms differ considerably in their structure and especially in their relation to the dome. We find no half-domes of the same diameter as the central dome nor walls of equal size throughout. These Byzantine forms are no longer in evidence, and while the forms employed are not new, they are smaller and are part of a new method of construction [4].

Figure 2.17. Interior view, looking up pendentives and dome [4]

The dome of this rectangular-plan mosque is stands over eight columns, four of which are octagonal and independent, with the other four are set on eight pillars which rise along the north and south walls. Measuring 15 m. in diameter, the dome is supported by four semi-domes and four arches. The interior of the mosque is divided into three sections. The large spherical spandrels (see the Mihrimah and Süleyman mosques) are now replaced by smaller half-domes. The semi-circular bases of these domes are connected to the walls by means of stalactites. Supporting walls fill the space between two such walls. The transition from the square to the dome is therefore achieved by an octagonal area, with walls supported by four more equally sized walls and half-domes. In this way we have a facetted transitional area. By replacing, the pendentives with half-domes, Sinan achieves more consistency in the interior of the mosque. As original Byzantine forms were abandoned, so other reminders also disappeared. Earlier Turkish elements, especially the stalactite, again begin to play an important role. Pillars merge into the background [4].

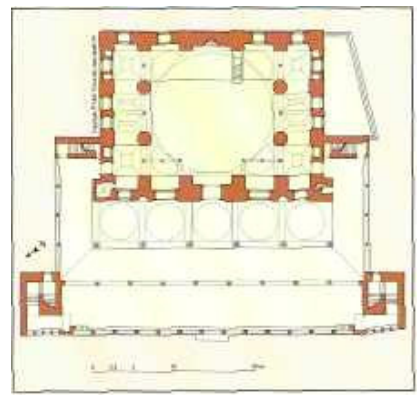

Figure 2.18. Plan of the Rüstem Pasha Mosque [4]

Figure 2.19. Interior view of the Rüstem Pasha Mosque [4]

Large, octagonal pillars, covered with tiles, already suggest the octagon from below. No capitals, but only a few stalactites on the corners are connected with the vaults. In this way, the sharp-cornered prismatic pillars appear so strongly merged that

the openings of the vaults appear to have been hollowed out. The new method of the transition to the dome makes a lower height for the inter- mediate zone possible. The half-domes at the corners connect the dome with the walls in a more rigid manner than the spherical spandrels. As the result of the effect of these details, the room gains a more solid and compact form. Three large windows on top of each other illuminate the interior and increase the effect of the wonderful tiles. All the walls of the mosque are decorated with tiles up to the skirts of the dome. These tiles are samples of the brightest period after red had been discovered in Iznik tile. It is observed that very rich and various motifs were used on these tiles. For instance; we can see 44 different tulip motifs. The elephantine pillars are adorned with tiles as well. Thus, the mosque bears the quality of a museum exhibiting 16th century Iznik tiles. The facade of its last outer congregation hall is also embellished with these tiles whereas the two niches on both sides of the entrance are adorned with tiles on the inside and outside. Covered with tiny domes, this section is separated by six columns into five smaller sections. Its single minaret is erected to the left of the mosque [6].

2.6. Historical background and architectural features of the Sehzade Mehmet Mosque

Figure 2.20. Aerial view of the Sehzade Mehmet Mosque [4]

“ The Sehzade Mosque is a work of art belonging to my apprenticeship days” Mimar Sinan [4]

The Prince's Mosque (Şehzade Camii) was built between 1543 and 1548 by Sinan to commemorate the memory of one of Süleyman's sons, the crown prince Mehmet. Although it has been debated how and when Sinan was commisioned the complex, it is his first large scale commision after he has been appointed as the 'chief architect'. Some sources indicate that he was asked by the prince himself, to start working on the plans and then, after his death Suleyman wanted the complex to be built. Other sources assert

that the complex was originally started for Suleyman himself, and was then converted to be in the name of Mehmet upon his death. Sinan handled the Mosque as a piece to commemorate the Prince, with a fresh approach [4].

Figure 2.21. Interior view, looking up pendentives and dome [4]

The decade stretching from 1538 to 1548, then, was a period in which Sinan developed his architectural skills by utilizing well-tested schemes to broaden his outlook. Sinan's own evaluation of the Sehzade Mehmed Mosque as the work of his "apprenticeship" shows that he regarded his first ten years in the Office of Chief Court Architect as his period of maturation. Needless to say, the Sehzade Mehmed Mosque was a striking monument to end the first phase of a promising career. It appealed to the eye, satisfied the mind, and elevated the spirit. It was a fitting climax to this phase because,

with an uncanny sense of timing, Sinan produced this orderly and well-balanced design as the Ottoman Empire reached the height of its power. To the beholder the symmetrical formation of the Sehzade Mehmed Mosque was symbolic of the political might and social harmony that the Ottoman State had achieved. Sinan was not content in externalizing the appearance of the mosque; he decorated its facades with great care to maximize the visual impact [4].

He combined two squares in plan, one for the courtyard, and one for the mosque itself. This original composition was not only the outcome of Sinan's experiments with architectural forms, but perhaps of his wish to come up with something new for the young Prince. He created a heavenly interior; full of light and a peaceful courtyard suurounded by a moderate portico. The complex was completed in 1548. Sehzade complex is situated between Fatih and Bayezid complexes. It stood on a flat site looking onto both the Golden Horn and Marmara Sea. However today, it has been surrounded by dense urban tissue that it is impossible to see neither the Horn, nor the sea. The complex consists of the mosque, the tomb of Prince Mehmet (which was built prior to the mosque), school, madrasa, kitchen for the poor and the caravansarail. The mosque and its courtyard are surounded by a wall that seperates them from the rest of the complex [7].

The Sehzade Mosque, which is the first major work of the architect Sinan, like the Bayezid comprises two equal squares as courtyard and prayer hall plus two graceful minarets, which adorn the corners where the two squares overlap. The prayer hall is crowned by a 19.OO m. dome that rises to a height of 37.OO m. at the center. Four halfdomes, augmented by two exedrae each, distend the central dome to rest on the outer walls. Smaller domes on the four corners complete the general composition of the upper structure. It must be observed that the piers to which the direct load of the central dome is transmitted through pendentives are treated in the Sehzade Mosque as lightly as possible to allow the space to move around them without visual obstruction. The objective of the sixteenth-century Ottoman architecture was no longer a compartmented, rigid mosque composed of recurrent domed-square units, but a spatially articulated and structurally complex mosque highlighted by a major dome descending through halfdomes, exedrae, and smaller domes It reached for a rational architectonic expression which was achieved by the mid-sixteenth century through the genius of Sinan. The

Ottoman ideal is perhaps best expressed in the Mosque of Sehzade, which I consider the zenith of the evolutionary pattern of the Ottoman multi-unit mosque [9].

Figure 2.22. Interior view, looking up pendentives and dome [21]

It portents the structural perfection aimed at by Sinan in mosque architecture. The work of this period is not only the most famous, but also some of the most daring and creative in Ottoman architecture. Sinan learned a great deal from Byzantine models like Hagia Sophia, but he also attempted to go beyond them. Beyazid Mosque was the first attempt to break away from Byzantine tradition; forty years later Sinan encountered problems that his predecessor had only touched on. With this building, Sinan begins his break with Byzantine architecture. Yet Beyazid Mosque enabled Sinan to ascertain how

far Byzantine styles could be adapted. In each of the three large mosques which Sinan built over the next fifteen years, he used variations on the scheme of St. Sophia. In the Sehzade Mosque, the symmetrical axes which form the Church of St. Sophia are translated into a form consisting of symmetrical points related to a center. The plan of Sehzade Mosque is symmetrical and central. The Sehzade Mehmed Mosque consists of two adjoining square masses — one closed, the other open — rivetted together by two minarets.This building could therefore be considered as an intermediate step, where Sinan is still experimenting with his new forms. In the Sehzade Mosque, Sinan had already been successful in transforming the stylistic character of early Ottoman architecture [6].

Figure 2.23. Interior view of the Sehzade Mehmet Mosque [21]

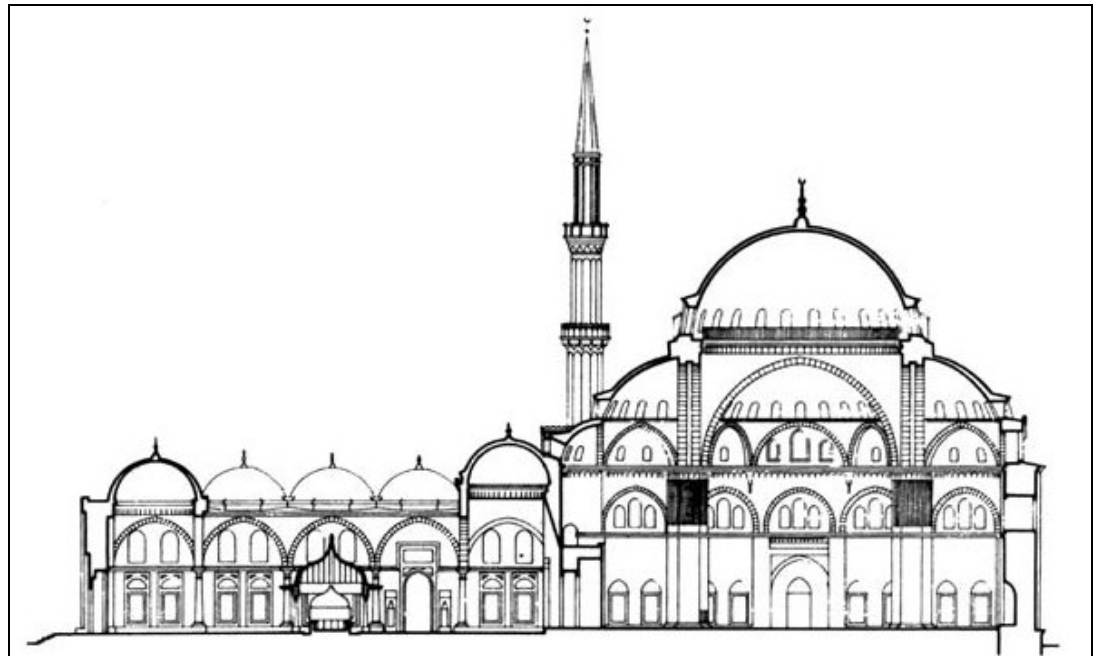

Figure 2.24. Plan section of the Sehzade Mosque [6]

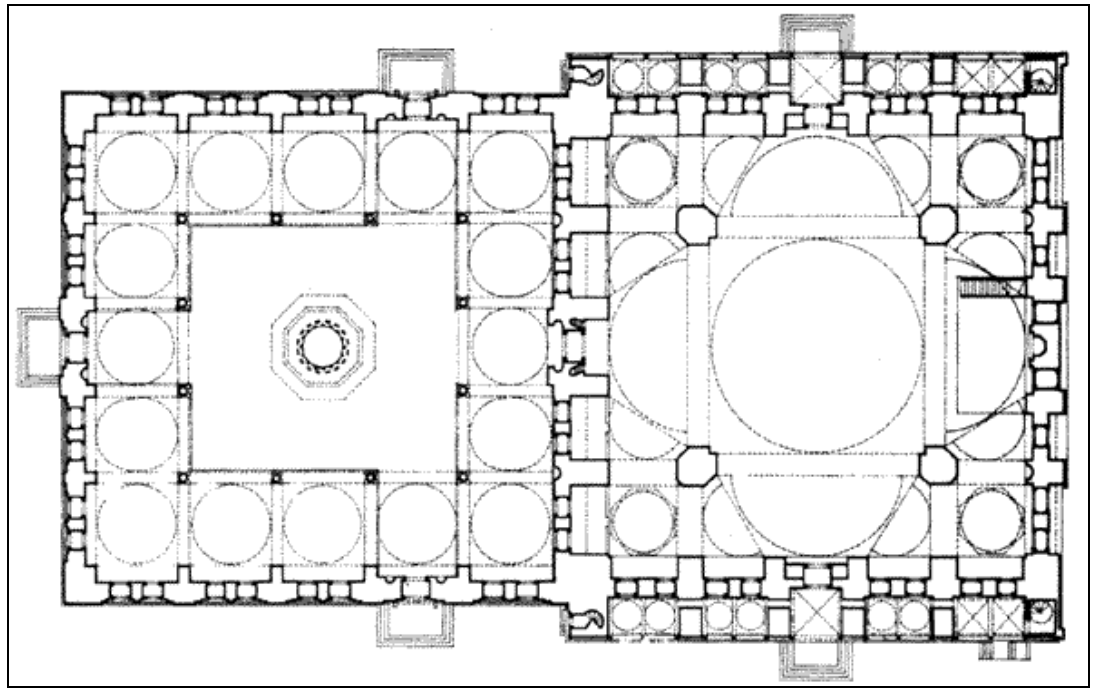

Figure 2.25. Plan section of the Sehzade Mosque [6]

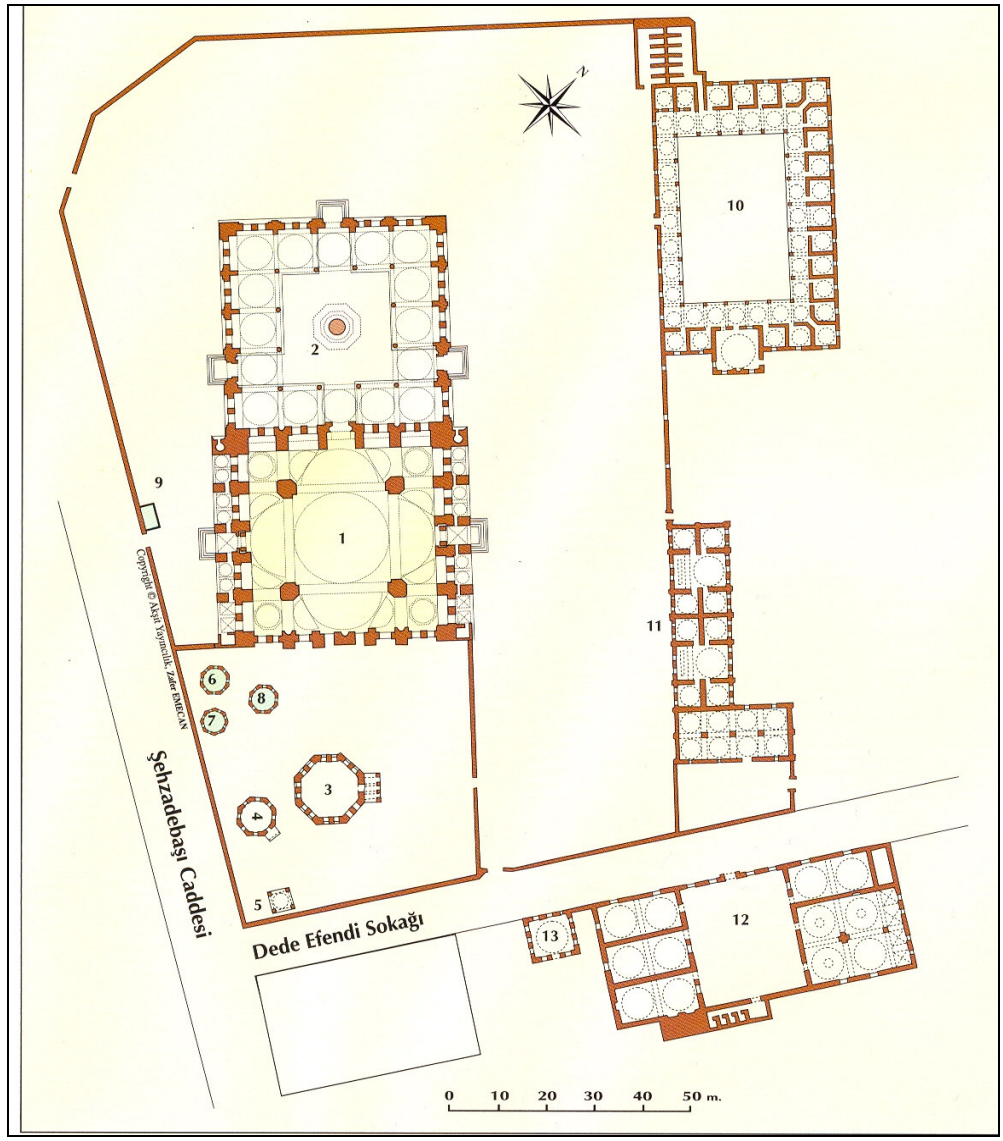

Figure 2.26. Plan of the Sehzade Complex [4]

1. Mosque; 2. Courtyard; 3. Tomb of Sehzade; 4. Tomb ofRustem Pasha; 5. Tomb ofFatma Sultan; 6. Tomb of Ibrahim Pasha; 7. Tomb of Hatice Sultan; 8. Tomb of Prince Mahmud; 9.Tomb of Destari Mustafa Pasha; 10 .School of Theology; 11. Hospice; 12. Caravanserai 13. School

The dome of Sinan's building forms the starting-point of the whole structure. From here the arches and smaller half-domes radiate outwards. The various components extend from the top to the bottom. They all form such a closely knit unit that it is impossible to distinguish at first sight just where, in this complex of spherical shells, the stress lies; whether the dome is supported by the arches and the latter by the pillars, or whether the dome itself supports everything [6].

These pillars, side arches and external walls together form an indissoluble unit. Sinan also tries to reduce the area between pillars and the effect of weight by stalactites. The use of stalactites between the walls and domes continues around the pillars and serves as a further connection between pillars and walls. The fluting on the upper part of the pillars draws attention to the downward bearing stress of the dome [6].

The mosque has a square plan, covered by a central dome, buttressed on four sides by semi-domes. The central dome is supported by four arches resting on four piers, and has a diameter of 19 meters and it is 37 meters high. Based on a square plan, the Sehzade Mehmet Mosque measures 38 m. x 38 m. in area and has a front courtyard. This hierarchical superstructure sits on walls that are fortified by five buttresses each. The drum has 24 windows. A similar treatment in the courtyard, which displays closely-set double two-tier windows on its three sides and the minarets, whose shafts are decorated with vertical. The court is surrounded by an arcade covered with 16 cupolas, linked together by arches supported by 12 columns. The structure and style of the mosque are totally innovative, employing features then as yet unknown in the Ottoman capital. This mosque is accessible through three gates [8].

Sinan has worked out a 5*5 modular plan, dedicating 3*3 area to the dome, to make the centrality more effective. Moreover, he has tried to make the piers more slender. Yet, the piers in Sinan's later mosques, are integrated more into the interior, sort of vanishing in the space and decoration. Whereas, in Sehzade Mosque, as it is the first large scale mosque by Sinan, the piers are still massive and visible. Transition from the piers to the dome is handled by four large arches. The arches have alternating rhytm of stones that add up to the interior decoration of the mosque. The exterior of the Sehzade Mosque gives the appearance of a single, massive block. The walls rise over and behind one another like

the steps of a pyramid. The exterior gives little hint of the light, airy interior [6].

As the structural system depends on the piers, arches, the dome and the semi-domes, the walls are freed of load and thus are perforated as much as possible to let daylight in. Its marble niche is skillfully decorated whereas the muezzin quarter is a very elegant piece of art and is propped up by eight columns. Mimar Sinan did not use tile in all parts of the mosque, but rather preferred to embellish the dome with calligraphy. Thus, it has quite a plain design. The mosque has two 41.1 m. high minarets with double balconies whereas the exterior of the minarets are adorned with relief decorations. The Sehzade Mehmet Mosque set the benchmark for architects of other mosques to follow after Mimar Sinan [4].

3. DESCRIPTION OF THE STRUCTURAL SYSTEM OF THE SEHZADE MEHMET MOSQUE

3.1. Superstructure

Early Ottoman buildings with domes (14'th and 15'th centuries) were based, either on the concept of a single dome of medium size covering the whole inner space or, on the series of small domes one neighboring the other at the same level. In both solutions, thrusts and seismic actions would thus be laterally transmitted to the massive exterior walls or piers. On the other hand building technique of Ottomans' had been improved during the sixteenth century by allowing the construction of masonry components in any curved, sophisticated geometry [27]. The structural elements of The Sehzade Mehmet Mosque are composed of:

- Domes
- Transition Elements(Elements used to pass from circular geometry to the polygon one; pendantives)
- Arches
- Counter Weight Towers
- Piers
- Walls and the buttresses
- Foundations

The plan of Sehzade Mosque is symmetrical and central. The mosque has a square plan (the interior, 38 meters long and 38 meters wide), covered by a central dome, flanked by four half-domes. The dome is supported by four piers, and has a diameter of 19 meters and it is 37 meters high. The mosque has two 41.1 m. high minarets with double balconies and the exterior of the minarets are adorned with relief decorations [4].

Sinan has worked out a 5*5 modular plan, dedicating 3*3 area to the dome, to make the centrality more effective [6]. Transition from the piers to the dome is handled

by four large arches. The arches have alternating rhytm of stones that add up to the interior decoration of the mosque. The dome is circled at the top of the arching system by a ring of 24 windows.

Due to the existence of these windows, the cross section of the dome and the short columns among the windows are enlarged. The circular base of the dome is transferred to the square geometry via the four decorated pendantives. The main four piers with huge and humble shape are connected to exterior buttersses via the double arches, at an elevation of 10 meters from bottom. The counter weight towers sitting on the top of the main piers have intended to provide lateral supports. But it is also believed that Sinan used these towers for architectural reasons.

3.2. Foundations

Little is known about the foundation system of the Sehzade Mehmet mosque. Some boreholes have been made in the different places around the mosque. The bores showed that the clay-silt and grovak layers were laying 8-10 meters below the ground level [10]. This means that there is approximately eight meters of thick fill layer exiting on the top of the rock. Unfortunately there is no significant and realistic study performed for the identification of the foundations of the mosque.

3.3. Construction materials

The structure is mainly constructed by stone, brick and mortar. Mortar was used as a conjuction material of stone blocks and bricks. The major part of it such as; main piers, arches, internal secondary arches, buttress piers, and walls are made of stone block masonary. The domes are made of brick masonary and covered by lead. Strength limit values for the masonary structure in compression and tension are taken as 15 Mpa and 1,4Mpa, respectively [1]. The stones used in the construction were mainly supplied from the mines in Istanbul and nearby regions and called "kufeki". The art of using this material can be observed on the sevaral historical edificies built by Sinan [25].

Among the various types of stones Architect Sinan used, the most widely used one

is küfeki stone the results of the tests of which is reported as following;

Table 3.1. Main characteristics of kufeki stone [12]

Definition: Limestone with high level of porosity and fossilation
Sources around İstanbul: Bakırköy, Sefaköy, Halkalı, Hadimköy, Sazlı Bosna
Physical Characteristics:

- Unit weight : 2.19g/cm^3
- Porosity : %12.6
- Water absorbtion (by weigth) : %5.70
- Water absorbtion (by volume) : %11.08
- Capillarity : 4.93.10-6 (sample of 3 months)
- Average weight loss during freezing and thawing : %0.28

Chemical Composition : %54.37 CaO, %0.22 Fe_2O_3, %0.39MgO, %0.34SiO2, %0.11 H_2O, %43.44 CO_2+H_2O

Historic mortars are complex systems formed of a binder material (aerial or hydraulic lime,gypsium), a variety of passive and active aggregates and some inorganic or organic additives (fibers,milk,pozzolan,white of eggs and others) to improve the mechanical strength of the mortar. The most important structural charactersitic of these materials used in mortar is that they increase the tension capacity of structural elements [13]. The historic mortars, in general, do not fit modern standards as their aggregates very ofen contain a considerable amount of fine components and also relatively high proportions of the mortar and bricks used in their masonary [13].

Previous structural studies to determine the earthquake worthiness of monumental buildings in Istanbul like Hagia Sophia have shown that the monuments' static and dynamic behaviour depends strongly on the mechanical and chemical properties of the mortar and bricks used in their masonary [13].

4. STRUCTURAL ANALYSIS BY FINITE ELEMENT METHOD

4.1. Structural model properties

The numerical model used for Sehzade Mehmet Mosque is created by Sap 2000 package program. Sap 2000 is a general purpose finite element analysis system which incorporates facilities for: linear and non-linear; natural frequency, buckling, spectral response, time history response; thermomechanical analyses.

Taking into considerations the complexities in preparing a three dimensional model of such a complicated structure by using Finite Element Method, one needs to make some simplifications and assumptions by using engineering judgment.

The main problem encountered in the preparation of the model, is the lack of technical documentation on Sehzade Mehmet Mosque. There are plenty of explanations in the references about the construction and the employment; but not enough technical information. There exists some architectural drawings in Vakıflar Library. But, they do not match exactly with the structure. The dimensions of the mosque were determined through an on-site study and the available simple sketches.

Sehzade Mehmet Mosque measures 38 m. x 38 m. in area. The height from the ground level to the top of the main dome is 37 meters [4]. The span between the two elephant feet is 17.50 meters. The height of the elephant feet from the ground level is 16.00 meters. The height of the main arches is 10.80 meters.

The finite element model consists of four elephant feet, four main arches, secondary buttress piers, secondary arches, the main dome, four semidomes and exedraes (on both sides of the semidomes) and four domes in the corners are included in the model. All piers, arches and pendatives were modeled by using solid elements and all domes and exedraes were modeled by shell elements. The size and complexity of the structure created a model consisting of 7739 joints, 2024 shell elements and 3064 solid elements.

Since little information is available about the boundary conditions, no special work was carried out for foundations. In the finite element model, piers are assumed to be fixed one meter below the ground level.

The structure is made of stone, brick and mortar. The elephant feet, butresses, arches are made of stone. All the domes are made brick and covered by lead.

Although there is no precise information about the material properties of the structure, the following material properties given in the table 4.1. are obtained from different researches previously made on Suleymaniye and Hagi Sophia [13], [14], [15].

Table 4.1. Material constants used in the finite element model [13], [14], [15]

	ELEMENT TYPE	MODULUS OF ELASTICITY (kN/m^2)	UNIT WEIGHT (kN/m^3)	POISSON RATIO	THICKNESS (m)
Arches	Solid Elements	850E+4	21 .9	0.20	
Piers	Solid Elements	850E+4	21.9	0.18	
Main Dome	Shell Elements	300E+4	20	0.18	0,5
Pendatives	Solid Elements	300E+4	20	0.20	
Semi domes	Shell Elements	300E+4	20	0.18	0,7

Shell elements used for modelling of domes have a three or four-node formulation that combines separate membrane and plate-bending behaviours. It activates all six degrees of freedom at each of its connected joints, 3 of them being in translation and the other 3 in rotation. The forces, moments and stresses at nodes are shown below [16], [17].

Maximum principal stress (Smax) shows generally tensile regions, i.e. positive. On the other hand, minimum principal stress (Smin) shows generally compressive regions being negative. Directions of the maximum and minimum principal stresses do not depend

on directions in either global or local axes [17].

Each shell element can be quadrilateral or triangular as shown in Figure 4.1. The positive forces and the moments are seen in Figure 4.2.

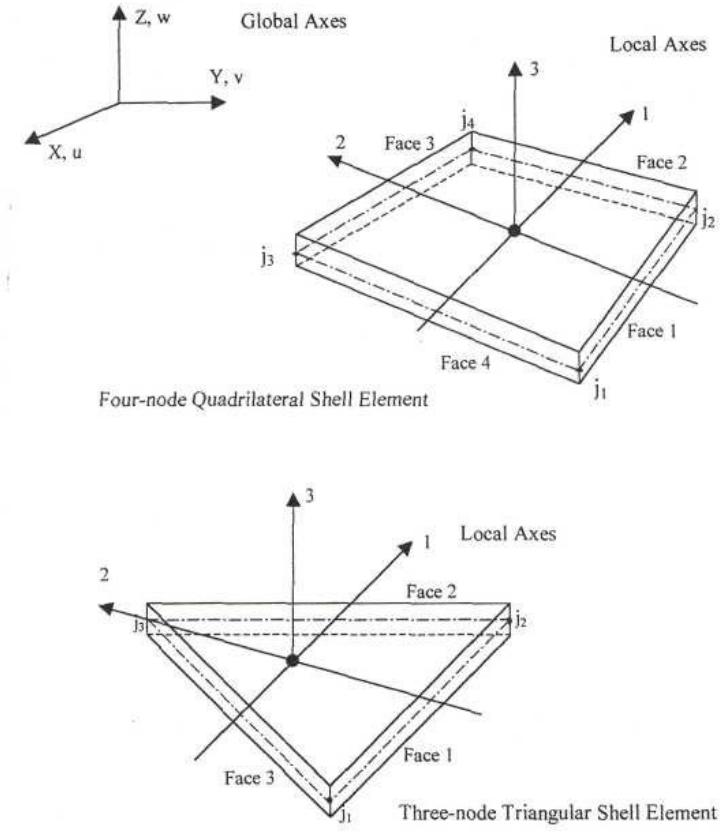

Figure 4.1. General types of shell elements [17]

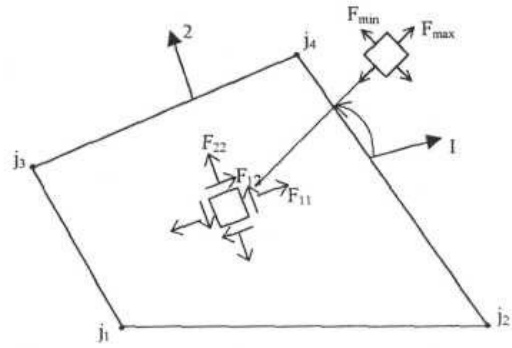

Membrane Forces

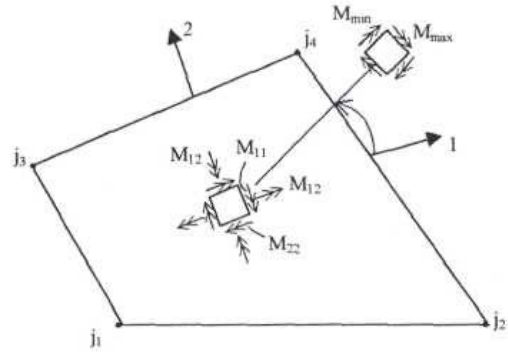

Plate Bending and Twisting Moments

Figure 4.2. Forces and moments in shell elements [17]

The solid element is an eight-node element for modelling of three-dimensional structures and solids. Solid elements are used in the case that frame or shell elements cannot represent the structural elements because of either the geometry of the structure or the location of the material. They are called according to their node numbers; hexahedral having 8 nodes, pentahedral having 6 nodes and tetrahedral having 4 nodes (Figure 4.3). Generally hexahedral solid elements are used in modelling of the structure in this study, while pentahedral elements are chosen in modelling of the pendentives. Tetrahedral elements are not used in the models considered in the study.

The local coordinate system for each Solid element is identical to the global system. The local coordinate system is used for defining material properties and loads, and for interpreting output. The Solid Element models a general state of stress and strain in a three-dimensional solid. All six stress and strain components are active for this element [17]. The forces, moments and stresses at nodes are shown below (Figure 4.3):

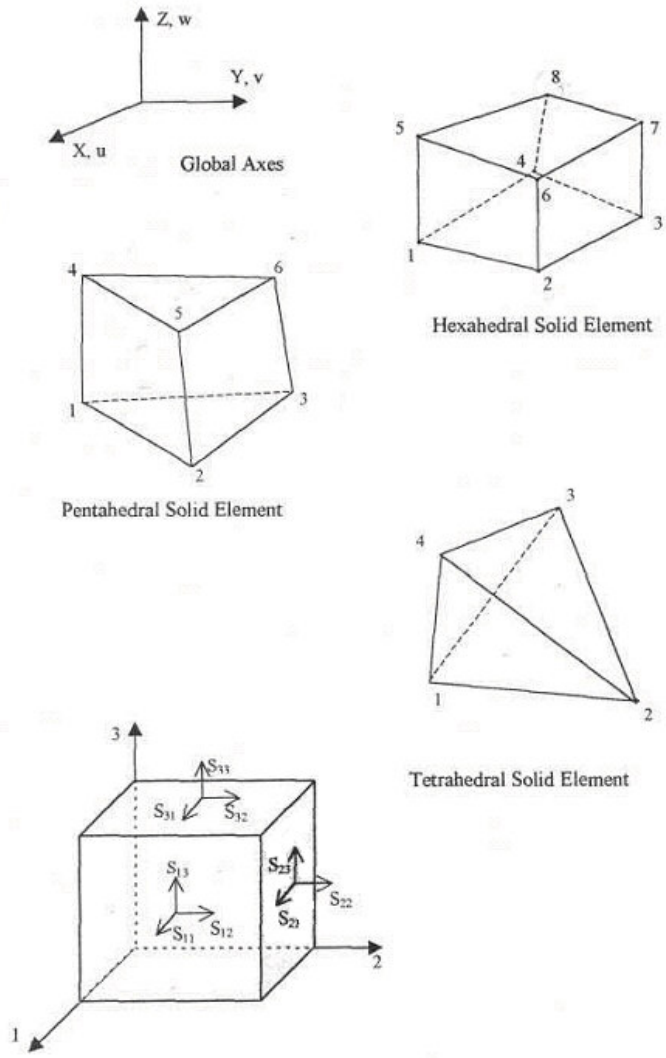

Figure 4.3. Solid elements [17]

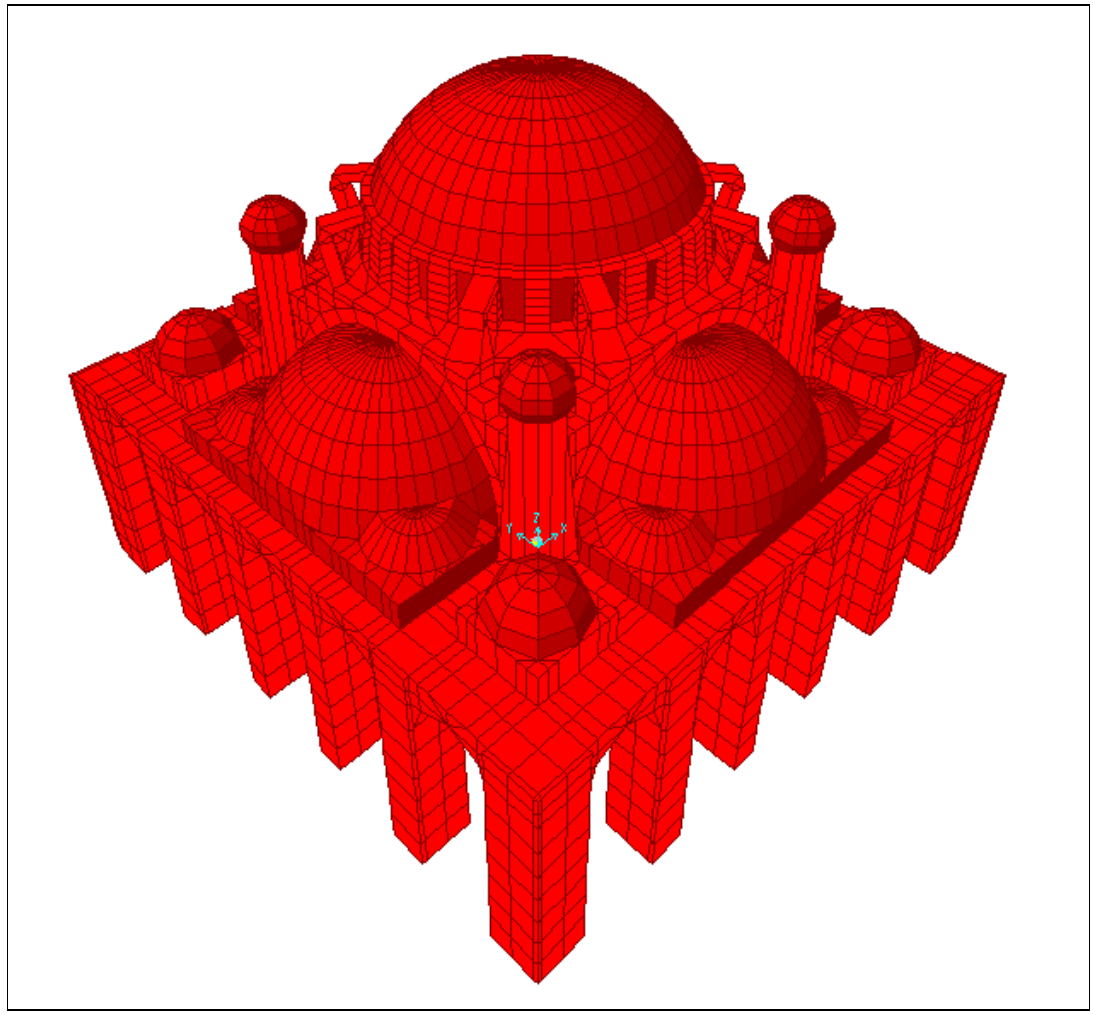

Figure 4.4. General 3-dimensional view from south-east

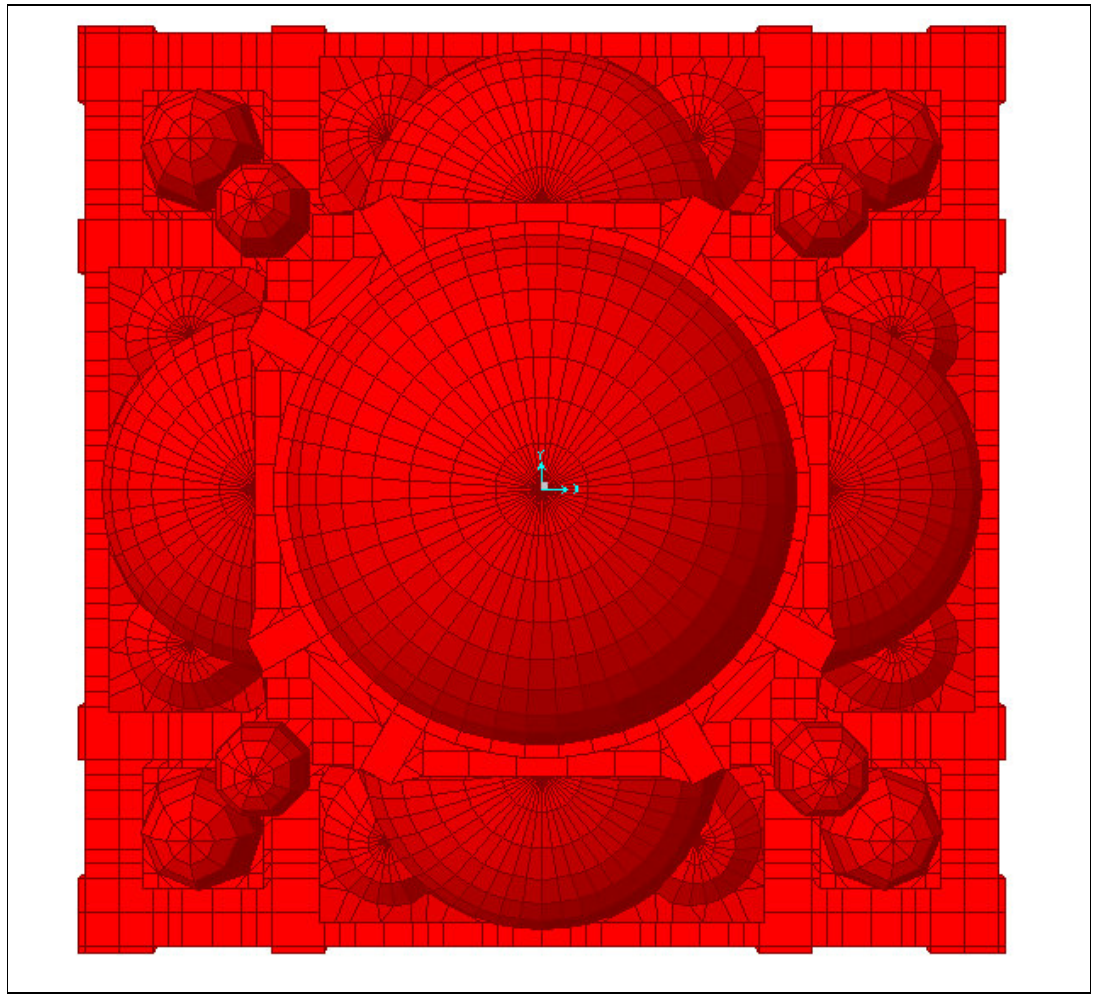

Figure 4.5. General view from top

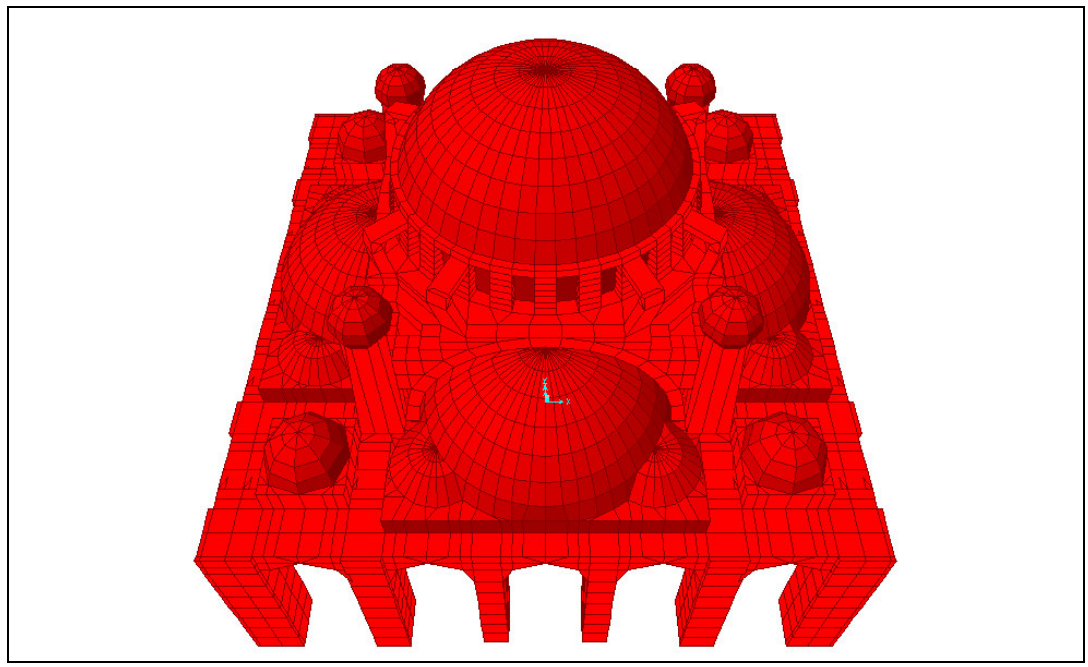

Figure 4.6. General view from east

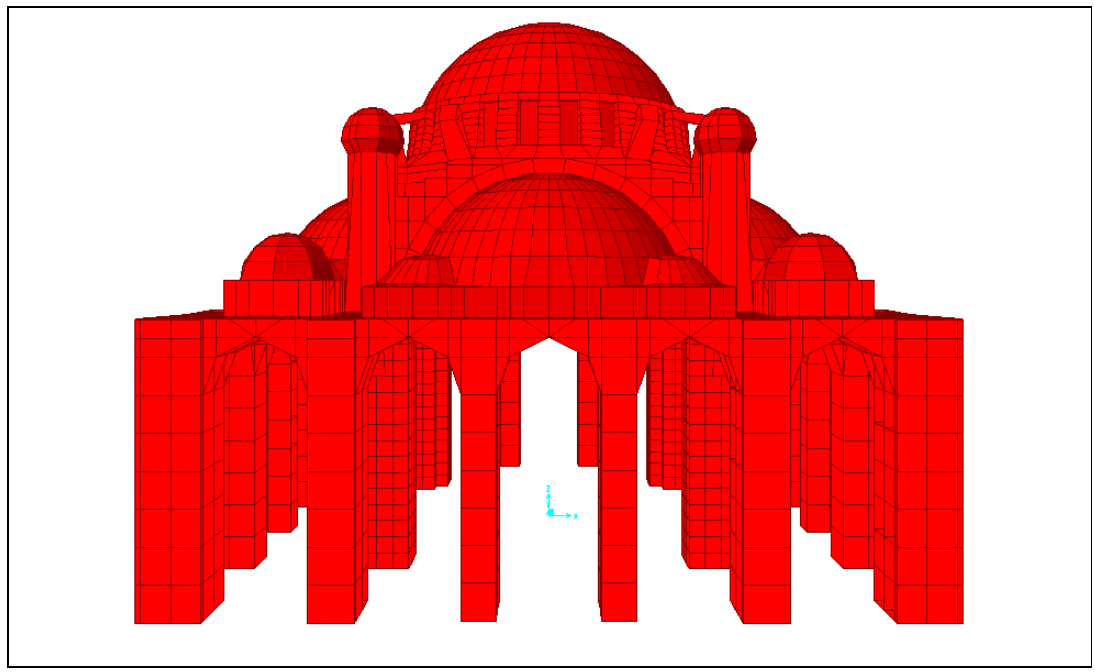

Figure 4.7. General view from east

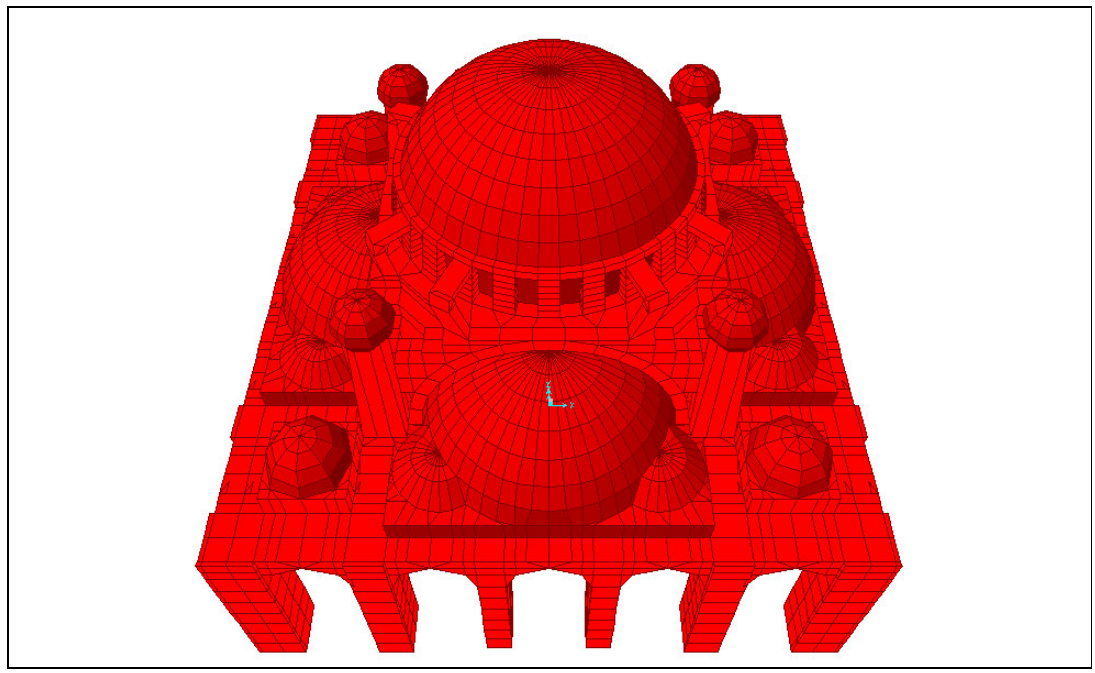

Figure 4.8. General view from north

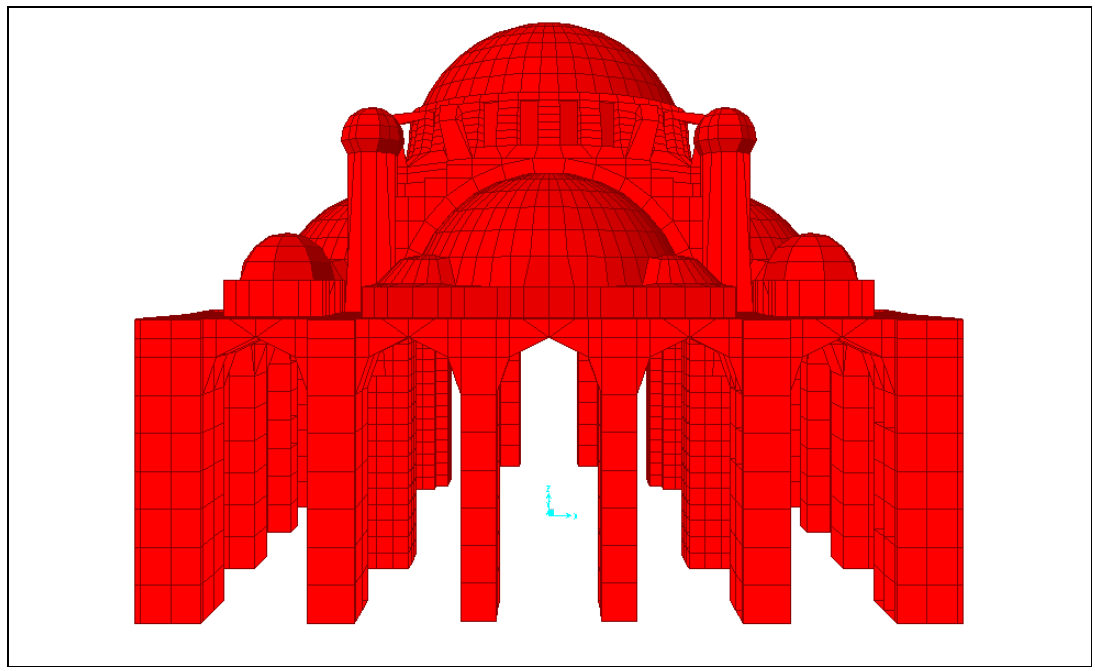

Figure 4.9. General view from north

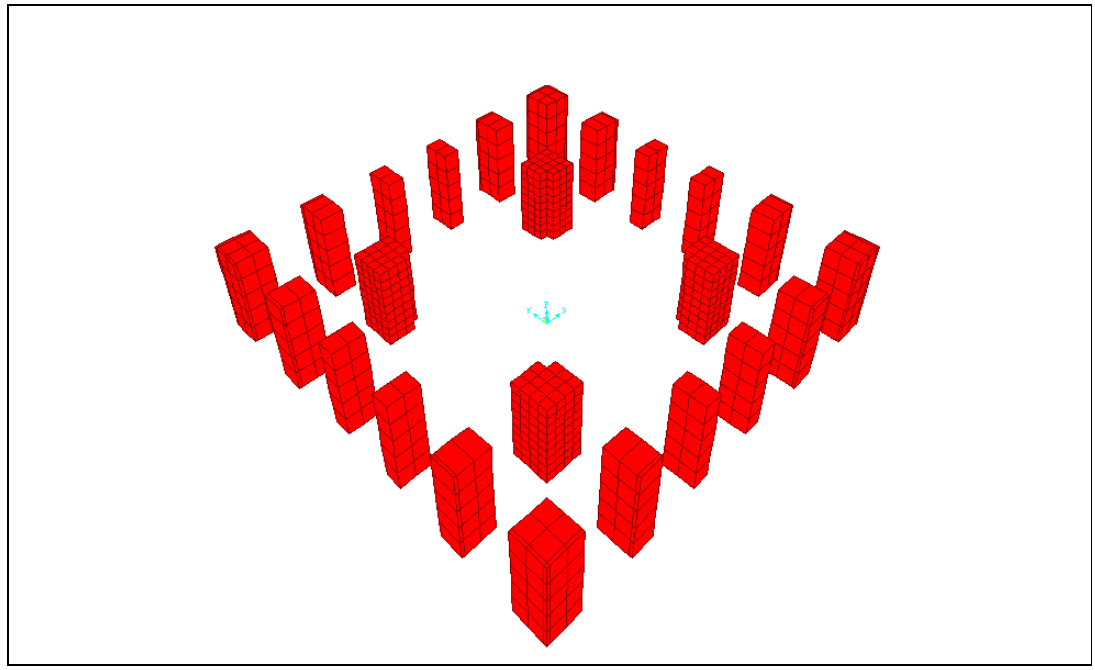

Figure 4.10. General view of the piers upto the middle

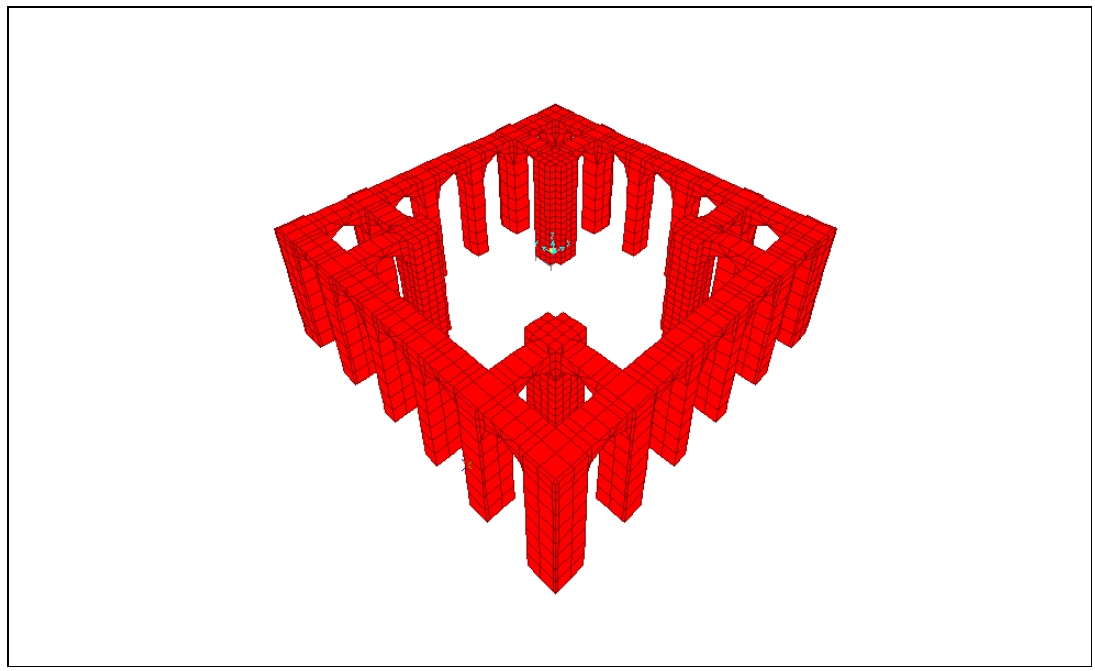

Figure 4.11. General view of the whole piers

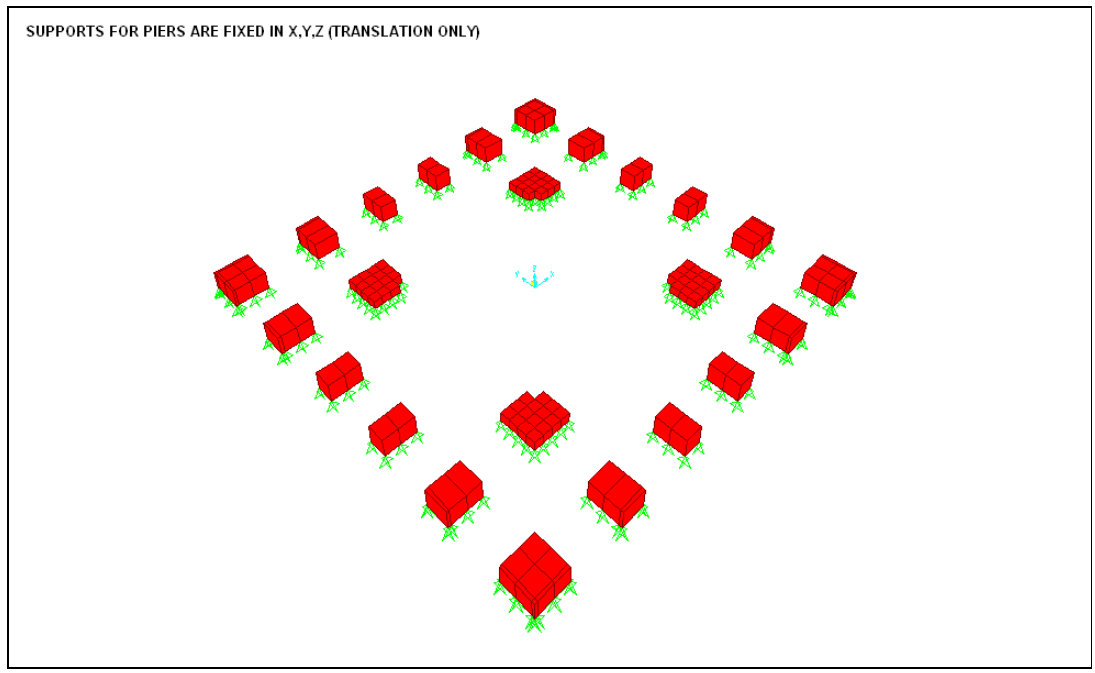

Figure 4.12. Position of supports

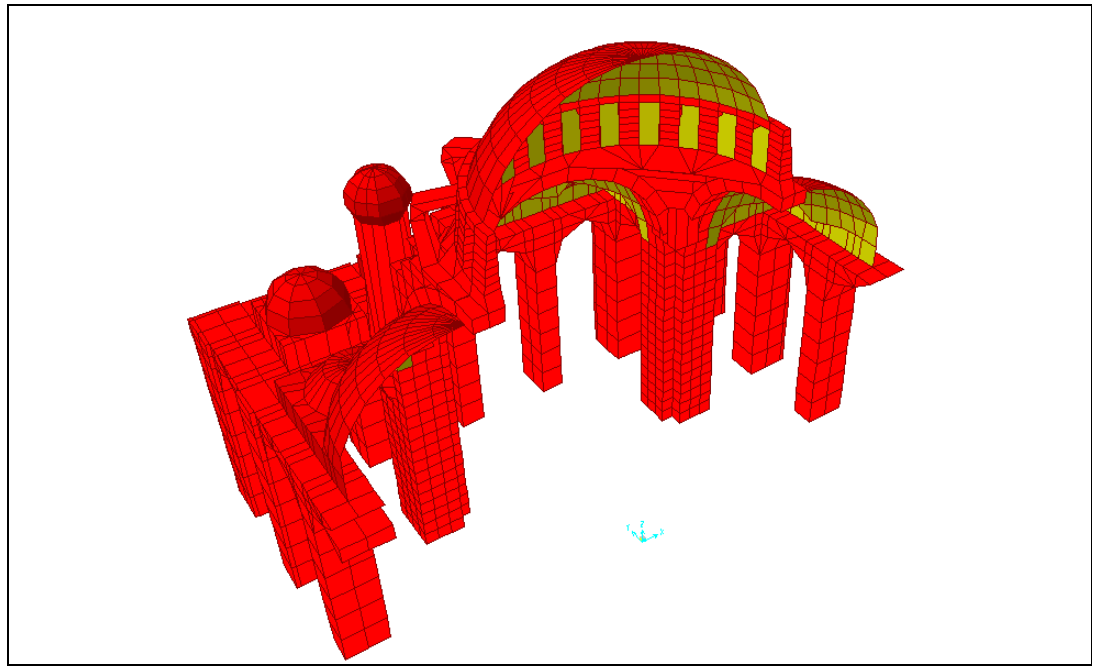

Figure 4.13. General 3-dimensional view In the half of model

5. STATIC ANALYSIS

5.1. Analysis under the self weight

The earthquake analysis necessitates the structure to be investigated under its own dead loads. For linear static analysis, it is assumed that the loaded body instantaneously develops a state of internal stress so as to equilibriate the total applied loads. The main aim from static analysis is to investigate;

- the possible stress distributions
- the deflections and possible crack locations on the structure

From the site inspeciton, it has been concluded that there is no major cracks existing on the structure. In other mean, all parts of the structure are in good condition.

In the static analysis, for deformations SAP2000 uses the linear equation system shown below:

$$[K]\{u\} = \{R\} \tag{5.1}$$

Where [K] is the stiffness matrix; {u} is the displacement vector; and {R} is the vector of applied loads. Equilibrium and compatibility equations can be used to calculate the global stiffness matrix [17].

The three dimensional view of the deformed structure is given in Figure 5.1. The resultant deformations of the linear static analysis are shown in Figure 5.1 to 5.6. The deformations predicted by this model are the deformations that would occur in a linear elastic homogenous system under its own weight. One should keep in mind that the deformations obtained from the model analysis are linear short term deformations. Whereas, the actual ones are long term and non-linear deformations combined with those caused by the experienced earthquakes.

Figure 5.2 shows deformations in global Z direction in meter with displacement contours. Dark areas indicate the higher values of deformations. In Figure 5.2 to 5.6, it can be easily observed that the deformations mainly concentrates in the middle are at dome and arches. The maximum vertical displacement computed from the static analysis of the model is 5,6 mm at the center of the main dome.

The second important point that should be drawn from the static analysis is the stress distributions. The following interpretations may be made for the stress experienced by the structure under dead load (See Figure 5.7 to 5.21).

The stresses under dead load are generally below the stress that can be resisited by the material. In other mean, maximum stress for all elements calculated doesn't exceed the strength limit (15 Mpa for compression and 1,4 Mpa for tension). So, the structure, under its own weight, has no stresses which can be classified as destructive. However, this analysis gives satisfactory results to determine the critical areas. The stresses and deformations output are in kN/m^2 and meter respectively for the solid elements. For the shell elements, the forces are in kN. Therefore, the real stresses are obtained by dividing the force by the thickness of the shell for each element.

It is easier to observe the stresses in half of the model. For the solid and shell elements, the stresses are in global axis. S11 denotes the hoop stresses for shell elements and the stress in X-direction for solid elements, while S22 denotes the radial stress for shell elements and the stress in the Y-direction for solid elements. Also, S33 denotes the vertical stress for solid elements.

The distributions of S33 (vertical stress), Smax (Maximum principal stress) and Smin((Maximum principal stress) which are the most important stress components for the dead load analysis show that;

In the main dome; compression stresses spread over at the middle part (apex part of the main dome) and tension stresses are observed around the middle part of the main dome in the circumferential direction (Figure 5.12 and 5.13).The maximum value for compression is -220 kN/m2 and the maximum for tension is about +220 kN/m2.

In the semidome; both tension and compression stresses are observed over the main semidomes (Figure 5.12 and 5.13). Compression stresses are observed around apex and also at the connection regions between the main semidomes and secondary semidomes. Tension stresses are observed around the middle part of the main semidome in the circumferential direction (Figure 5.12 and 5.13). The maximum value for compression is -220 kN/m2 and the maximum for tension is about +220 kN/m2 around apex and the maximum value for compression is -440 kN/m2 and the maximum for tension is about +660 kN/m2 at the connection regions.

In the arches, pendentives and piers; bottom fibers of the main arches are in compression and the upper fibers are in tension. The highest tension stresses occurs at the top of the key region in the stress range, 0,55-0,60 10^3 kN/m^2. This stress value is observed at a very limited region. The highest compression stresses occurs at the bottom parts in the stress range, -1,65 to -2,20 10^3 kN/m^2 (Figure 5.16).

Tension stresses concentrate at the four pendentives as compared to the arches and piers, reaching to the value of 0,55 10^3 kN/m^2.(Figure 5.16 and Figure 5.20).

Tension stresses spread over upper parts of the piers. However, these stresses do not cause any important effect for the structure because they occur at very small regions relative to the main structural parts. Compression stresses generally spread over almost all parts of the piers and the stresses ranges increase towards the bottom parts of the piers and their highest value of -1.1 10^3 kN/m^2 (at the bottom of the main piers), (Figure 5.16 and Figure 5.20).

5.2. Analysis under the self weight and snow load

Snow Loads are calculated according to the following:

$$Pk = m * Po \tag{5.2}$$

Where m is a constant, Po is selected as 75 kg/m2, 1. region from TS498 and m=1 for $\alpha < 30$ (α is slope of roof) or $m = 1 - (\alpha - 30°)/40°$ for $\alpha < 30°$ (α is slope of roof) [26].

The stressses under dead load + snow load are almost same as the stresses under only dead load because there is not an important effect of snow load on the analysis in comparison with the effect of structure weight. Also, there is not observed any difference between the compression and tension regions in shell and solid elements of two analyses(See Figure 5.22 to 5.26).

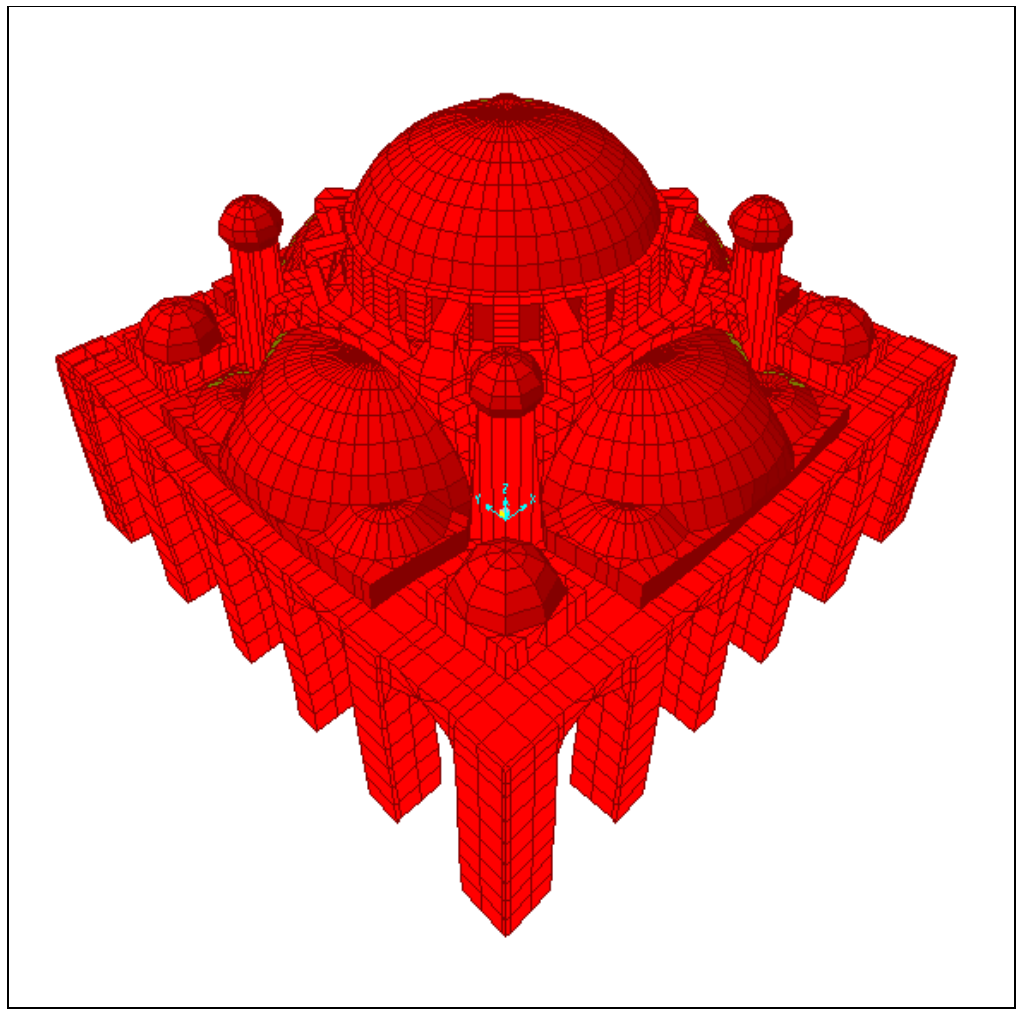

Figure 5.1. General deformed configuration (3-D view from south-east) for static analysis under self weight

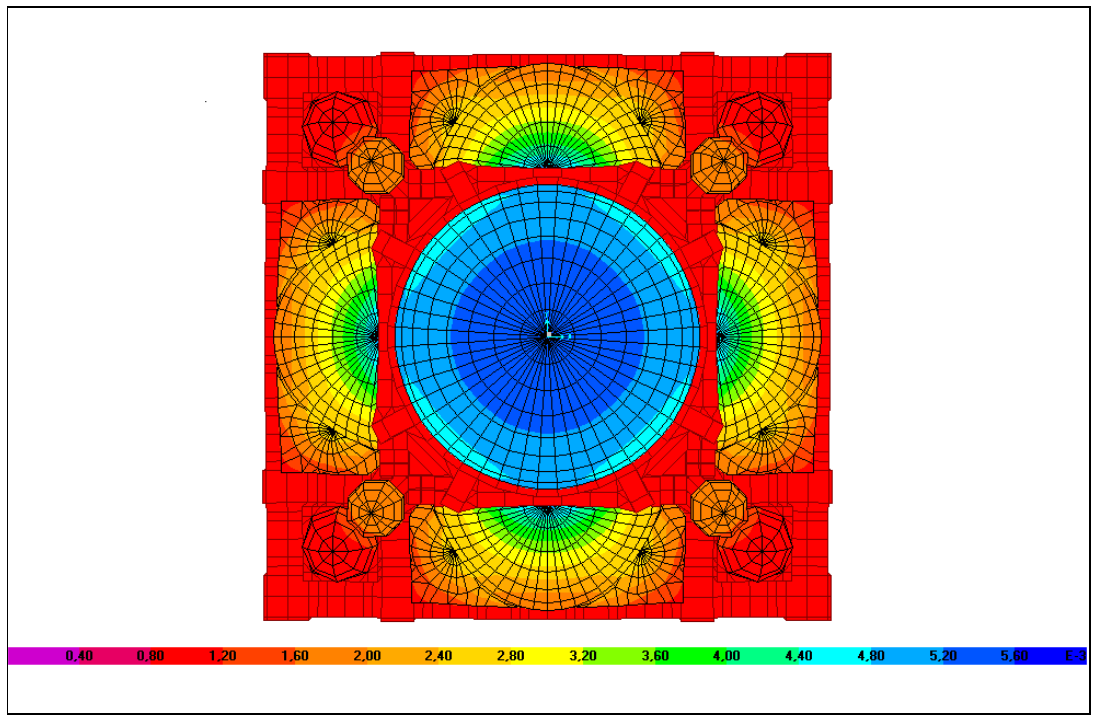

Figure 5.2. Displacement contours in the shell elements for static analysis under self weight

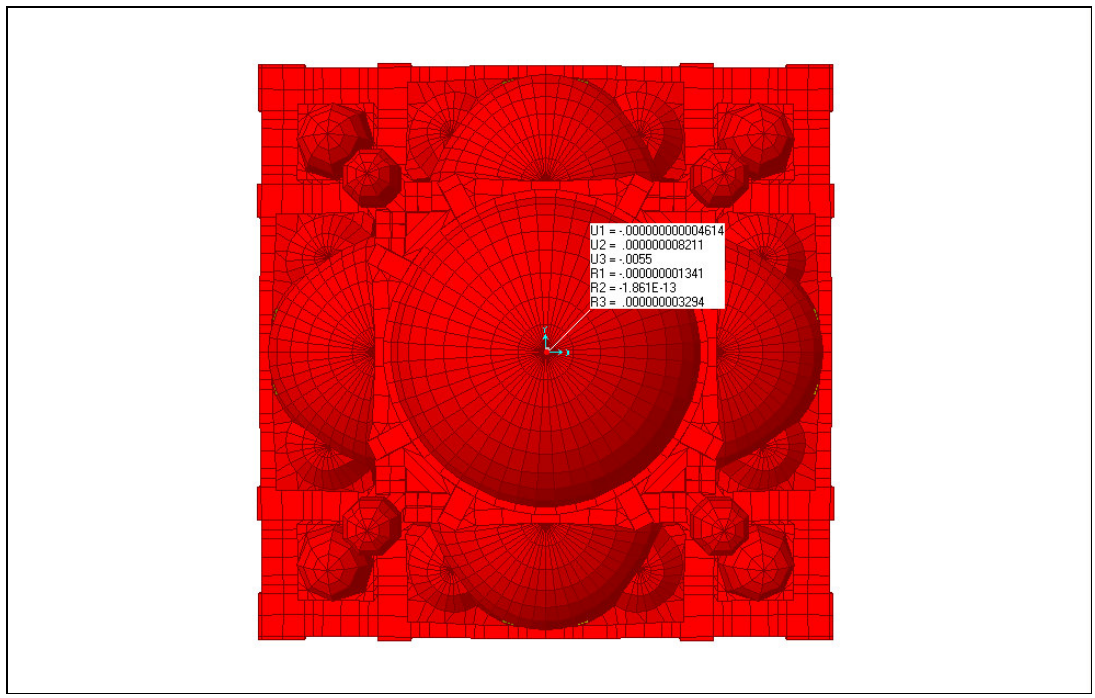

Figure 5.3. Displacement of the top point of the main dome (view from top) for static analysis under self weight

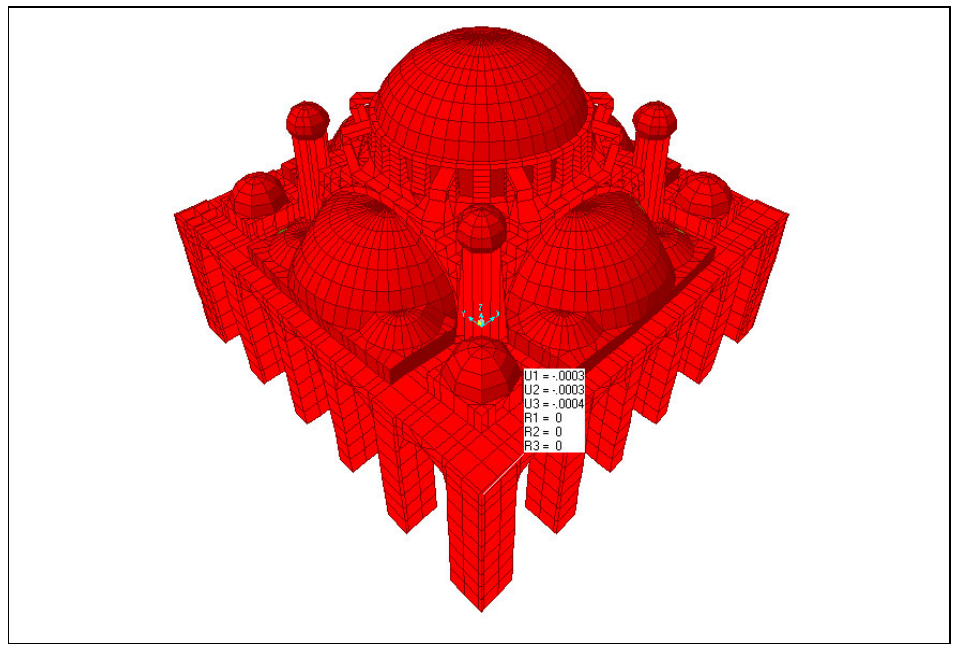

Figure 5.4. Displacement of the top point of the pier from south- east (3-D view from south- east) for static analysis under self weight

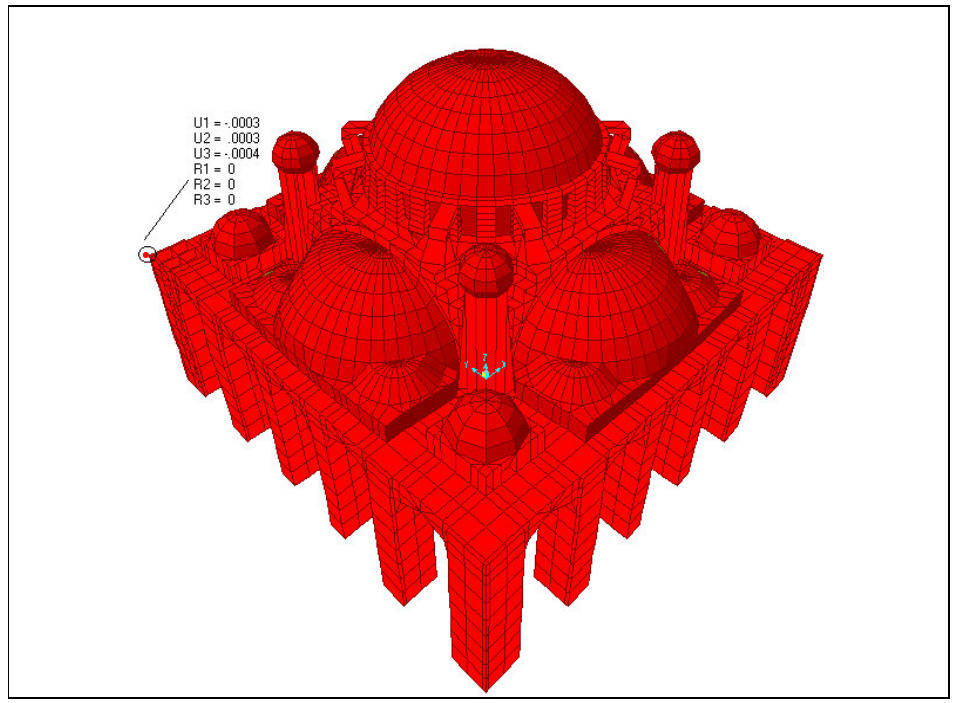

Figure 5.5. Displacement of the top point of the pier from south- west (3-D view from south- east) for static analysis under self weight

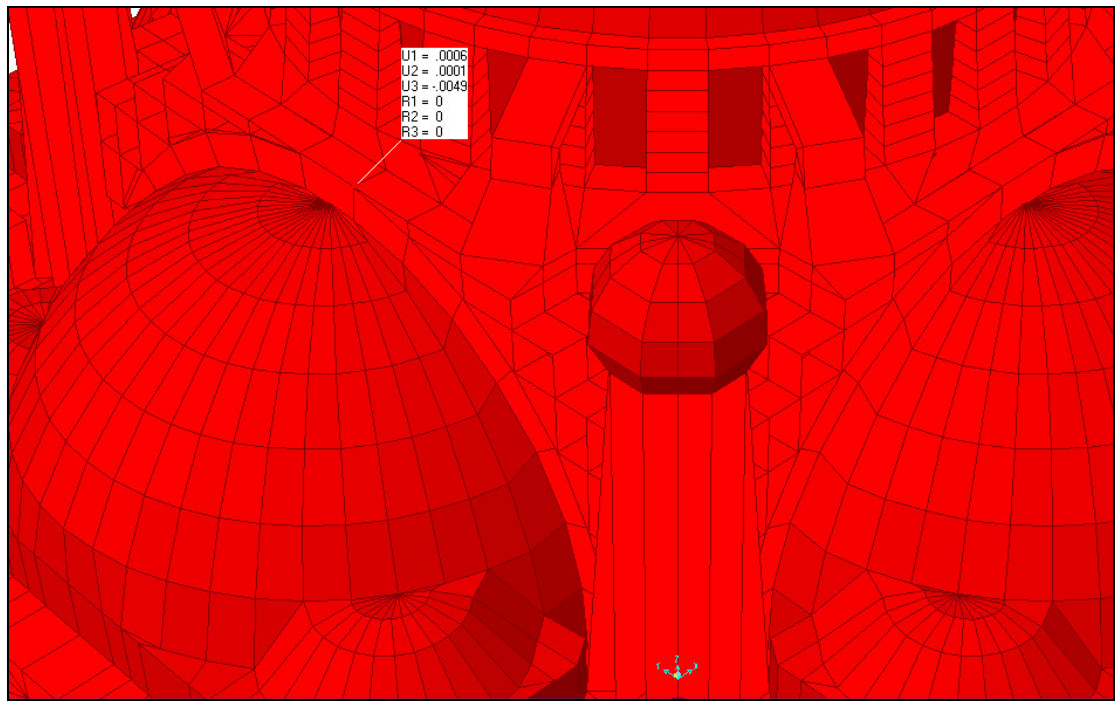

Figure 5.6. Displacement of the top point of the main arch from south (3-D view from south- east) for static analysis under self weight

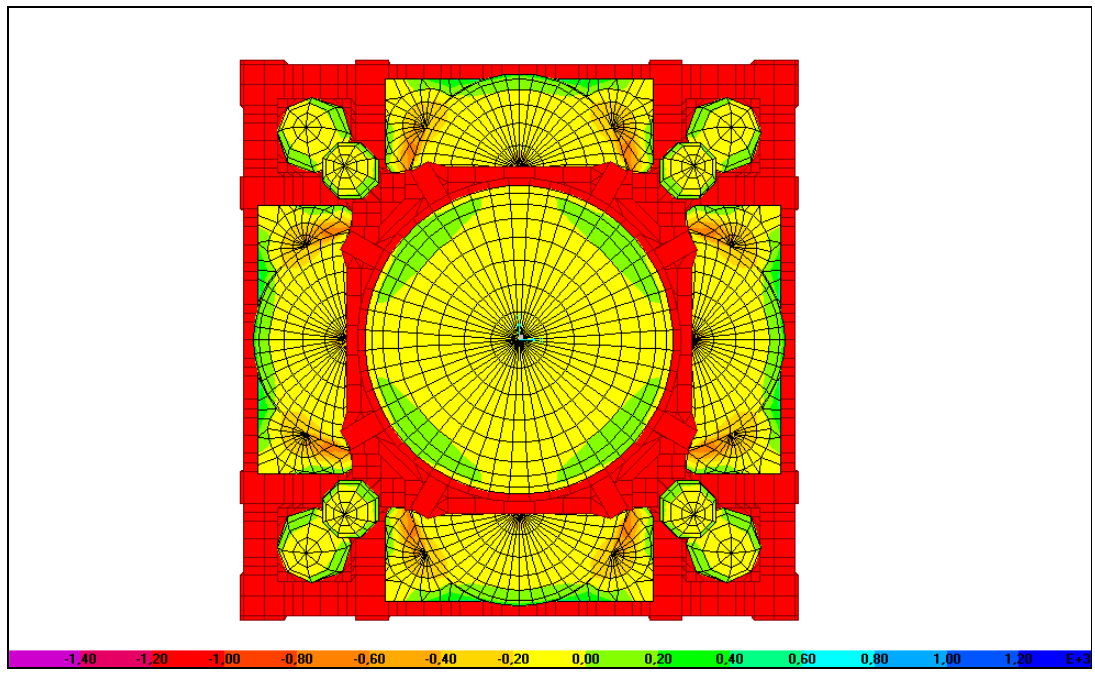

Figure 5.7. S11 stress contours in the shell elements (view from top) for static analysis under self weight

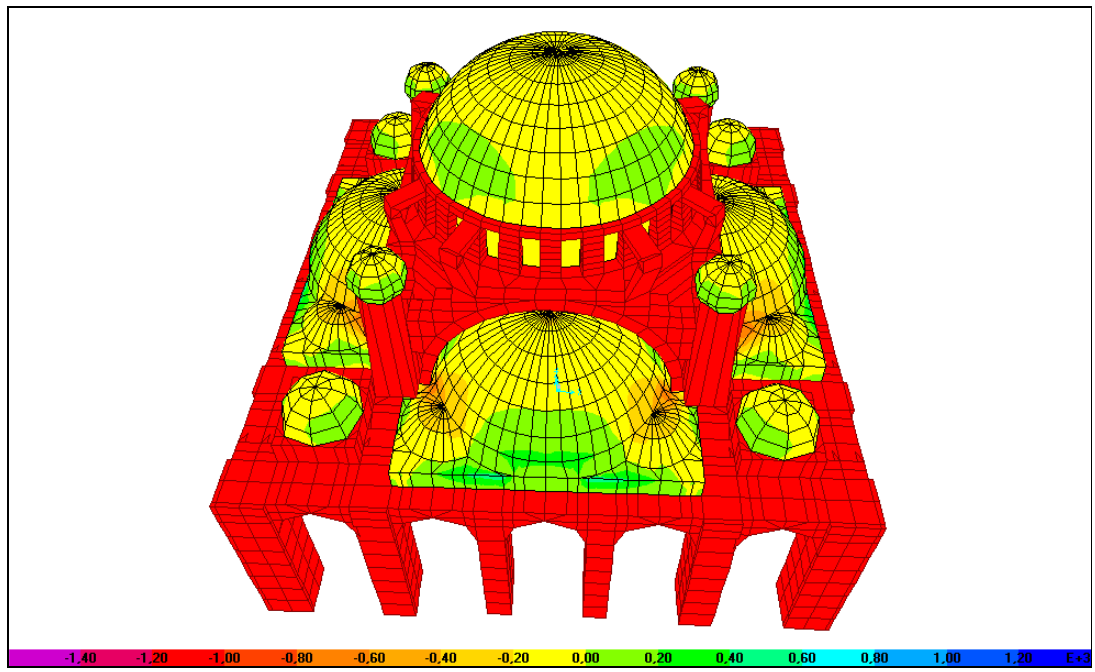

Figure 5.8. S11 stress contours in the shell elements (view from side) for static analysis under self weight

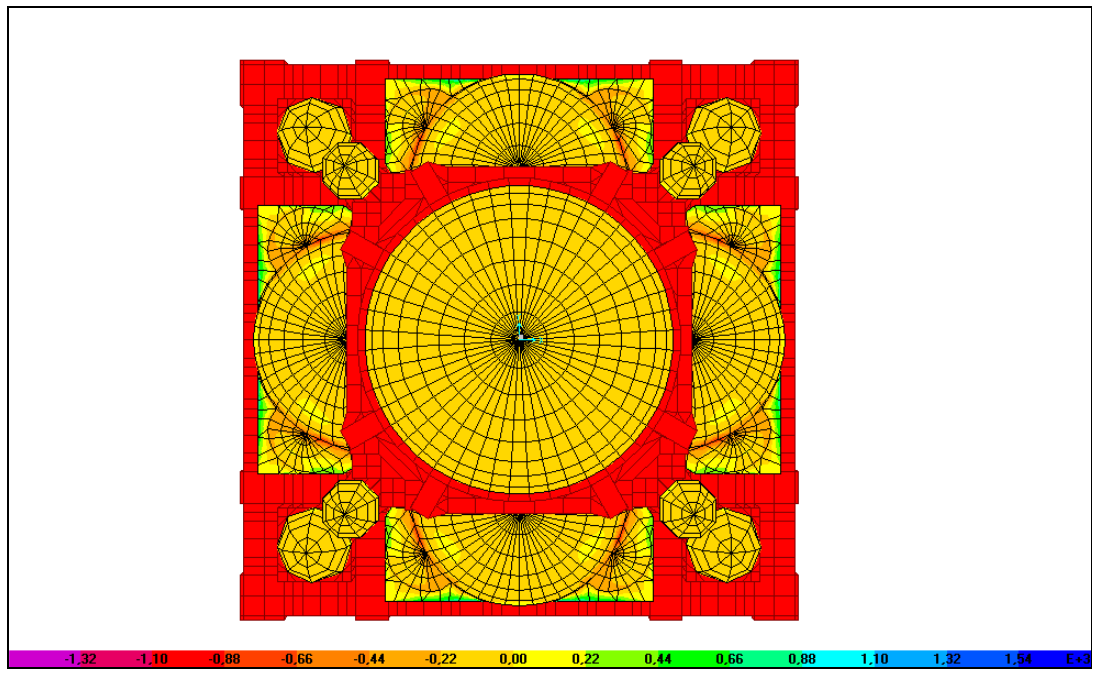

Figure 5.9. S22 stress contours in the shell elements (view from top) for static analysis under self weight

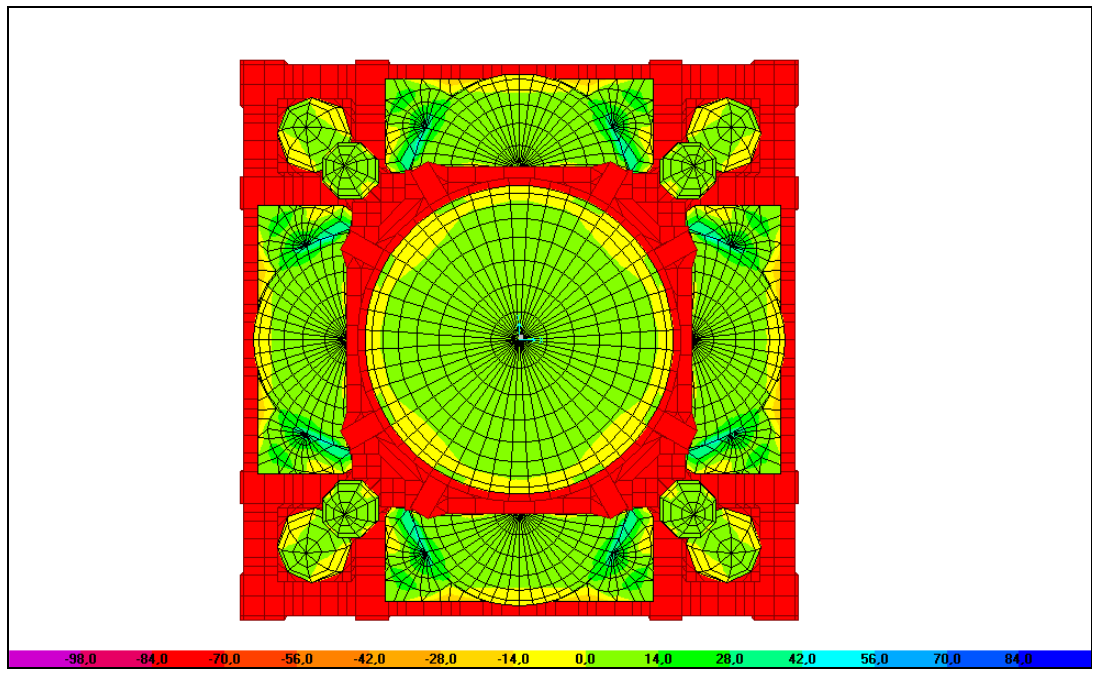

Figure 5.10. M11 bending moment contours in the shell elements (view from top) for static analysis under self weight

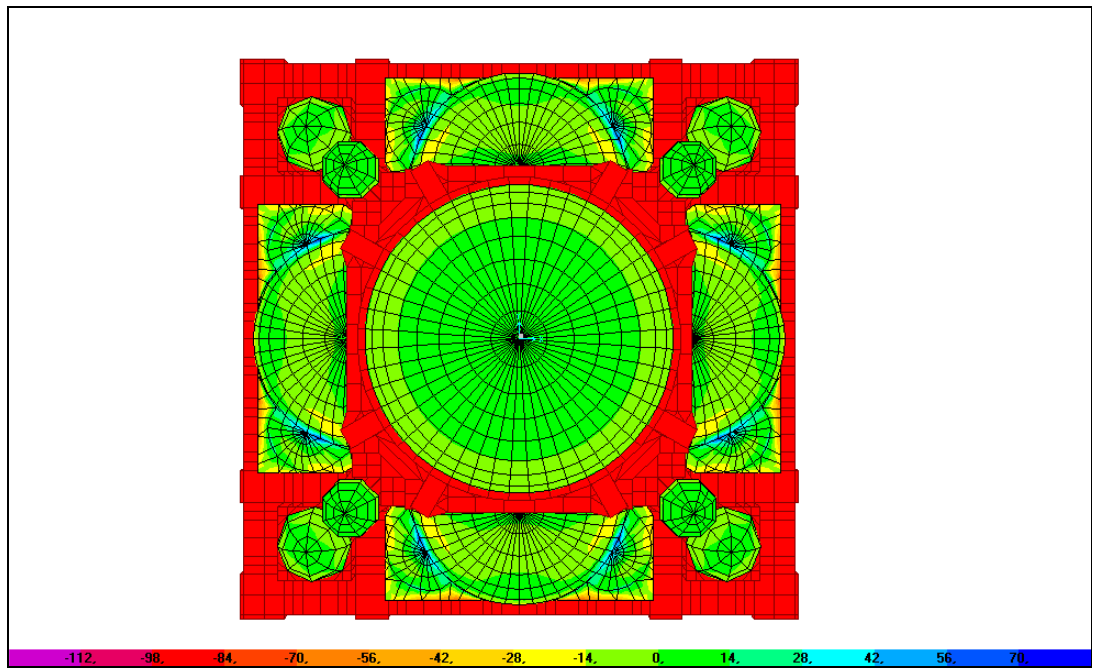

Figure 5.11. M22 bending moment contours in the shell elements (view from top) for static analysis under self weight

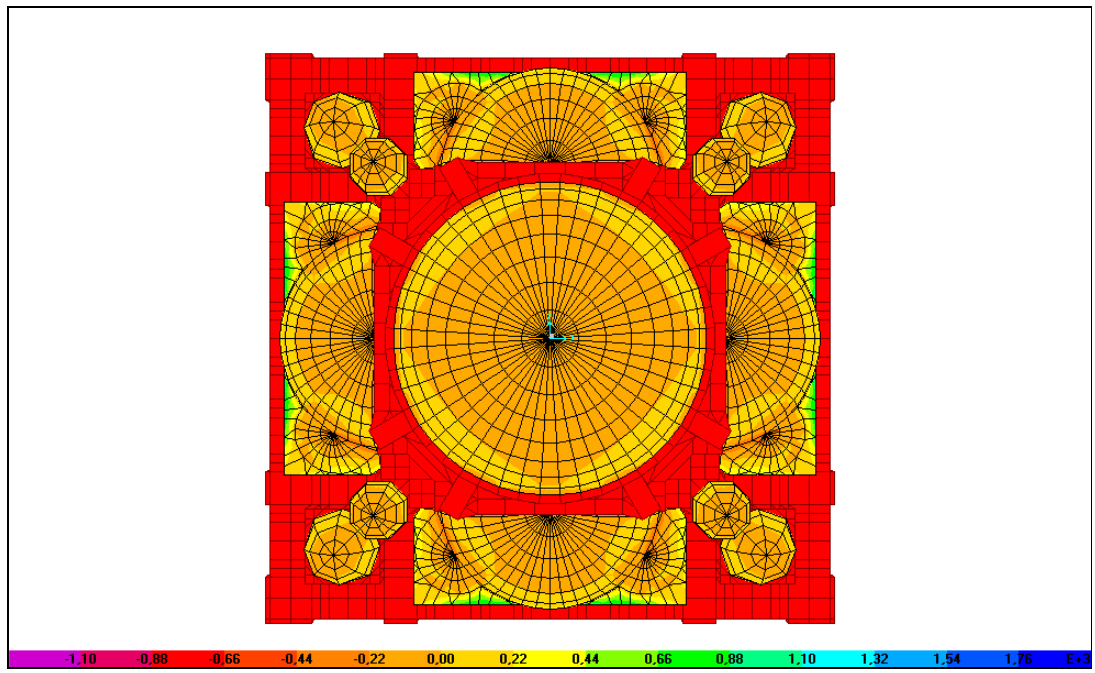

Figure 5.12. Smax (maximum principal stress) stress contours in the shell elements (view from top) for static analysis under self weight

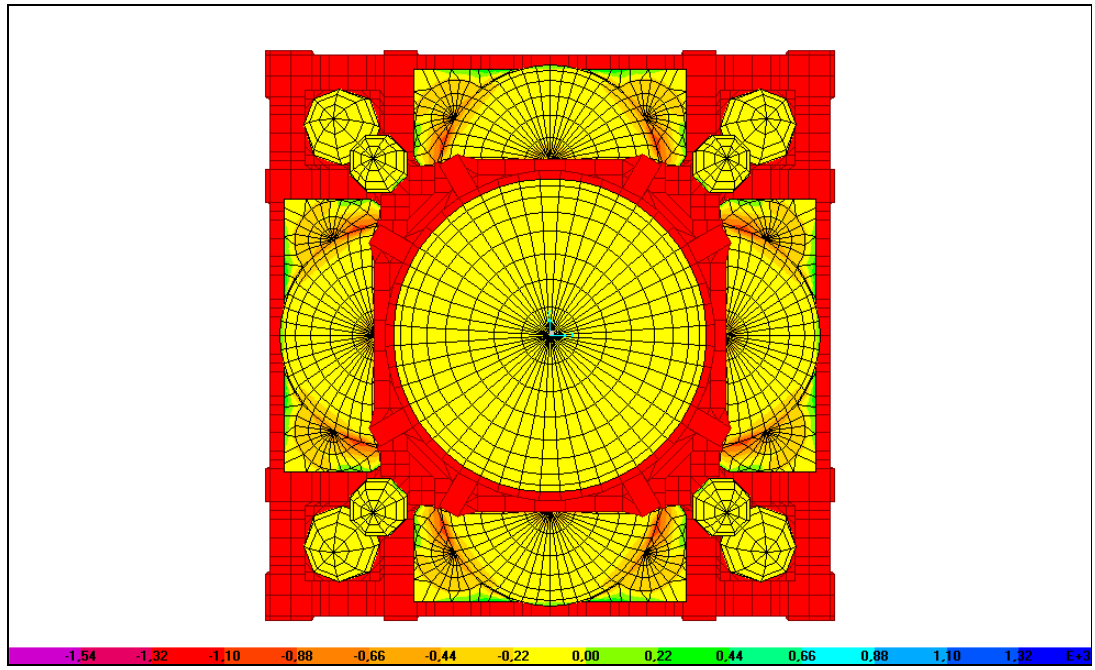

Figure 5.13. Smin (minimum principal stress) stress contours in the shell elements (view from top) for static analysis under self weight

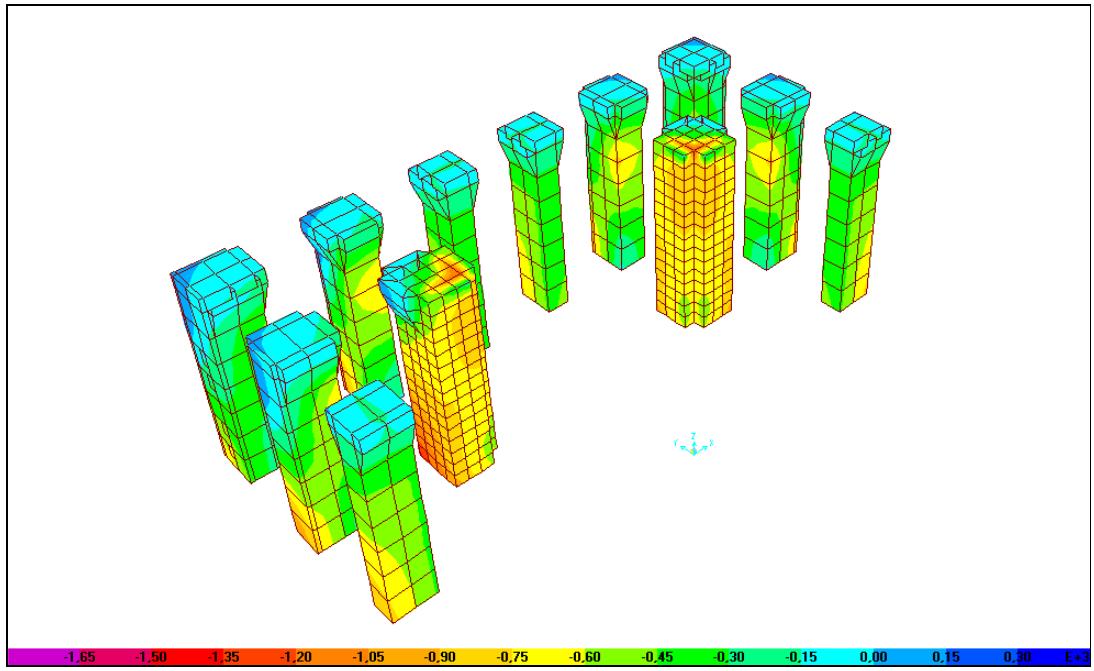

Figure 5.14. S33 stress contours in the solid elements (in half of piers) for static analysis under self weight

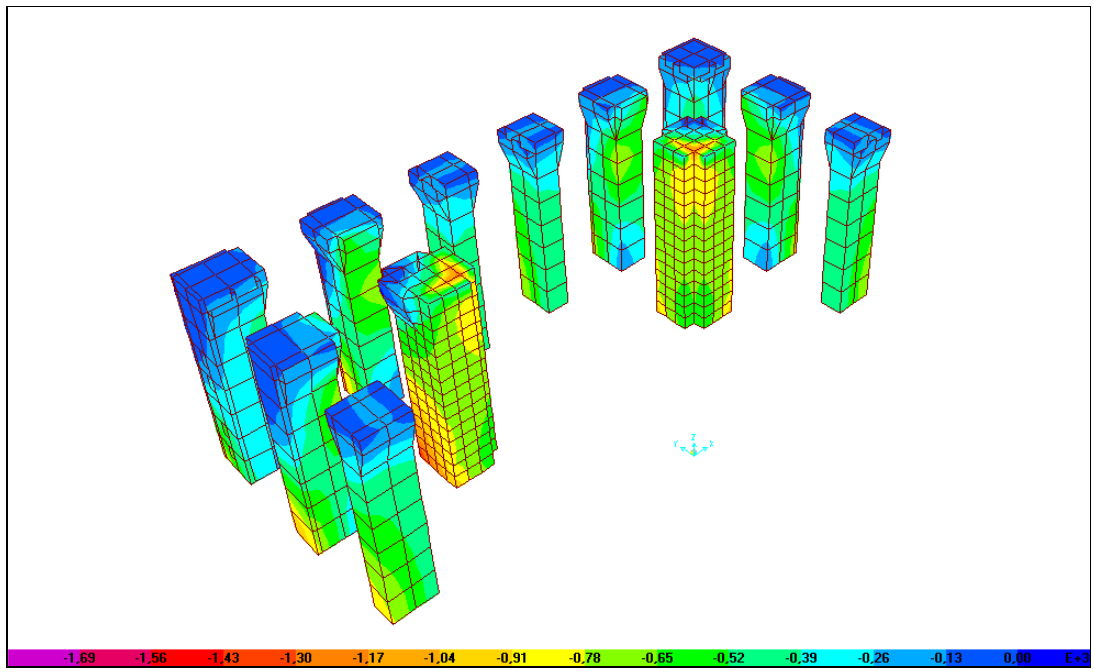

Figure 5.15. Smin stress contours in the solid elements (in half of piers) for static analysis under self weight

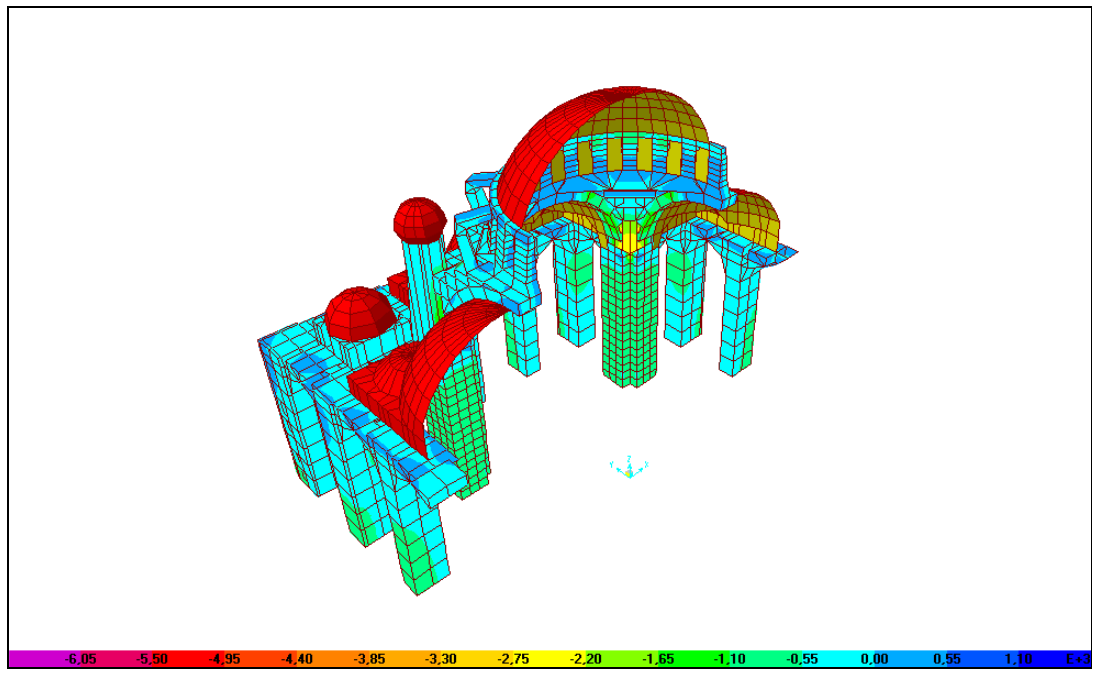

Figure 5.16. S33 stress contours in the solid elements (in half of model) for static analysis under self weight

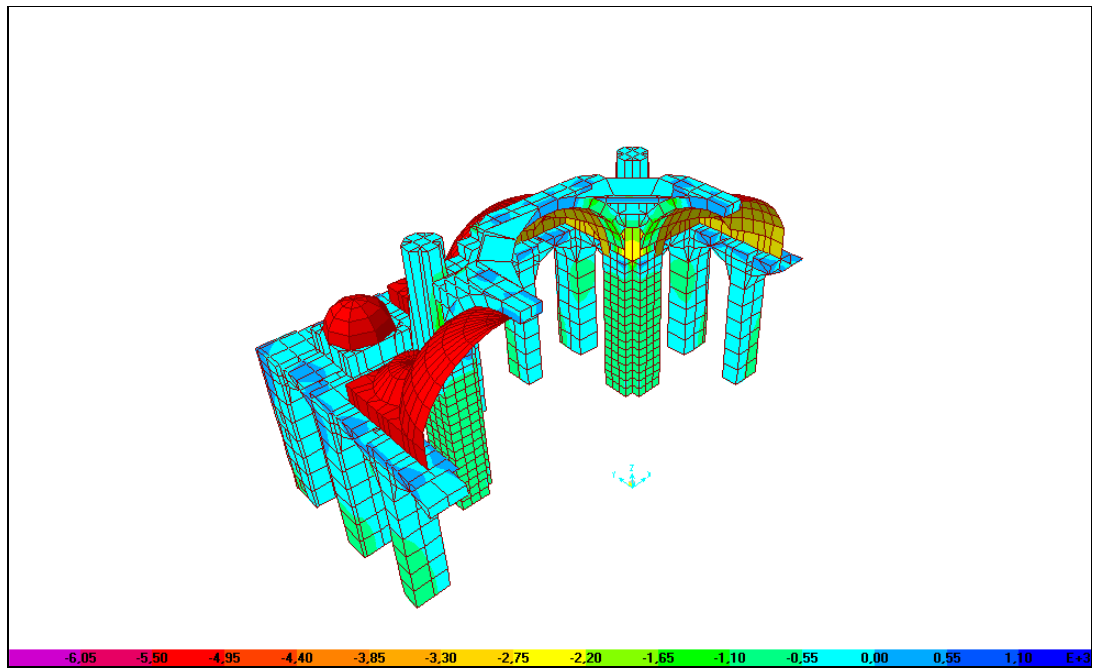

Figure 5.17. S33 stress contours in the solid elements (in half of model) for static analysis under self weight

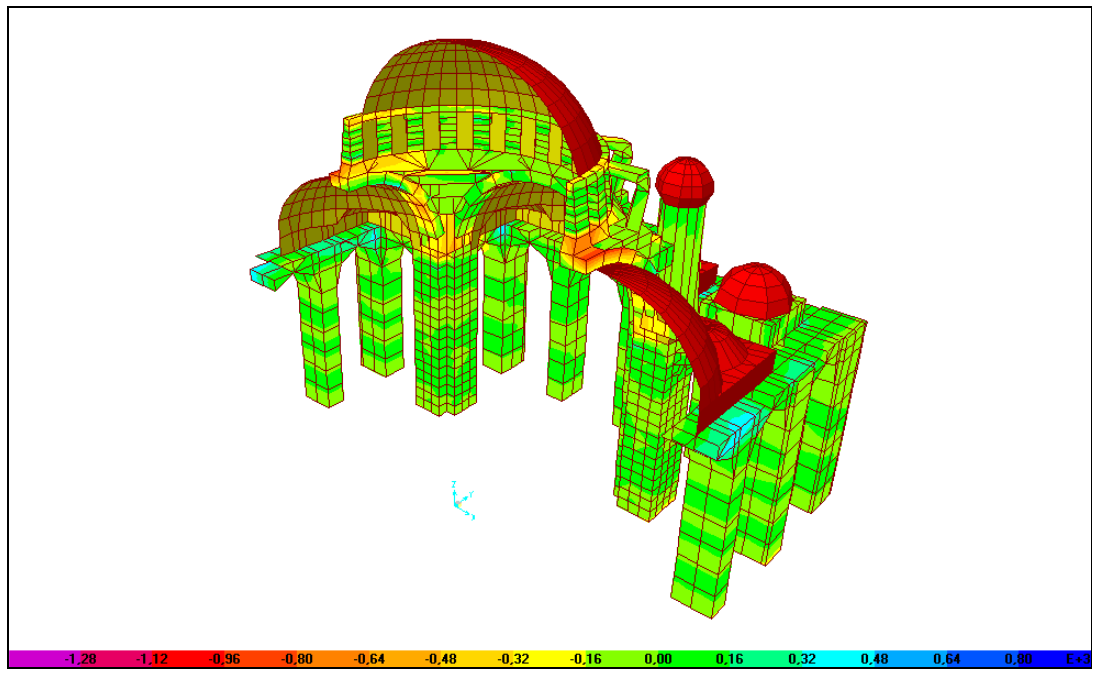

Figure 5.18. S22 stress contours in the solid elements (in half of model) for static analysis under self weight

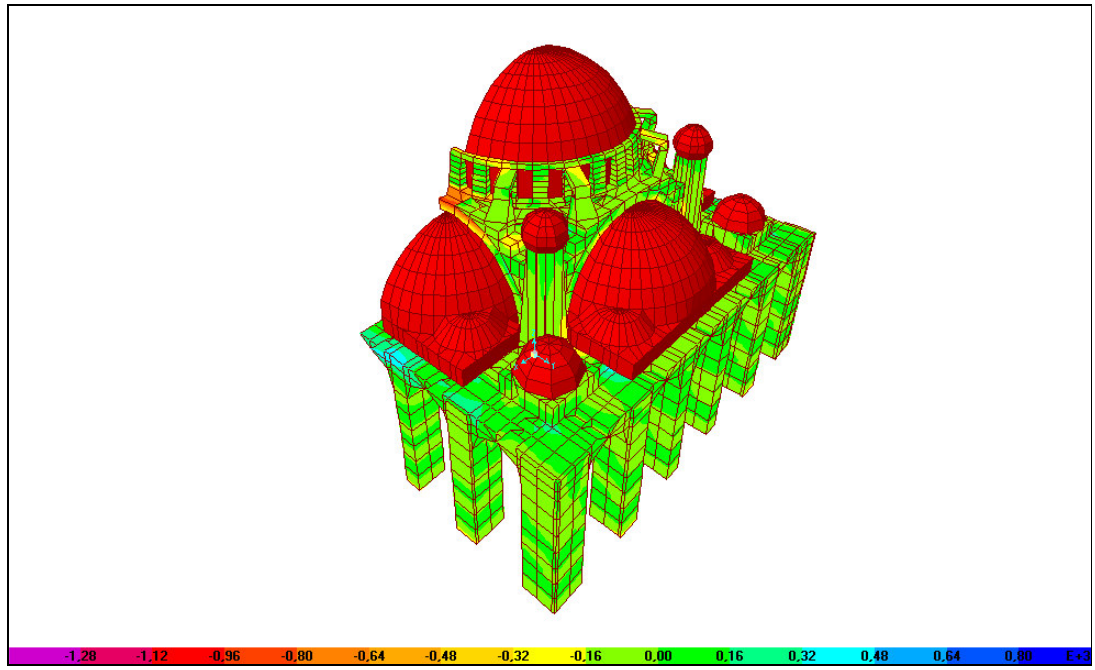

Figure 5.19. S22 stress contours in the solid elements (in half of model) for static analysis under self weight

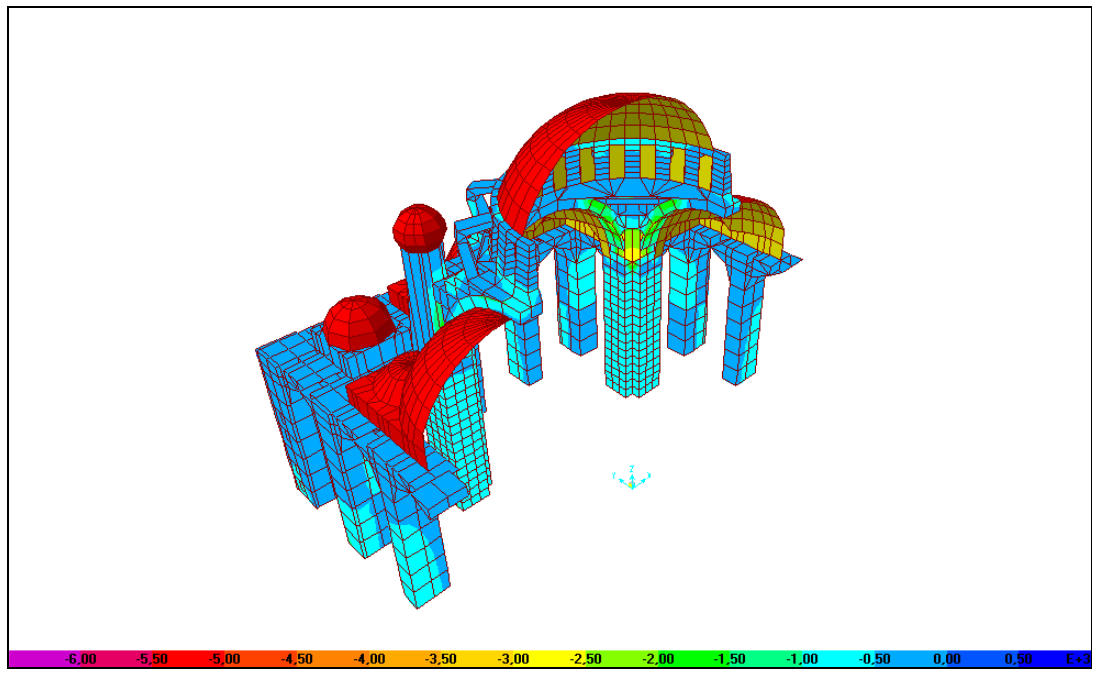

Figure 5.20. Smin stress contours in the solid elements (in half of model) for static analysis under self weight

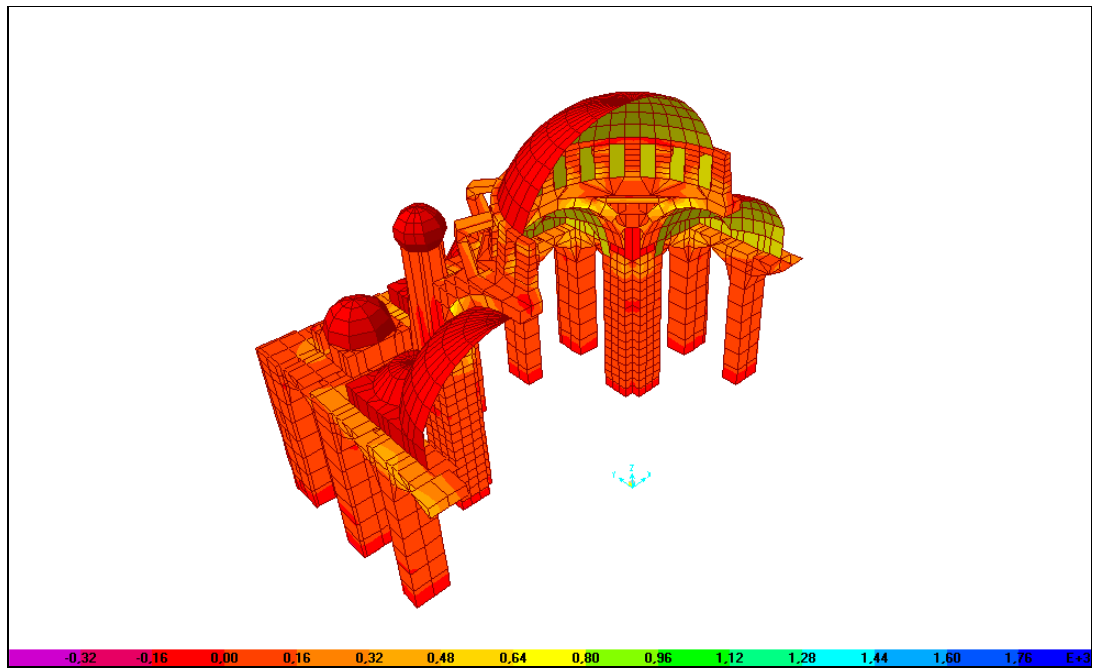

Figure 5.21. Smax stress contours in the solid elements (in half of model) for static analysis under self weight

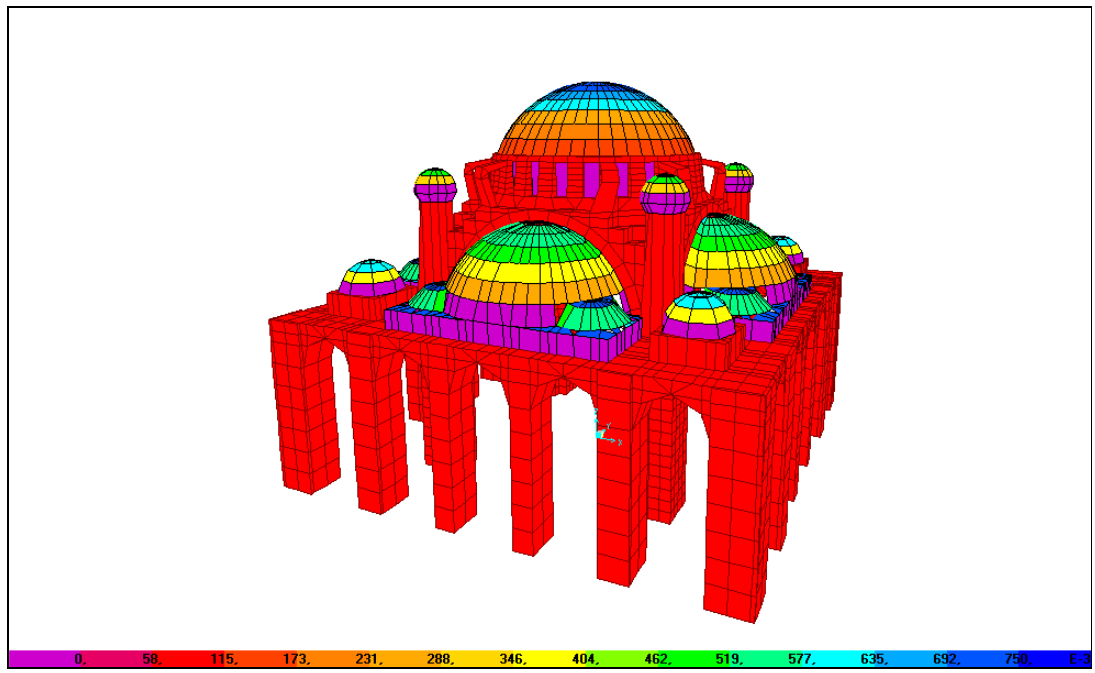

Figure 5.22. Snow load contours in the shell elements (3-D view from south-east)

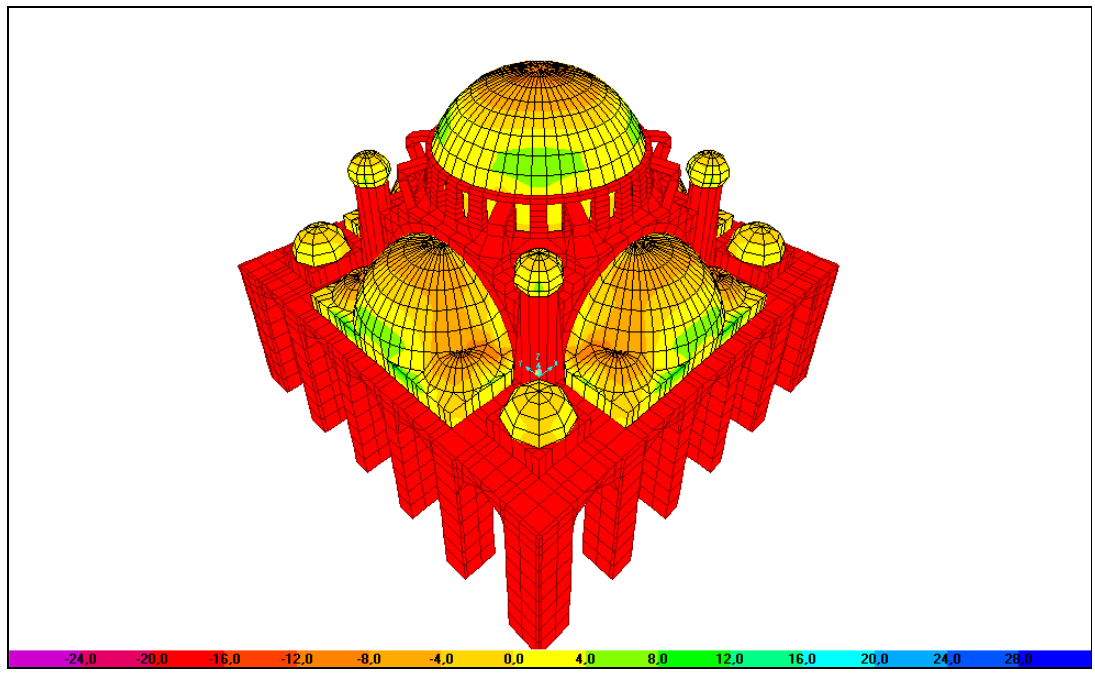

Figure 5.23. S11 stress contours in the shell elements (3-D view from south-east) for static analysis under snow loading

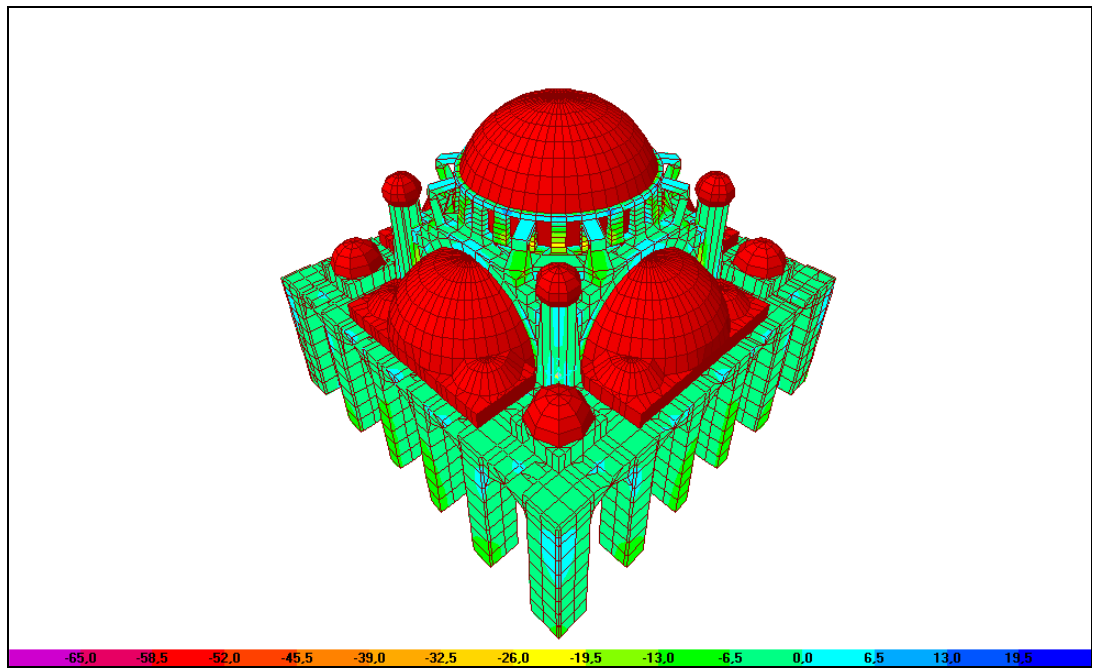

Figure 5.24. S33 stress contours in the solid elements (3-D view from south-east) for static analysis under snow loading

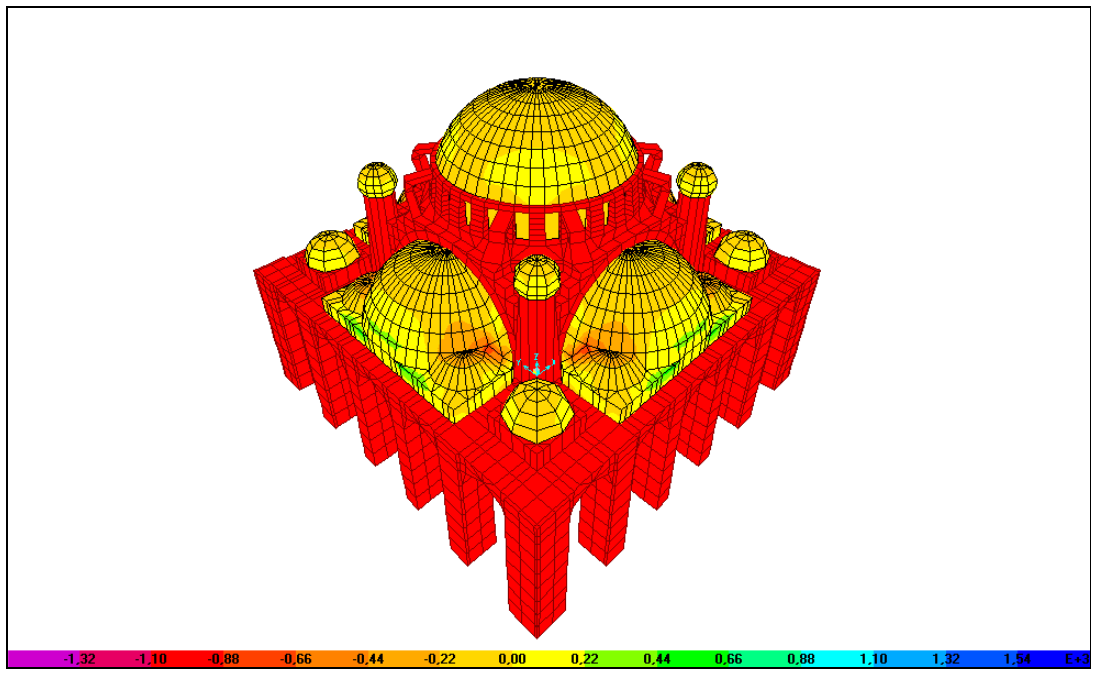

Figure 5.25. S11 stress contours in the shell elements (3-D view from south-east) for static analysis under self weight + snow loading

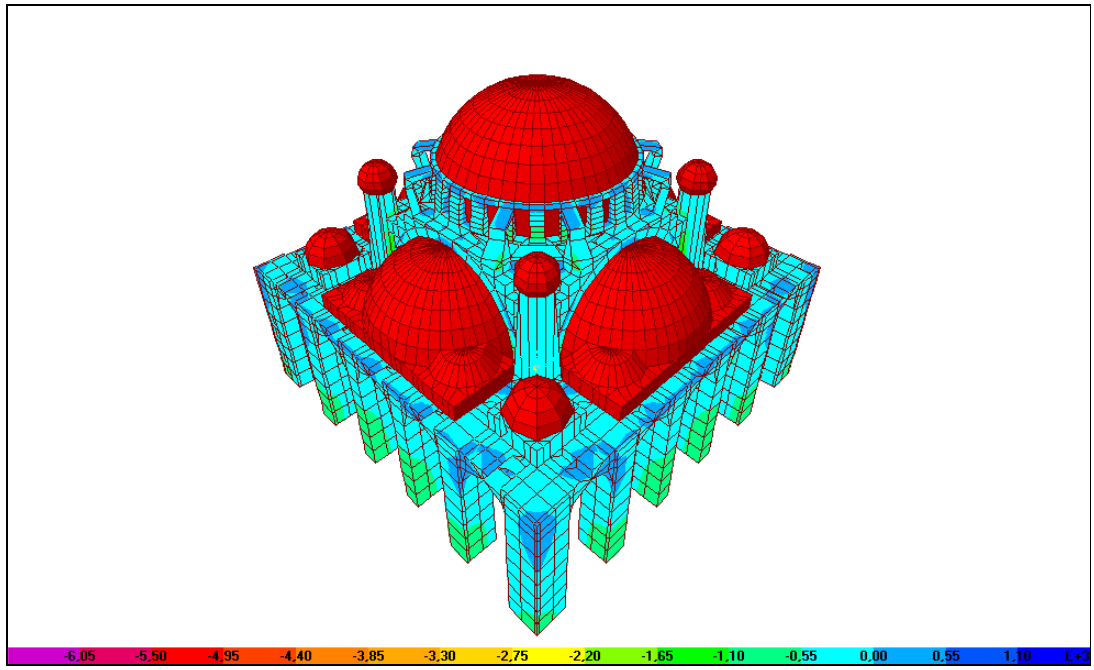

Figure 5.26. S33 stress contours in the solid elements (3-D view from south-east) for static analysis under self weight + snow loading

6. DYNAMIC ANALYSIS

Dynamic Analysis is achieved by adjusting the value of elastic moduli by assuming that the geometry and mass distribution of the structure are modelled correctly.

6.1. Eigenvalue analysis of the model

The frequencies and mode shapes can be obtained performing the Eigen-value analysis. In the Eigen-value analysis, the equation system shown below is used;

$$[M]\{\ddot{u}\}+[K]\{u\}=\{0\} \tag{6.1}$$

Where [M] is the mass matrix, [K] is the stiffness matrix, $\{\ddot{u}\}$ is the acceleration vector and, $\{u\}$ is the displacement vector.

The equation system 6.1 can be solved with the equation shown below:

$$[K]\{\Ø\}=[M]\{\ \Ø\ \}[\Omega^2] \tag{6.2}$$

Where $[\Omega^2]$ is the diagonal matrix giving Eigen-values (modal frequencies) and $\{\Ø\}$ is the vector of mode shapes corresponding with the modal frequencies.

6.2. Definition of response spectrum

To study the effects of the ground motion excitations on structure it is necessary to measure the intensity of the motion. One practical measure can be obtained from a knowledge of the response spectra for a generic ground motion. The spectral response analysis seeks to estimate the maximum displacement or pseudo velocity or acceleration of the structure during a design earthquake without recourse to direct integration of the model over the complete duration of an event.

Response-spectrum analysis seeks the likely maximum response to these equations rather than the full time history. The earthquake ground acceleration is given as a digitised response-spectrum curve of pseudo-spectral acceleration response versus period of the structure.

Even though accelerations may be specified in three directions, only a single positive result is produced for each response quantity. The response quantities include displacements, forces, and stresses. Each computed result represents a statistical measure of the likely maximum magnitude for that response quantity. The actual response can be expected to vary within a range from this positive value to its negative. No correspondence between two different response quantities is available. No formation is available as to when this extreme value occurs during the seismic loading, or as to what the values of other response quantities are at that time. Response-spectrum analysis is performed using load superposition. Modes may have been computed using Eigen-vector analysis or Ritz-vector analysis.

A scale factor is specified to multiply the ordinate, i.e. pseudo spectral acceleration response of the function. This is often needed to convert values given in terms of the acceleration due to gravity to units consistent with the rest of the model.

For a given direction of acceleration, the maximum displacements, forces and stresses are computed throughout the structure for each vibration mode. These modal values for a given response quantity are combined to produce a single, positive result for the given direction of acceleration. CQC (Complete Quadratic Combination) method is used in this study for combination. Obtaining the single, positive result for each direction of acceleration, these directional values are combined with SRSS (Square Root of the Sum of their Squares) method.

The CQC method takes into account the statistical coupling between closely spaced Modes caused by modal damping. Increasing the modal damping increases the coupling between closely spaced modes. If the damping is zero for all Modes, this method degenerates to the SRSS method. CQC combines the modal results by the Complete Quadratic Combination technique. SRSS method combines the modal results

by taking the Square Root of the Sum of their Squares [17].

6.3. Modal effect

For visualization and to get familiar with all of the modes, about 200 eigenvalues were calculated and the total modal effect has been taken into consideration. The results show slight difference among 50, 100 and 200 modes. The effective mass of each mode shows its modal contribution. Some modes assigned a smaller mass density have no structural importance since they vibrate locally and prevent finding the other important modes which have higher effective mass.

In Table 5.1 the first five modes with the model frequencies and modal shapes are given and in Table 5.2 the first 50 modes with all parameters are given. It is important to note that for the first 50 modes the effective mass in both horizontal directions (Global X and Y) is about 85%. But when we look at for the first 100 modes these percentage increases only 1-2%.

Table 6.1. Results of the eigenvalue analysis

Modes	Frequencies	Modal Shapes
Mode 1	2,8569	N-S lateral
Mode 2	2,8569	E-W lateral
Mode 3	3,3394	Squeezing
Mode 4	3,5371	Torsional
Mode 5	4,2489	Breathing

Table 6.2. Modal participating mass ratios

Output Case	Step Type	Step Num	Period	Frequency	UX	SumUX	UY	SumUY	UZ	SumUZ
Text	Text	Unitless	Sec		Unitless	Unitless	Unitless	Unitless	Unitless	Unitless
MODAL	Mode	1	0,350	2,857	0,763	0,763	0,000	0,000	0,000	0,000
MODAL	Mode	2	0,350	2,857	0,000	0,763	0,763	0,763	0,000	0,000
MODAL	Mode	3	0,299	3,339	0,000	0,763	0,000	0,763	0,000	0,000
MODAL	Mode	4	0,283	3,537	0,000	0,763	0,000	0,763	0,000	0,000
MODAL	Mode	5	0,235	4,249	0,000	0,763	0,000	0,763	0,000	0,000
MODAL	Mode	6	0,209	4,783	0,000	0,763	0,001	0,763	0,000	0,000
MODAL	Mode	7	0,209	4,784	0,001	0,763	0,000	0,763	0,000	0,000
MODAL	Mode	8	0,206	4,860	0,000	0,763	0,000	0,763	0,002	0,002
MODAL	Mode	9	0,191	5,233	0,000	0,763	0,000	0,763	0,000	0,002
MODAL	Mode	10	0,190	5,271	0,012	0,775	0,000	0,763	0,000	0,002
MODAL	Mode	11	0,190	5,272	0,000	0,775	0,012	0,775	0,000	0,002
MODAL	Mode	12	0,183	5,476	0,000	0,775	0,000	0,775	0,000	0,002
MODAL	Mode	13	0,169	5,916	0,000	0,775	0,000	0,775	0,000	0,002
MODAL	Mode	14	0,152	6,577	0,000	0,775	0,049	0,824	0,000	0,002
MODAL	Mode	15	0,152	6,577	0,050	0,824	0,000	0,824	0,000	0,002
MODAL	Mode	16	0,148	6,766	0,000	0,824	0,000	0,824	0,085	0,087
MODAL	Mode	17	0,141	7,110	0,000	0,824	0,021	0,846	0,000	0,087
MODAL	Mode	18	0,141	7,110	0,021	0,846	0,000	0,846	0,000	0,087
MODAL	Mode	19	0,136	7,339	0,000	0,846	0,000	0,846	0,000	0,087
MODAL	Mode	20	0,134	7,464	0,000	0,846	0,000	0,846	0,000	0,087
MODAL	Mode	21	0,127	7,889	0,000	0,846	0,000	0,846	0,000	0,087
MODAL	Mode	22	0,127	7,889	0,000	0,846	0,000	0,846	0,000	0,087
MODAL	Mode	23	0,119	8,397	0,000	0,846	0,000	0,846	0,000	0,087
MODAL	Mode	24	0,118	8,480	0,000	0,846	0,000	0,846	0,000	0,087
MODAL	Mode	25	0,110	9,102	0,000	0,846	0,000	0,846	0,109	0,196
MODAL	Mode	26	0,106	9,416	0,000	0,846	0,000	0,846	0,000	0,196
MODAL	Mode	27	0,106	9,416	0,000	0,846	0,000	0,846	0,000	0,196
MODAL	Mode	28	0,097	10,307	0,000	0,846	0,000	0,846	0,081	0,277
MODAL	Mode	29	0,096	10,379	0,000	0,846	0,000	0,846	0,000	0,277
MODAL	Mode	30	0,091	10,961	0,000	0,846	0,000	0,846	0,000	0,277
MODAL	Mode	31	0,091	10,961	0,000	0,846	0,000	0,846	0,000	0,277
MODAL	Mode	32	0,085	11,735	0,003	0,849	0,000	0,846	0,000	0,277
MODAL	Mode	33	0,085	11,736	0,000	0,849	0,003	0,849	0,000	0,277
MODAL	Mode	34	0,082	12,211	0,000	0,849	0,000	0,849	0,000	0,277
MODAL	Mode	35	0,077	12,906	0,000	0,849	0,000	0,849	0,000	0,277
MODAL	Mode	36	0,076	13,078	0,000	0,849	0,000	0,849	0,000	0,277
MODAL	Mode	37	0,074	13,447	0,001	0,849	0,000	0,849	0,000	0,277
MODAL	Mode	38	0,074	13,447	0,000	0,849	0,001	0,849	0,000	0,277
MODAL	Mode	39	0,069	14,436	0,000	0,849	0,000	0,849	0,036	0,313
MODAL	Mode	40	0,069	14,502	0,000	0,849	0,002	0,851	0,000	0,313
MODAL	Mode	41	0,069	14,502	0,002	0,851	0,000	0,851	0,000	0,313
MODAL	Mode	42	0,069	14,567	0,000	0,851	0,000	0,851	0,000	0,313
MODAL	Mode	43	0,068	14,741	0,000	0,851	0,000	0,851	0,000	0,313
MODAL	Mode	44	0,067	15,009	0,000	0,851	0,000	0,851	0,000	0,313
MODAL	Mode	45	0,066	15,103	0,003	0,854	0,000	0,851	0,000	0,313
MODAL	Mode	46	0,066	15,103	0,000	0,854	0,003	0,854	0,000	0,313
MODAL	Mode	47	0,066	15,161	0,000	0,854	0,000	0,854	0,056	0,369
MODAL	Mode	48	0,066	15,182	0,000	0,854	0,000	0,854	0,000	0,369
MODAL	Mode	49	0,066	15,256	0,000	0,854	0,000	0,854	0,000	0,369
MODAL	Mode	50	0,066	15,256	0,000	0,854	0,000	0,854	0,000	0,369

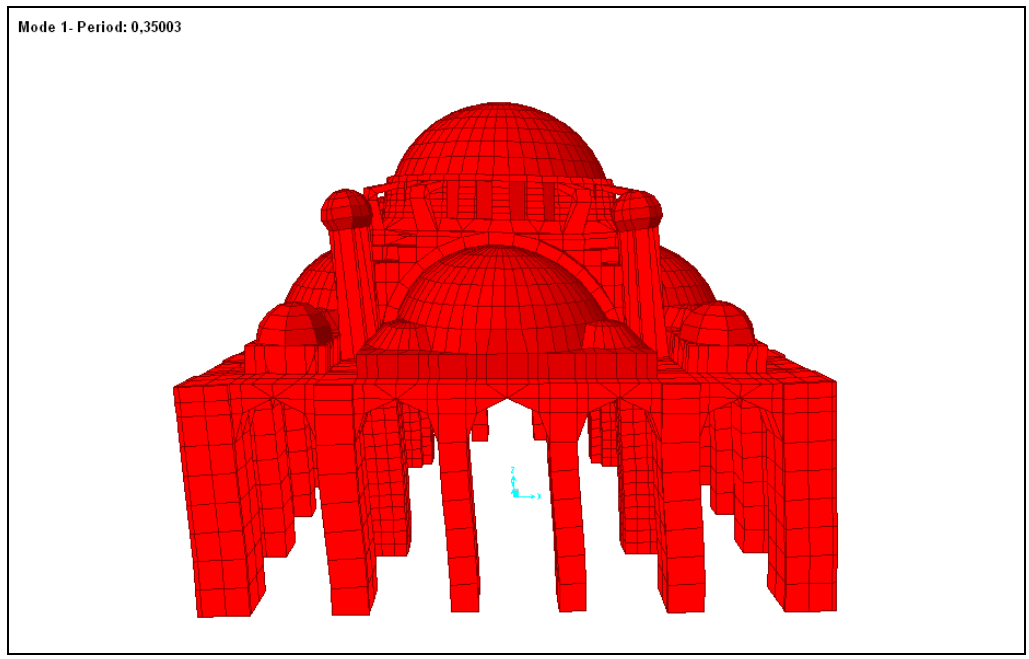

Figure 6.1. Modal analysis, mode 1(side view)

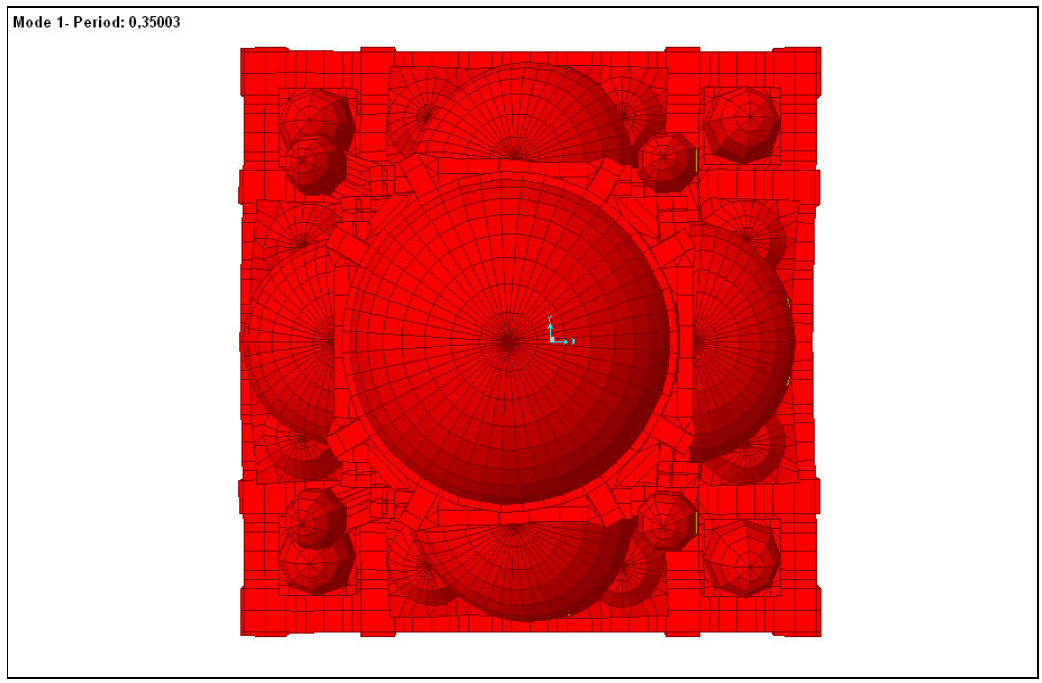

Figure 6.2. Modal analysis, mode 1 (view from top)

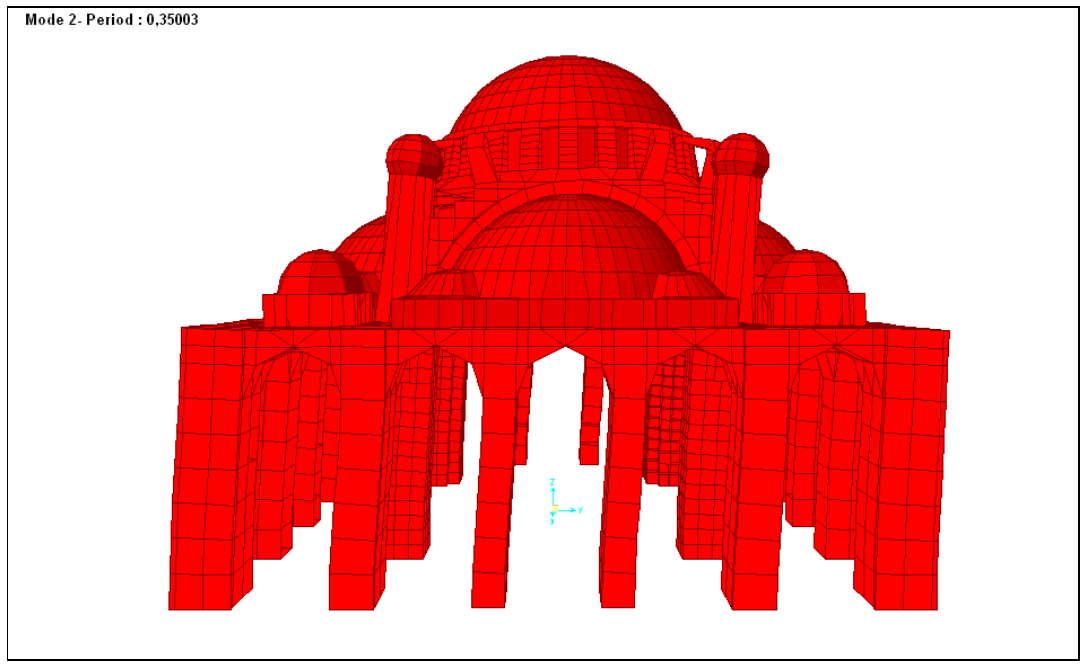

Figure 6.3. Modal analysis, mode 2 (side view)

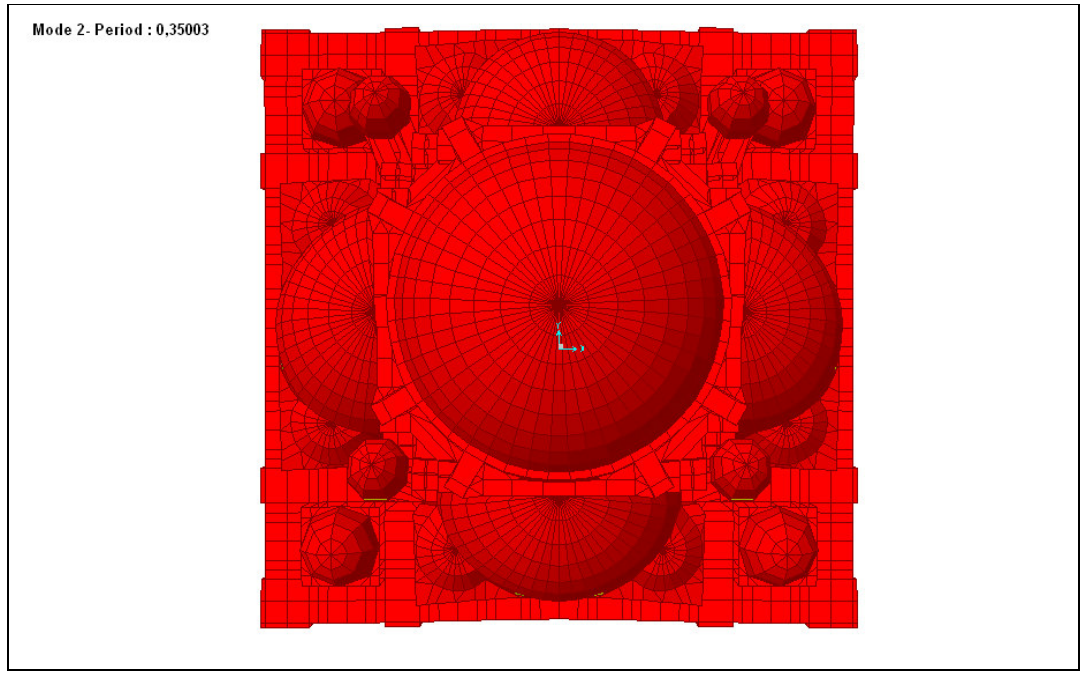

Figure 6.4. Modal analysis, mode 2 (view from top)

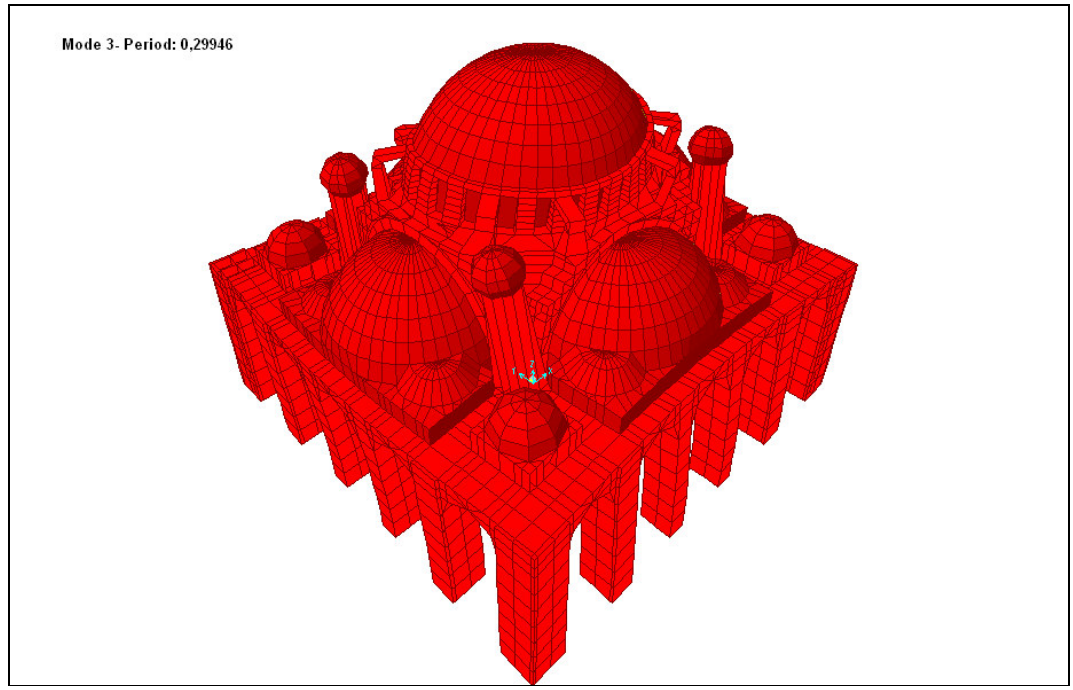

Figure 6.5. Modal analysis, mode 3 (3-D view from south-east)

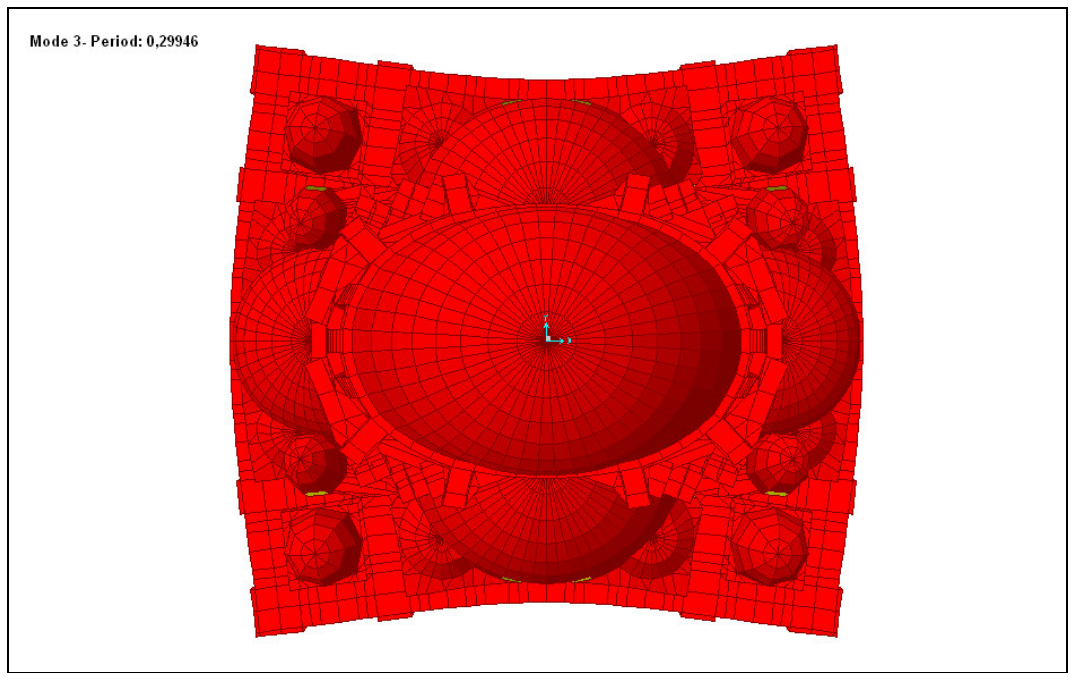

Figure 6.6. Modal analysis, mode 3 (view from top)

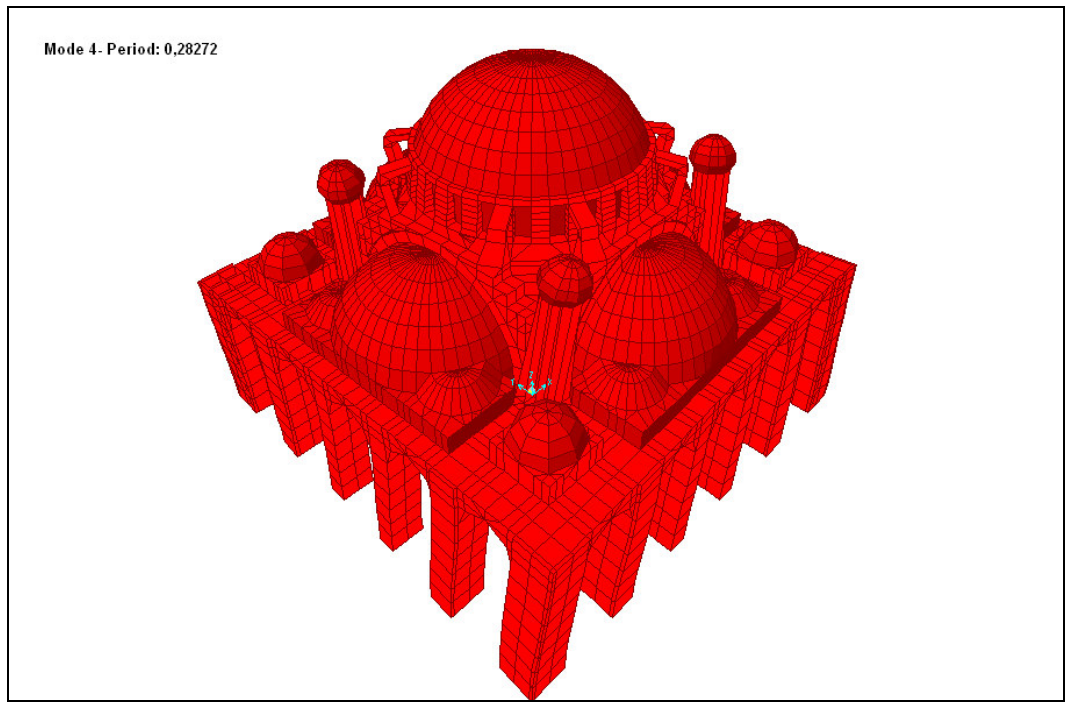

Figure 6.7. Modal analysis, mode 4 (3-D view from south-east)

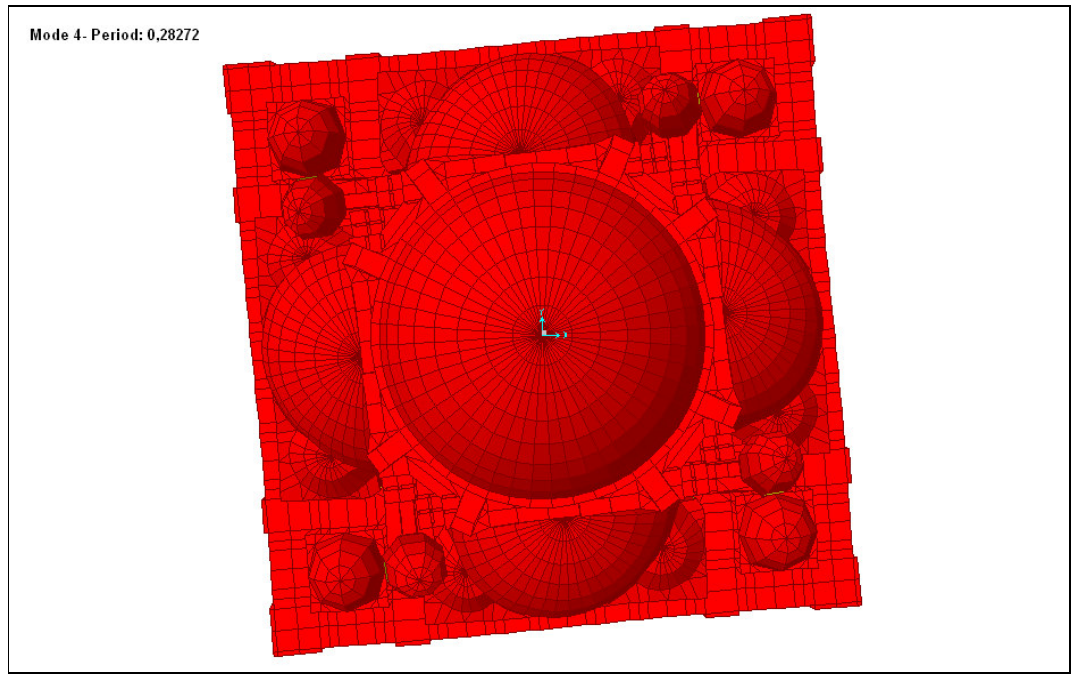

Figure 6.8. Modal analysis, mode 4 (view from top)

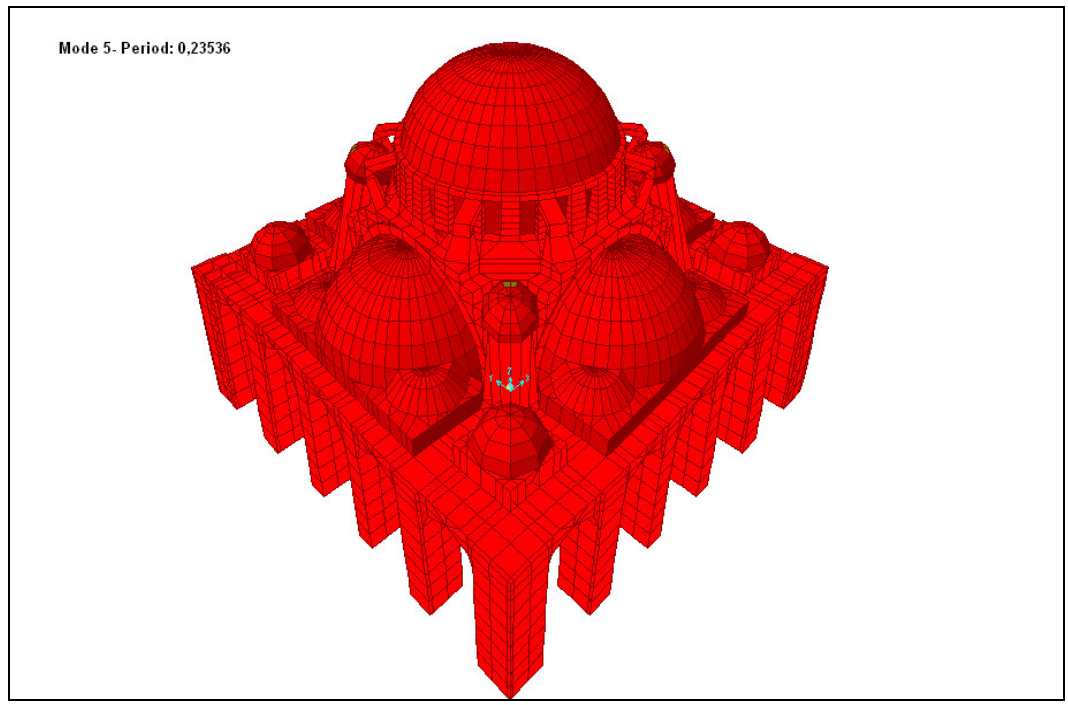

Figure 6.9. Modal analysis, mode 5 (3-D view from south-east)

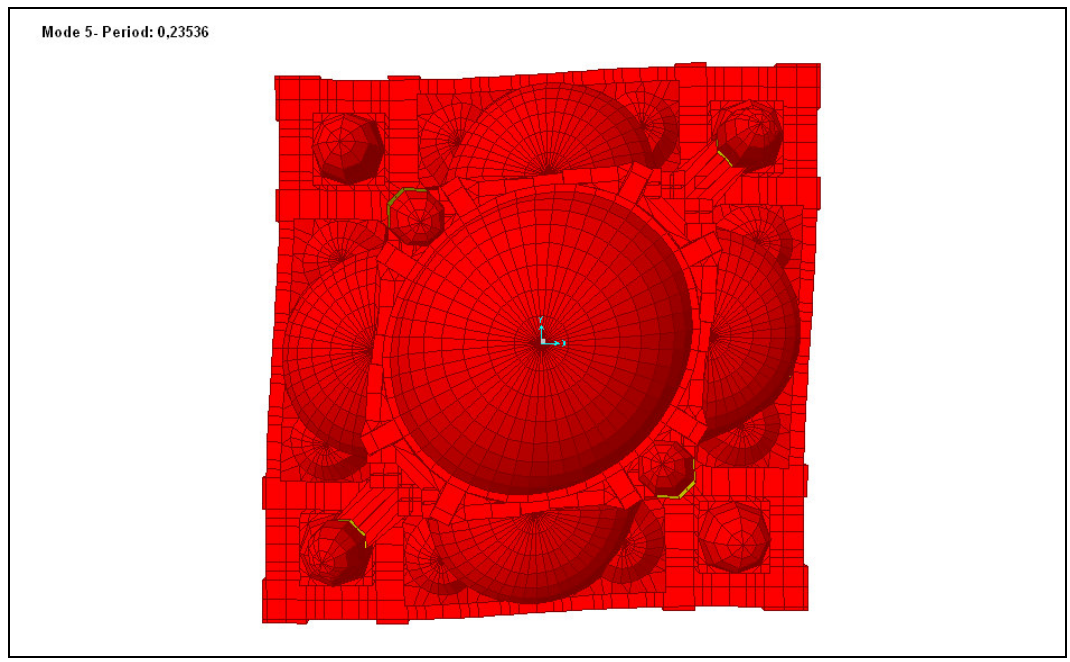

Figure 6.10. Modal analysis, mode 5 (view from top)

7. SPECTRAL RESPONSE ANALYSIS OF THE IMPROVED MODEL UNDER A SCENARIO EARTHQUAKE FOR ISTANBUL

Istanbul in general, is expected to be exposed to earthquakes occuring mainly as a result of the activity of the graben system in Marmara Sea associated with the North Anatolian Fault Zone. The nearest fault is about 20 km south of Istanbul. The improved model is analysed under a scenario earthquake of magnitude 7 with an epicentral distance of 20 km to Istanbul [18].

To study the effects of the ground motion excitations on structure it is necessary to measure the intensity of the motion. One practical measure can be obtained from a knowledge of the response spectra for a generic ground motion. The spectral response analysis seeks to estimate the maximum displacement or pseudo velocity or acceleration of the structure during a design earthquake without recourse to direct integration of the model over the complete duration of an event.

Earthquakes are unique events. Therefore, for design, spectra have been evaluated which envelope the peak response of one degree of freedom systems to a series of earthquakes. Such design spectra are given in terms of the maximum displacement or pseudo-velocity or acceleration of the structure for a range of circular frequencies.

As the modes do not necessarily occur at the same time they may not be superimposed directly to obtain design values. Therefore, two averaging methods have been incorporated in Sap 2000 which are CQC (Complete Quadratic Combination and SRSS (Square-Root-of the Squares).

The numerical values of ground spectral acceleration are given in Table 7.1. Table 7.2 gives the distribution factors of spectral amplitude ratios in x direction. Figure 7.2 to 7.14 show the results of this analysis.

Table 7.1. Spectral accelaration values [18]

Period (sec)	Acceleration (m/sec^2)
0	3,021
0,034	4,532
0,067	6,043
0,101	7,554
0,503	7,554
0,628	6,043
0,785	4,836
0,982	3,865
1,227	3,090
1,534	2,472
2,301	1,648
3,451	1,099
5,177	0,736
7,765	0,491
11,647	0,324

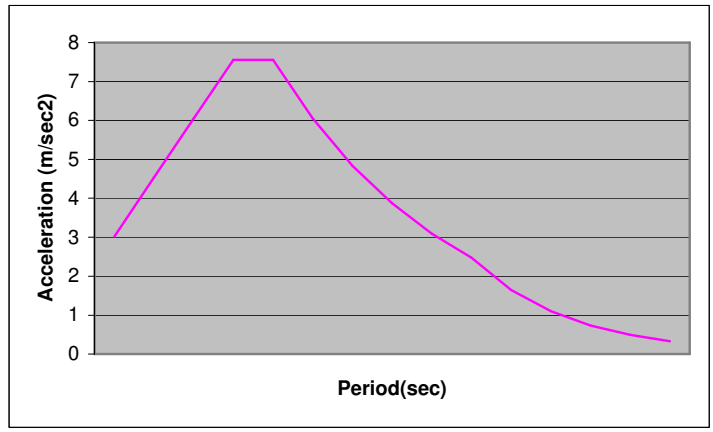

Figure 7.1. Spectral acceleration curve used in this study [18]

Table 7.2. Spectral amplitude used in the analysis [18]

Earthquake direction	**Combination**	**Percentage Amplitude**
Global X direction	Self weight	100%
	Global X	50% (R=2)

Figure 7.5 shows deformations in global X direction in meter with displacement contours. Dark areas indicate the higher values of deformations. In Figure 7.5 and 7.6, it can be easily observed that the deformations. The maximum horizontal displacement computed from the analysis of the model is 15mm at the north face of the main dome.

According to S_{11} stress resultants in the main dome, both tension and compression stresses develop at the main dome. Compression stresses spread over at the middle part (apex part) and tension stresses are observed around the middle part of the main dome in the circumferential direction (Figure 7.7). The maximum value for compression is -280 kN/m2 and the maximum for tension is about +280 kN/m2.

According to S_{22} stress resultants in the main dome, almost all the surface of the main dome is covered by compression stresses except for some regions (around the middle part of the main dome in the circumferential direction). The maximum value for compression is -260 kN/m2 and the maximum for tension is about +260 kN/m2 (Figure 7.8).

According to S_{11} stress resultants in the semi domes, both tension and compression stresses develop at the semi domes (Figure 7.7). The maximum value for compression is around -280 kN/m2 and the maximum for tension is around +840 kN/m2.

According to S_{22} stress resultants in the semi domes, both tension and compression stresses develop at the semi domes (Figure 7.8). The maximum compression and tension streses are respectively -260 kN/m2 and +520 kN/m2 on the surface of the dome. But at the connection regions, the maximum value of tension reachs around +1100 kN/m2.

According to S_{11} stress resultants in the arches, pendentives and piers, compression stresses are observed at the top of the key regions of the east and west main arches, while tension stresses develop at the top surface of the main north and south arches, pendentives and main piers. The highest tension stress in the arches is around +1050 kN/m2 and also the compression stress is around -700 kN/m2 (Figure 7.9). Tension stresses are observed almost all main piers and secondary piers. Also, compression stresses develop at the bottom surfaces of the secondary piers. The maximum value for compression in the piers is around -350 kN/m2 and the maximum for tension is in the range, 1050-1400 kN/m2 at the connection regions (Figure 7.9 and 7.10). The maximum value of tension in the regions is rather near to the strength limit value of crack (the crack strength limit value for tension is 1.4 Mpa).

According to S_{22} stress resultants in the arches, pendentives and piers, tension stresses are observed at the top key regions of all arches, pendentives and piers, and their highest values are around 1 10^3 kN/m2. Compression stresses develop at the bottom surfaces of the arches and their highest values are around -0,50 10^3 kN/m2 (Figure 7.13 and 7.14).

According to S_{33} stress resultants in the arches, pendentives and piers, while tension stresses are observed at top regions of arches, compression stresses develop in the other parts of arches (Figure 7.11 and 7.12). The maximum tension and compression stresses in arches are around 0,60 10^3 kN/m2 and -1,80 10^3 kN/m2 respectively. Both tension and compression stresses are observed in the pendentives. The highest tension value is around 0,60 10^3 kN/m2 and the highest compression value is around -1,80 10^3 kN/m2 (Figure 7.11 and 7.12). Both tension and compression stresses are observed in the piers. Tension stresses occur in many regions of the piers. Also tension stresses increase at the top and bottom of the piers (critical regions). Especially, it reachs maximum value on the surfaces at the bottoms of main and some secondary piers. While the maximum compression stress in the piers is -1,80 10^3 kN/m2, the maximum tension stress is 2,40 10^3 kN/m2 (on the surfaces at the bottoms of main piers). The tension stresses on the surfaces at the bottoms of main and some secondary piers reach or exceed the crack strength limit value for tension. So, cracks are observed on these surfaces (Figure 7.11 and 7.12).

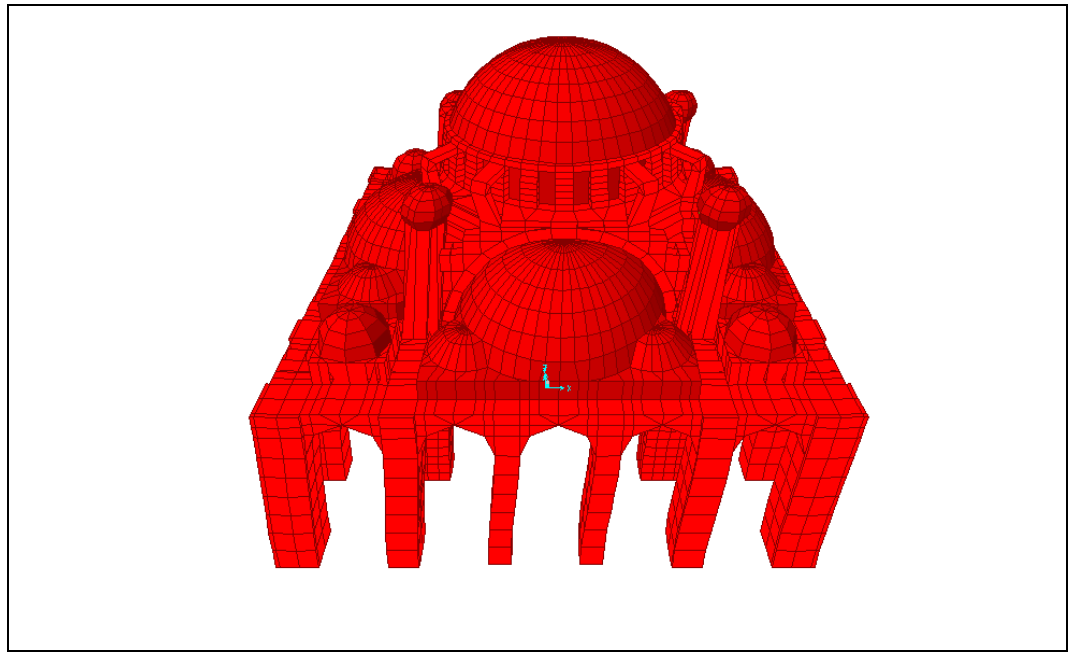

Figure 7.2. General deformed configuration (side view) for spectral response analysis

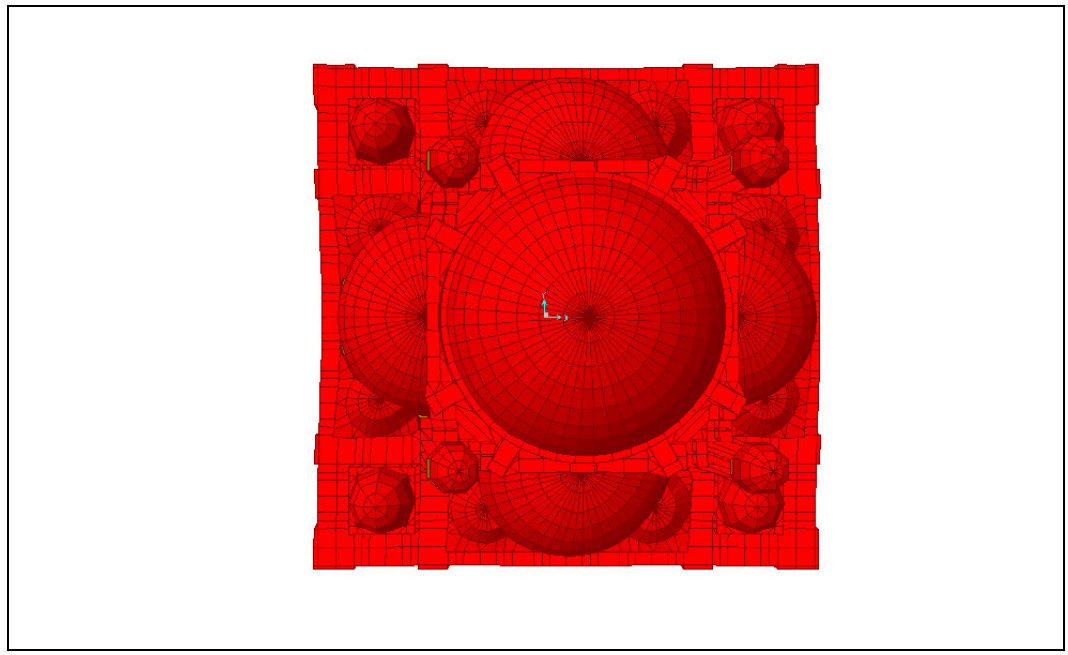

Figure 7.3. General deformed configuration (top view) for spectral response analysis

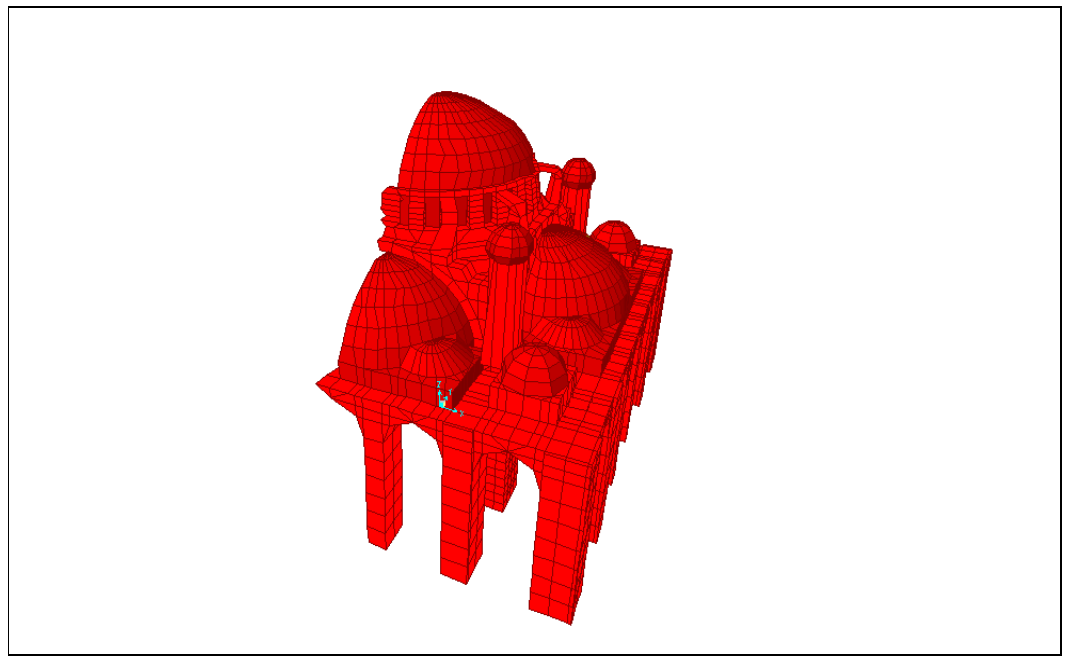

Figure 7.4. General deformed configuration (3-D view from north-east) for spectral response analysis

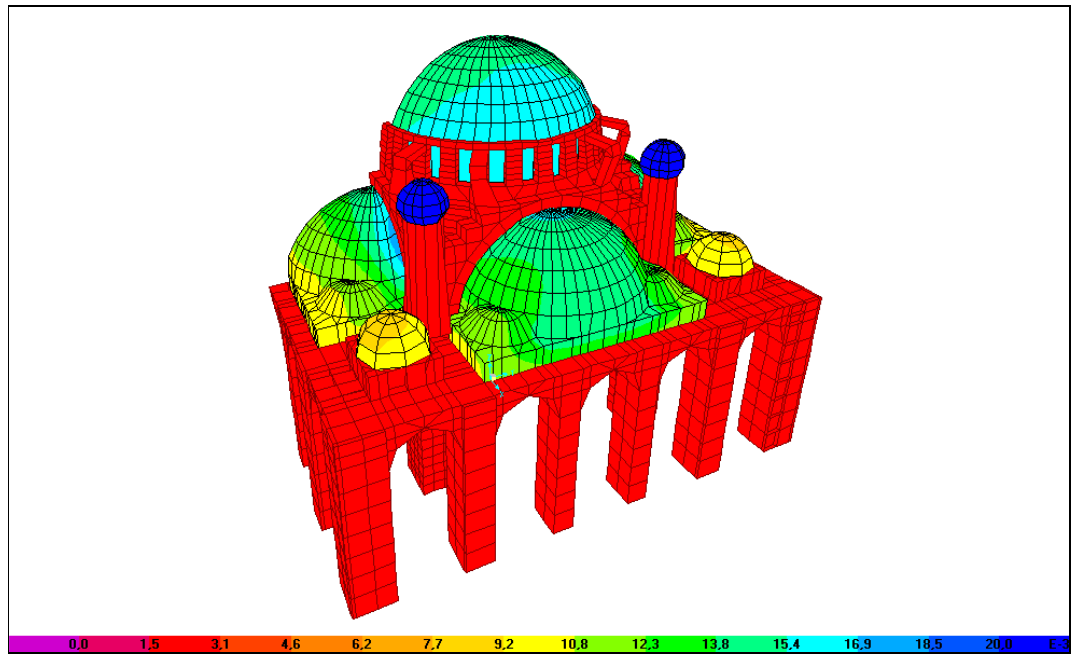

Figure 7.5. Displacement contours in the shell elements (3-D view from north-east) for spectral response analysis

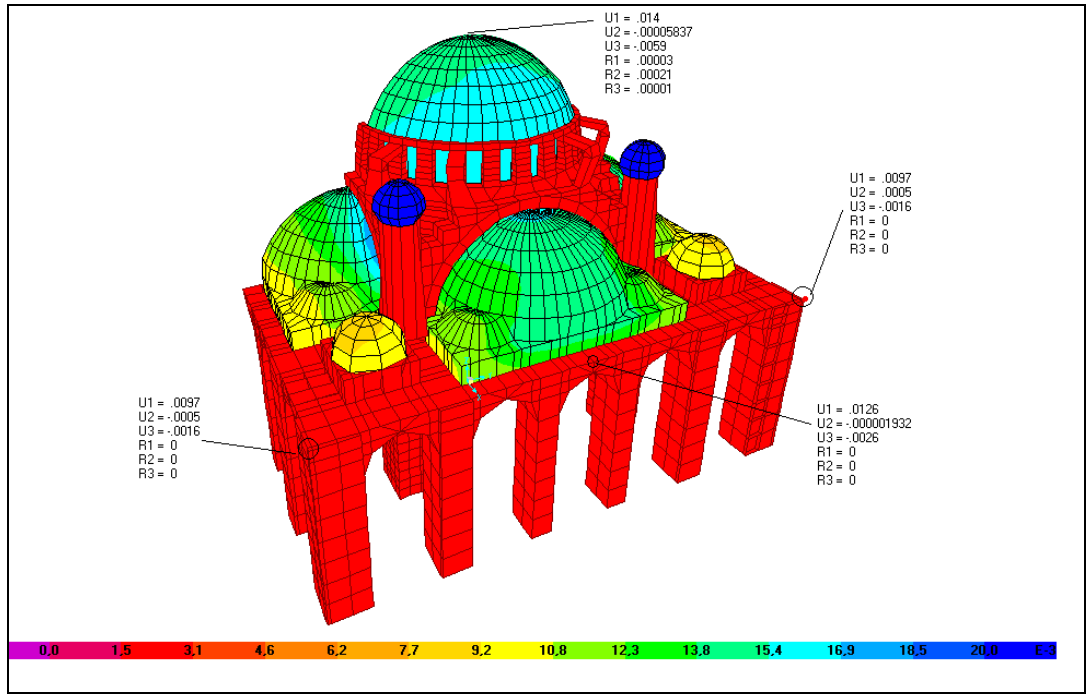

Figure 7.6. Displacement values of some specific points in the half of model (3-D view from north-east) for spectral response analysis

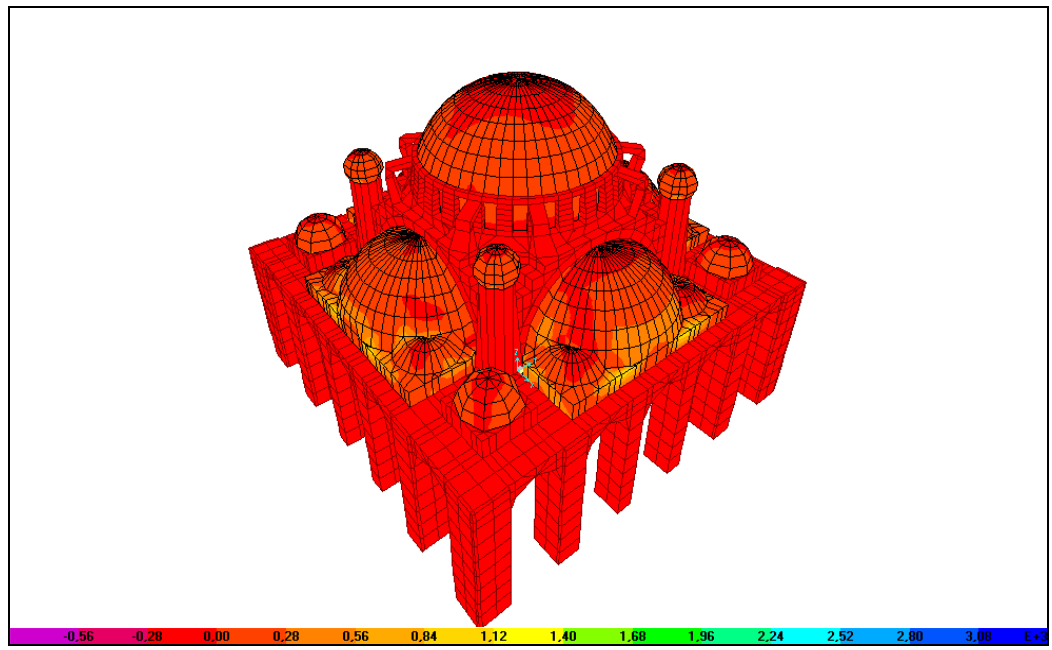

Figure 7.7. S11 stress contours in the shell elements (3-D view from north-east) for spectral response analysis

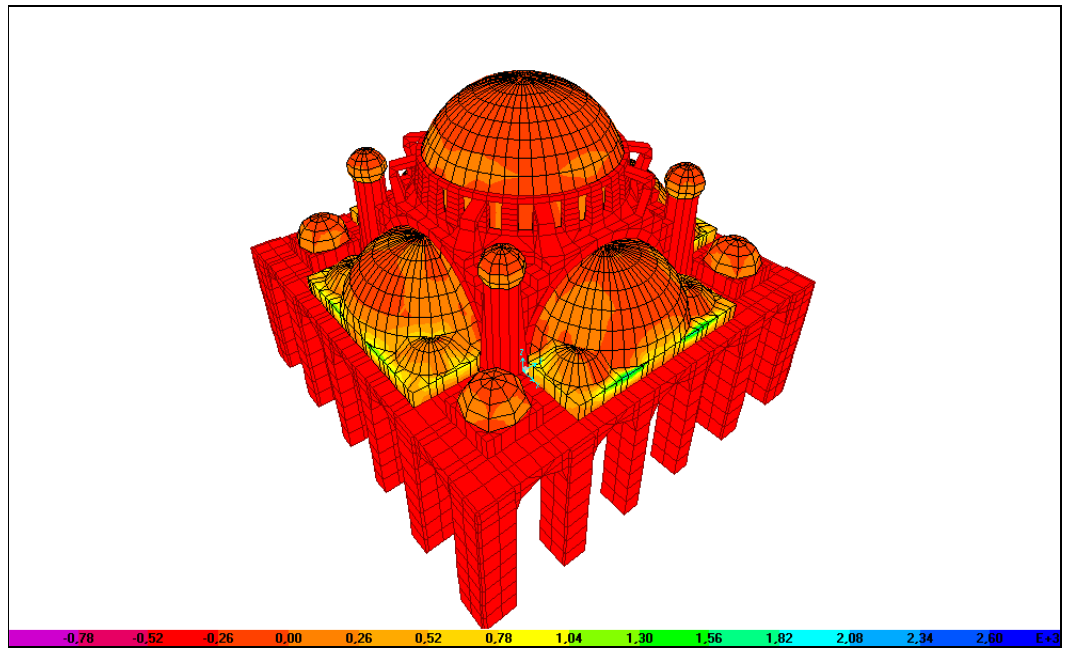

Figure 7.8. S22 stress contours in the shell elements (3-D view from north-east) for spectral response analysis

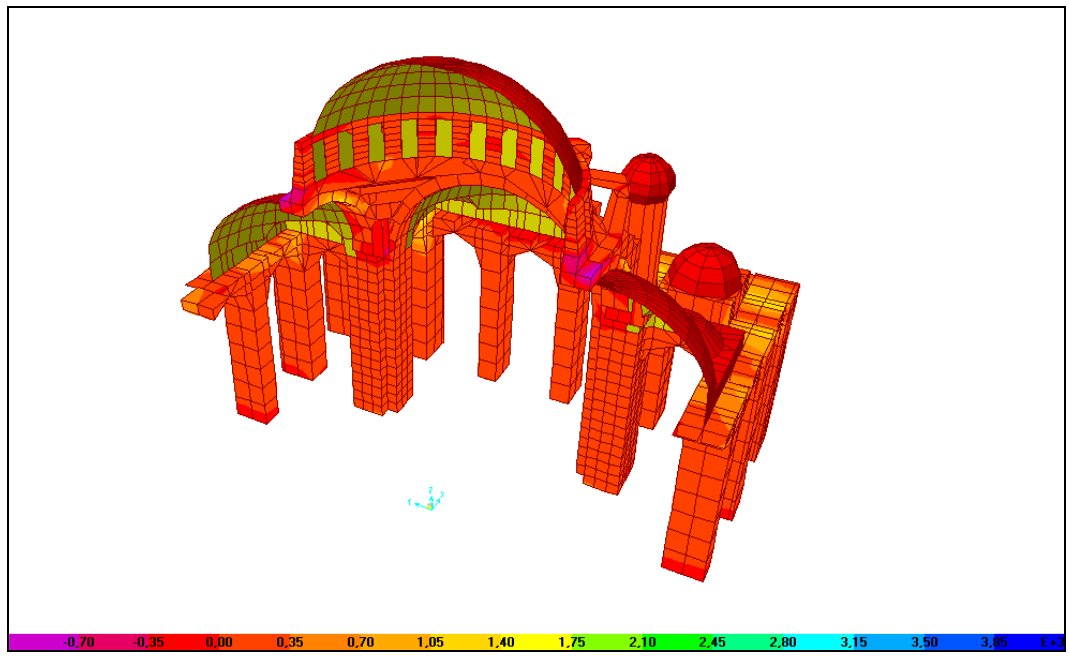

Figure 7.9. S11 stress contours in the solid elements (3-D view from south-east) for spectral response analysis

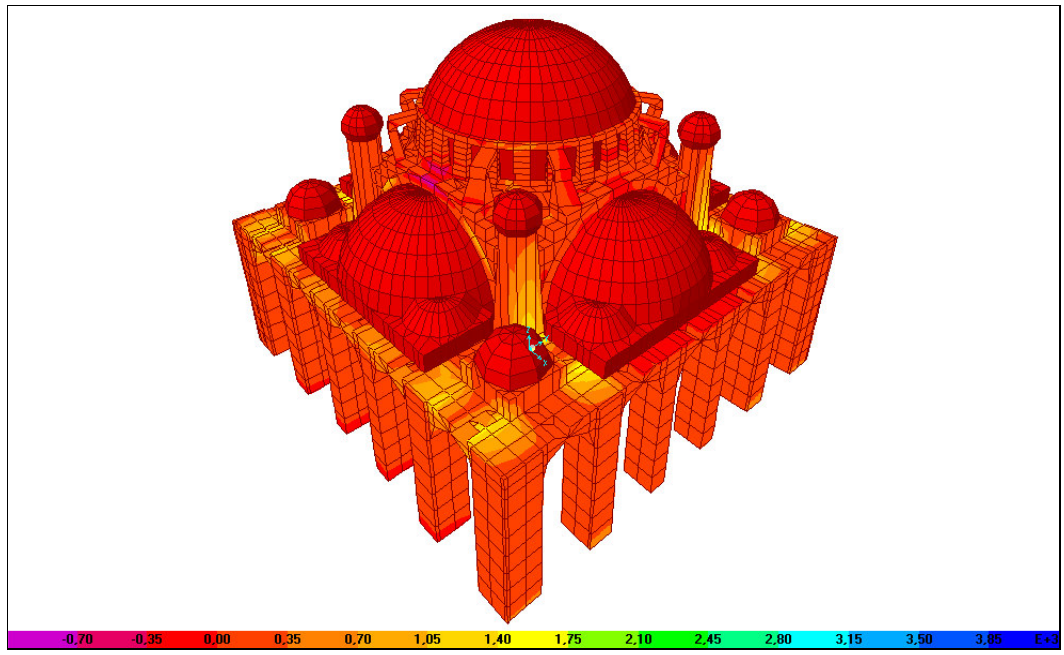

Figure 7.10. S11 stress contours in the solid elements (3-D view from north-east) for spectral response analysis

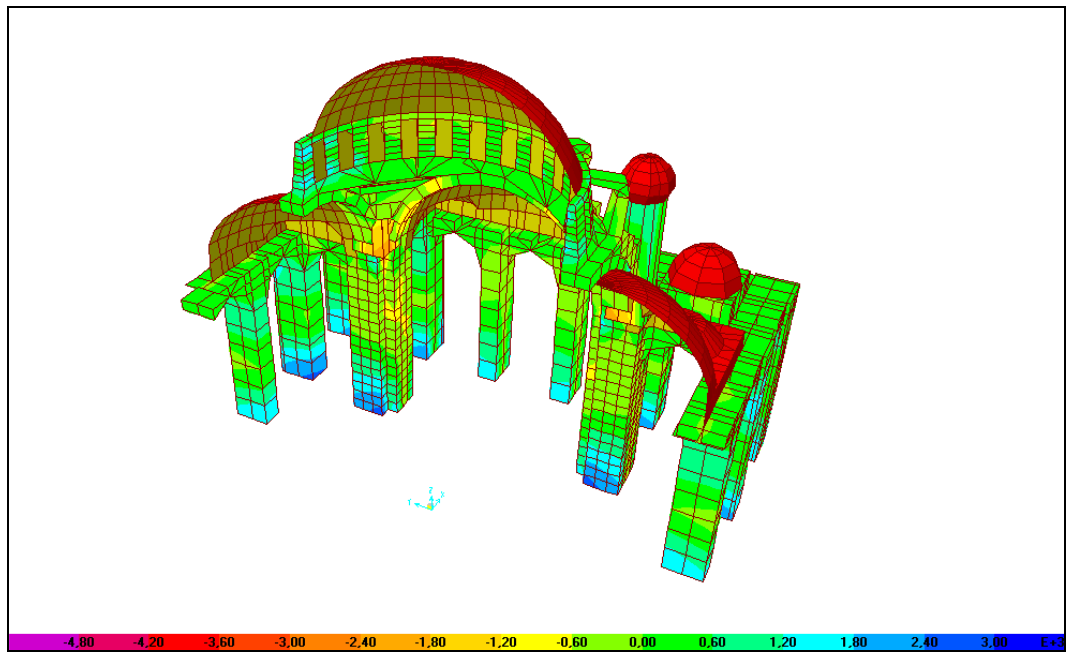

Figure 7.11. S33 stress contours in the solid elements (3-D view from south-east) for spectral response analysis

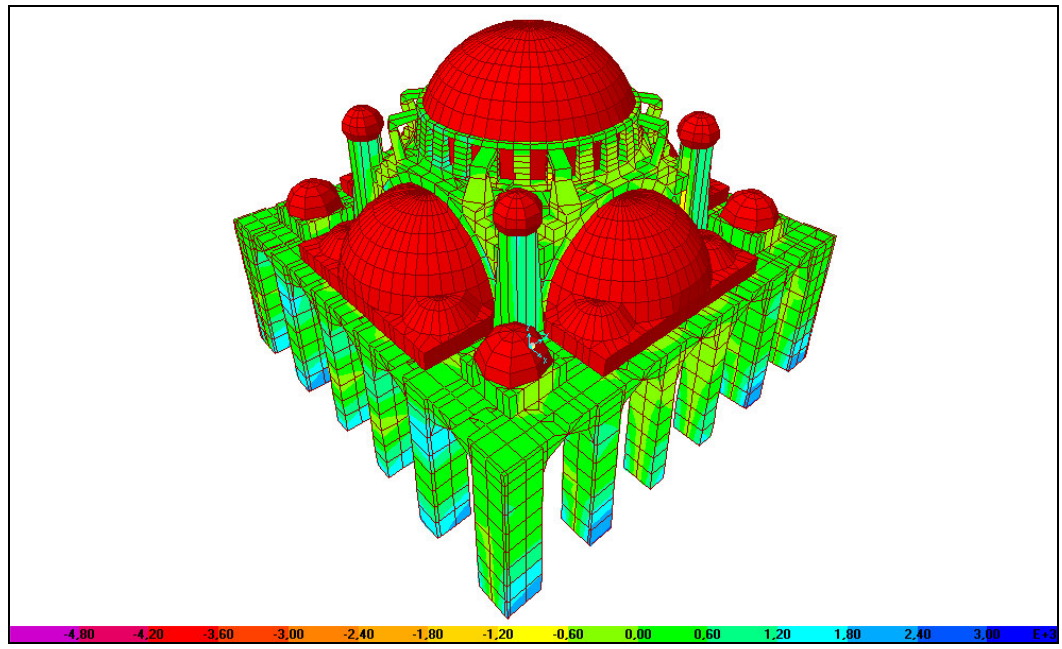

Figure 7.12. S33 stress contours in the solid elements (3-D view from north-east) for spectral response analysis

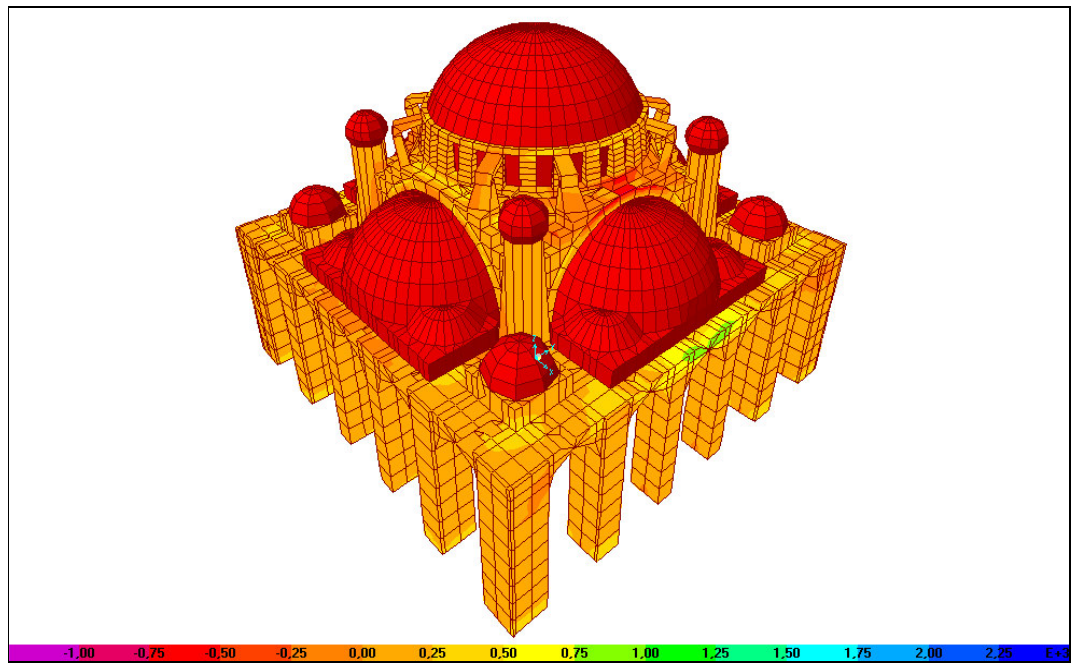

Figure 7.13. S22 stress contours in the solid elements (3-D view from north-east) for spectral response analysis

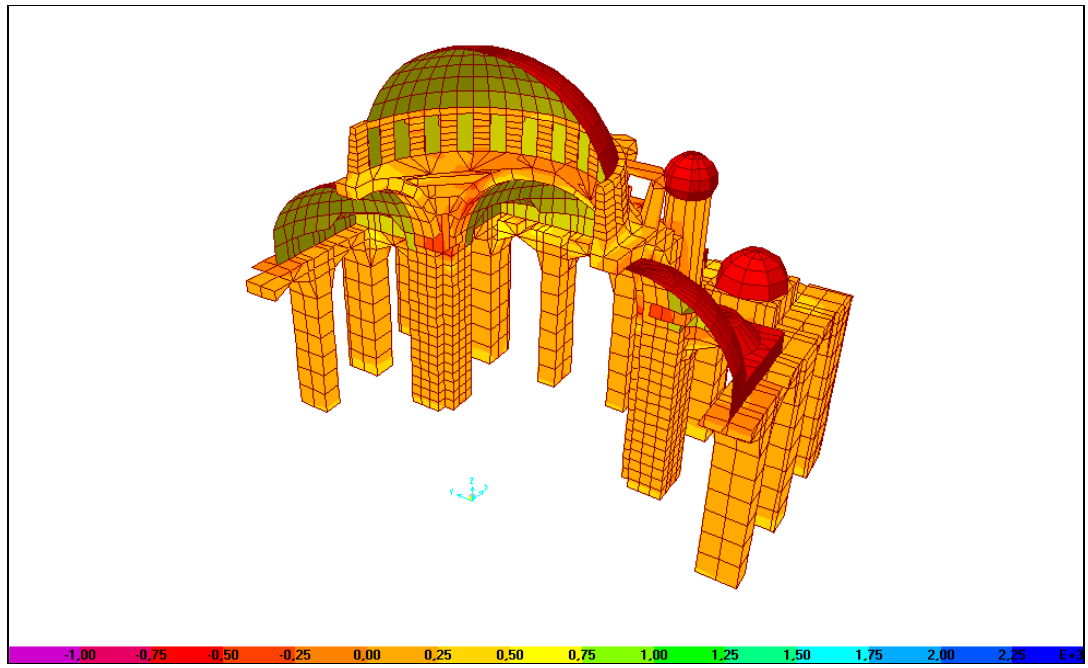

Figure 7.14. S22 stress contours in the solid elements (3-D view from south-east) for spectral response analysis

8. CONCLUSIONS

Notwithstanding the lack of technical documents, the constructed three dimensional finite element model reflects the main characteristics of the Sehzade Mehmet Mosque by static, dynamic and spectral response analyses.

Under the own weight, according to short-term and linear analysis, the structure is generally understressed. So, the structure, under its own weight, has no stresses which can be classified as destructive. However, this analysis gives satisfactory results to determine the critical areas. One should keep in mind that the deformations obtained from the static analysis are linear short term deformations. Whereas, the actual ones are long term and non-linear deformations combined with those caused by the experienced earthquakes. Also, snow loads are added in the static analysis but there are not observed any important effect of snow loads on the analysis. In the dynamic analysis, it has been possible to determine the first five modes of the Sehzade Mehmet Mosque precisely as;

Table 6.1. Results of the eigenvalue analysis

Modes	Frequencies	Modal Shapes
Mode 1	2,8569	N-S lateral
Mode 2	2,8569	E-W lateral
Mode 3	3,3394	Squeezing
Mode 4	3,5371	Torsional
Mode 5	4,2489	Breathing

In the spectral response analysis, the critical areas are observed at the some connection regions and bottom and top of piers. The tension stresses on the surfaces at bottoms of main and some secondary piers reach or exceed the crack strength limit value for tension. So, cracks are observed on these surfaces (Figure 7.9, Figure 7.10, Figure 7.11 and Figure 7.12).

It is a fact that the research studies carried out up to today towards the determination of the erthquake performance of this masterpiece of Ottoman-Turkish architecture is very limited. Aimed at the exploration of the earthquake performance of the Sehzade Mehmet Mosque, the present study is the first extensive master thesis study prepared on the Sehzade Mehmet Mosque. A large number of elements are improved to achieve maximum precision. These improvements were reliased after the preliminary investigation on the structural system, historical backround and material properties.

From the site inspeciton, it has been concluded that there is no major cracks existing on the structure. In other words, all parts of the structure are in good condition. The Sehzade Mehmet Mosque is considered to be one of the first masterpieces of the Ottoman architecture and has successfully sustained against more than 89 major earthquakes without any severe damages [11], [19].

Unfortunately, precise documents of the works are not found in the archives. As a future work, some parts of the finite element model may be refined after the exact determination of the geometrical and material properties of the structure. In order to identify material properties, laboratory and field tests should be performed. Furthermore, soil investigation should be done to have a clear information about the boundary conditions as well as the dimensions of the foundations. Also, a non-linear analysis may be performed to be a better solution to represent more accurately the dynamic behavior and to identify the deformation patterns of the actual structure.

APPENDIX A: HISTORICAL EARTHQUAKES OF ISTANBUL [27]

- 24 August 358 — Damage in Istanbul
- 2 December 362 — Damage in newly finished Hagia Sophia
- 396 — Strong earthquake in Istanbul
- June 402 — Strong earthquake in Istanbul
- 403 — Strong earthquake in Istanbul
- 1 April 407 — Many houses were damaged in Bakırköy. Tsunami wave observed.
- 412 — Damage in the city walls
- 6 November 447 — Many buildings were damaged during the earthquake. An important portion of the city walls and 57 of 96 fortification towers collapsed.
- 25 September 478 — Significant damage in Istanbul. Partial collapse of the inner city walls.
- 16 August 542 — Significant damage in Istanbul.Damage in Constantin and Arcadius churches, collapse of the statues and obelisks
- 6 September 543 — Strong earthquake in Istanbul.Damage in Hagia Sophia
- 16 August 554 — Damage in many buildings and the city walls, damage in the east main arch of Hagia Sophia
- 14 December 557 — Many Buildings damaged. Previously damaged east main arch of the Hagia Sophia collapsed with the eastern part of the main dome.
- 26 October 740 — Significant damage in Istanbul, damage in the city walls and Aya Irini Church
- 10 April 861 — Many buildings were damaged.
- 9 January 869 — Partial collapse in Hagia Sophia. Many buildings were collapsed.
- 25 October 989 — Damage in Hagia Sophia and Valens Aquaduct (Bozdogan Kemeri), west main arch of Hagia Sophia collapsed causing damage in the main dome and in the west semidome.

- 1 June 1296 Many buildings were damaged.
- 1323 Many buildings were damaged.
- 18 October 1343 Many buildings were damaged. Tsunami wave observed. Hagia Sophia were damaged.
- 6 November 1344 Strong earthquake in Istanbul, partial damage in city walls
- 19 May 1346 East side of Hagia Sophia collapsed because of the fall of its east main arch.
- 16 January 1489 Many minarets collapsed. One of the strongest earthquakes hit IstanbuI. Nearly every building was damaged. Liquefaction observed. About 1000 houses and lots of mosques collapsed. About 5000 (5% of the population) casuaIties. Damage in Hagia Sophia, Bayazit, Fatih, Atik Ali Pasa and Davut Pasa mosques, in Topkapi Palace, Galata Tower, Theodosius Obelisk, Anadolu and Rumeli Fortresses and city wall.
- 10 May 1556 Many buildings were damaged. Cracks in the walls of Hagia Sophia, damage in the Fatih mosque
- 17 February1659 Damage in many old buildings, damage in Süileymaniye mosque
- 25 April 1689 Slight damage through Istanbul
- 11 July 1690 Damage in some buildings, Fatih mosque and Topkapi Palace
- 25 May 1719 Damage in 40 mosques and 27 towers, damage in Bayazit, Sinan Pasa, Bali Pasa and Pertev Pasa mosques
- 2 September1754 Damage in many buildings, intensive damage in Usküdar and Balat
- 22 May 1766 Damage in many buildings, damage in Hagia Sophia, Bayazit, Fatih, Süleymaniye and a number of mosques
- 10 July 1894 Extensive damage in Istanbul, damage in Hagia Sophia, Fatih and a number of mosques and churches and Topkapi Palace.

APPENDIX B: DESTRUCTIVE EARTHQUAKES IN ISTANBUL [27]

	Date	Epicenter N	Epicenter E	Magnitude	Intensity (MM) (at epicenter)	Distance from Epicenter (km)	Intensity (MM) In İstanbul	Acc %g
1	30-04-1557	41	29	6,4	VIII	0	VIII	12
2	30-07-1633	41	29	5,5	VII	0	VII	-
3	28-06-1648	41	29	7,0	IX	0	IX	18
4	1718	41	29	6,2	VII	0	VII	-
5	25-05-1719	40,8	29,4	7,3	X	25	IX	18
6	03-09-1763	41	29	5,8	VII	0	VII	-
7	23-04-1766	40,8	28,2	7,6	X	72	IX	17
8	28-02-1855	40,2	29,1	7,7	X	90	VIII	14
9	10-07-1894	40,6	28,7	7,8	X	54	IX	21
10	09-08-1912	40,5	27,0	7,8	X	177	VII	-
11	04-01-1935	40,5	27,5	6,9	IX	137	VI	-
12	18-03-1953	40,0	27,3	8,0	XI	182	VII	-
13	06-10-1964	40,3	28,2	7,0	IX	102	VI	-
14	22-07-1967	40,7	30,8	7.2	IX	150	VI	-

REFERENCES

1. Smith, J. V., *Hagia Sophia: Advancement of Nonlinear Modelling*, Senior Thesis, Princeton University, 1996.

2. Ceylan, O., *Turkish Architecture*, Mimar Sinan University /Department of Restoration, http://www.lesartsturcs.com/general_arts/archi_turk_overview.html, 2003.

3. Macaulay, D., *Mosque*, Houghton Mifflin Co., Boston, 2003.

4. Aksit, İ., *İstanbul*, Ali Rıza Baksan Güzel Sanatlar Matbaası A.Ş., İstanbul, 1981.

5. Özer, B., "The Architect of Domed Mosques as a Master of Pluralism", *Journal of the Islamic Environmental Design Research Centre*, pp.146-155, 1987.

6. Vogt, U., *Living Architecture; Ottoman*, Grosset & Dunlop, NewYork , pp. 97-104, 1996.

7. Kuran, A., *The Grand Old Master of Ottoman Architecture,* Ada Press Publishers, Istanbul, pp.64-68, 1987.

8. Kuran, A., *The Mosque in Early Ottoman Architecture*, University of Chicago Press, Chicago, pp.191-217, 1968.

9. Stierlin, H., *Turkey, from the Selçuks and to the Ottomans*, Taschen, Köln; New York, 1998.

10. İlkışık, M., *Boring Log Archives,* Anadolu Yerbilimleri, İstanbul, pp.1-6, 2000.

11. Arıoğlu, E. and K. Anadol, "On the Earthquake Resistance of the Süleymaniye Mosque (Istanbul) in the Historical Perspective", *Fifth World Conference on Earthquake Engineering*, Roma, pp.289, 1973.

12. Arıoğlu, E. and N. Arıoğlu, "Mimar Sinan'ın Taşıyıcı Olarak Kullandığı Küfeki Taşının Mühendislik Gizemi", *Mimar Sinan Dönemi Yapı Etkinlikleri Semineri*, İstanbul 1999.

13. Durukal, E. and Ö.Yüzügüllü, *Non-destructive Testing Techniques of Structural Materials in Historical Structures*, Compatible Materials for the Protection of European Cultural Heritage Pact 55, Athens, pp.221-223, 1998.

14. Durukal, E. and M.Erdik, *Dynamic Response of Hagia Sophia and Süleymaniye in Istanbul inferred from the recordings of 1999 Kocaeli and Düzce earthquakes*, Compatible Materials for the Protection of European Cultural Heritage Pact 59, pp.19-28, 2000.

15. Kaya, S. M., M. N. Aydınoglu, M. Erdik, Ö. Yüzügüllü, *Determination of Dynamic Characteristics of Süleymaniye Mosque by Analytical and Experimental Methods*, Compatible Materials for the Protection of European Cultural Heritage Pact 56, İstanbul, 1998.

16. Şahin, M., *Dynamic Response of Hagia Sophia Considering Cracks*, Doktora Tezi, Mimar Sinan Üniversitesi, 2002.

17. SAP2000, *Integrated Structural Analysis and Design Software*, Computer and Structures Inc., Berkeley, California 2005.

18. Keypour, H., *Nonlinear Dynamic analysis of Historical Structure and Application to Ayasofya Mosque*, Ph.D. Thesis, Boğaziçi Üniversity, 2001.

19. Kuran, A., *Mimar Sinan'ın İstanbul'daki Eserleri; Külliyeler, Camiler ve Mescidler*, Türk Tarih Kurumu, 1972.

20. Cerasi, M., "The Commerce of Forms and Types Between the West and the Ottoman East from the sixteenth to the Eighteenth Century", *Journal of the Islamic Environmental Design Research Centre*, pp.114-133, 1997.

21. Yerasimos, S., *İstanbul, İmparatorluk Başkenti*, Tarih Vakfı Yurt Yayınları, İstanbul, pp.245-247, 2000.

22. Peker, A. U., *Edirnekapi Mihrimah Sultan Mosque*, http://www.metu.edu.tr/home/ wwwissch /ozgurey / istanbul /mihrimah.htm, 2005.

23. Burelli, R., "Vision and Representation of Urban Space", *Journal of the Islamic Environmental Design Research Centre*, pp. 42-51, 1987

24. Demir, A. H., *Fatih Camileri ve Diğer Tarihi Eserler*, Türkiye Diyanet Vakfı, İstanbul, pp: 39-40, 1991.

25. Selahiye, A., *A Study on the Identification of Natural Vibration Frequencies of The Süleymaniye Mosque*, M.S. Thesis, Boğaziçi University, 1994.

26. Odabaşı, Y., *Ahşap ve Çelik Yapı Elemanları*, Beta BasımA.Ş. İstanbul, p:108,1997.

27. Kaya, S. M. *Determination of Earthquake Performance of the Süleymaniye Mosque*, M.S. Thesis, Boğaziçi University,1999.